AD-A095 931 NAVAL OCEAN SYSTEMS CENTER SAN DIEGO CA F/G 17/1
AN EXPERIMENT IN SELF-COHERING A FLEXIBLE LINEAR ARRAY.(U)
APR 80 J V THORN, N O BOOTH
UNCLASSIFIED NOSC/TR-597 NL

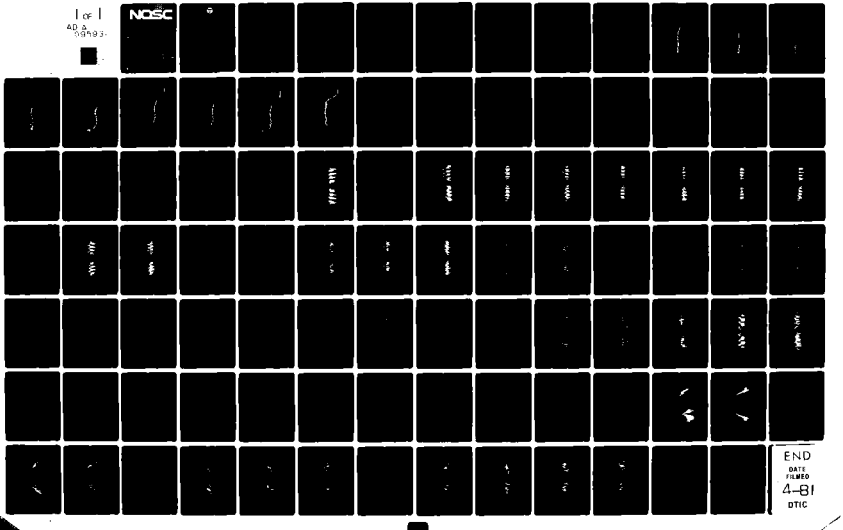

END
DATE FILMED
4-81
DTIC

(12) LEVEL II

NOSC

NOSC TR 597

NOSC TR 597

Technical Report 597

AD A095931

AN EXPERIMENT IN SELF-COHERING A FLEXIBLE LINEAR ARRAY

JV Thorn
NO Booth
April 1980

Final Report: June - October 1978

Prepared for
Naval Electronic Systems Command

Approved for public release; distribution unlimited.

NAVAL OCEAN SYSTEMS CENTER
SAN DIEGO, CALIFORNIA 92152

NAVAL OCEAN SYSTEMS CENTER, SAN DIEGO, CA 92152

AN ACTIVITY OF THE NAVAL MATERIAL COMMAND

SL GUILLE, CAPT, USN
Commander

HL BLOOD
Technical Director

ADMINISTRATIVE INFORMATION

The research reported herein was conducted for the Naval Electronic Systems Command, Code 320, under Program Element 62711N, XF11-101-100 over the period June to October 1978. The authors would like to acknowledge the valuable assistance rendered by Dr. Bruce Geelhood and Mr. Steve Bryant of the Naval Ocean Systems Center.

Released by
IP Lemaire, Head
Advanced Systems Division

Under authority of
HR Talkington, Head
Ocean Technology Department

UNCLASSIFIED

SECURITY CLASSIFICATION OF THIS PAGE (When Data Entered)

(14) NOSC/TR-597

REPORT DOCUMENTATION PAGE

READ INSTRUCTIONS BEFORE COMPLETING FORM

1. REPORT NUMBER: NOSC Technical Report 597 (TR 597)	2. GOVT ACCESSION NO.: AD A095 031
3. RECIPIENT'S CATALOG NUMBER:	
4. TITLE (and Subtitle): AN EXPERIMENT IN SELF-COHERING A FLEXIBLE LINEAR ARRAY	5. TYPE OF REPORT & PERIOD COVERED: Final Report, June - October 1978
	6. PERFORMING ORG. REPORT NUMBER:
7. AUTHOR(s): JV Thorn, NO Booth	8. CONTRACT OR GRANT NUMBER(s):
9. PERFORMING ORGANIZATION NAME AND ADDRESS: Naval Ocean Systems Center, San Diego, CA 92152	10. PROGRAM ELEMENT, PROJECT, TASK AREA & WORK UNIT NUMBERS: 62711N, XF11 101 100
11. CONTROLLING OFFICE NAME AND ADDRESS: Naval Electronic Systems Command, Washington, DC 20360	12. REPORT DATE: April 1980
	13. NUMBER OF PAGES: 91
14. MONITORING AGENCY NAME & ADDRESS (if different from Controlling Office): 12 95	15. SECURITY CLASS. (of this report): Unclassified
	15a. DECLASSIFICATION/DOWNGRADING SCHEDULE:

16. DISTRIBUTION STATEMENT (of this Report)

Approved for public release; distribution unlimited.

17. DISTRIBUTION STATEMENT (of the abstract entered in Block 20, if different from Report)

18. SUPPLEMENTARY NOTES

19. KEY WORDS (Continue on reverse side if necessary and identify by block number)

Passive sonar
Beamforming
Towed array

20. ABSTRACT (Continue on reverse side if necessary and identify by block number)

Self-cohering is a method of using the signals from strong sources to locate the elements of a towed array accurately enough that beamforming may be successful on weaker sources at other frequencies arriving from different directions.

An experiment was conducted to test this method with a mile-long, 40-element towed line array. Results indicate that whereas it is sometimes possible to perform self-cohering successfully by means of very simple algorithms, some of the phenomena involved are only poorly understood, and care must be exercised in applying these algorithms if failure is to be avoided.

DD FORM 1 JAN 73 1473 EDITION OF 1 NOV 65 IS OBSOLETE S/N 0102-014-6601

UNCLASSIFIED

SECURITY CLASSIFICATION OF THIS PAGE (When Data Entered)

393159

CONTENTS

ILLUSTRATIONS

ILLUSTRATIONS (continued)

INTRODUCTION

Beamforming with large acoustic arrays suffers from inaccurate knowledge of array element locations. Self-cohering is a method of using the signals from strong sources to locate array elements accurately enough that beamforming may be successful on weaker sources at other frequencies arriving from different directions.

This report describes an attempt to test self-cohering with a mile-long, 40-element towed line array in order to answer the following questions:

(1) How "straight" is the line array under "ideal" towing conditions?

(2) Can array elements be located accurately enough that the array can be used for beamforming even when the towing ship is turning?

(3) Are the beam patterns of a "crooked" line array good enough to be useful if the towing ship were slowed down (to reduce self-noise) until the array sagged?

The results of this experiment indicate that it is sometimes possible to successfully perform self-cohering by means of very simple algorithms. However, some of the phenomena involved are only poorly understood. Thus care must be exercised in applying these algorithms if failure is to be avoided. All of the work described here uses frequency-domain beamforming. As indicated in Ref. 1, there are many other ways to implement self-cohering; the method described here is not necessarily the best, but does at least establish feasibility.

DATA

The data used in this experiment come from magnetic tape recordings of an actual at-sea exercise performed several years ago with a towed line array. The exercise itself lasted for more than a week, but only 1-1/2 hours of data, taken from 3 separate days, were used for the self-cohering experiment. Ship's logs and data recorder logs were scanned to find data representative of times when the towed array was "working well" (ie, presumably straight) and "very noisy" (ie, presumably crooked). The purpose of the exercise had nothing to do with self-cohering, of course, so even these carefully chosen data do not provide many answers to questions about self-cohering beyond simple feasibility.

The towed array itself consisted of 40 omnidirectional hydrophones equally spaced at 125-ft intervals along the towed line (a total length of 4875 ft). The array was attached to the towing ship via a 4000-ft length of towing cable, part of which was a compliant section for strain relief. A few of the elements were equipped with depth sensors, but their accuracy is disputed among persons connected with the data-collecting exercise.

Electronic preamplifiers associated with the array elements were calibrated in such a manner that recorded data were supposedly compensated for nonuniformities in sensitivity and phase between individual hydrophones.

Actual data recording was done on analog recorders, but the data segments used for self-cohering were transcribed onto digital tapes using 8-bit analog-to-digital converters running at 260.42 samples per second.

No attempt was made during the data-collecting exercise to measure actual element locations. The quality of beam patterns is the only indication of how well self-cohering is working, since the self-cohered array shapes cannot be compared with independent measurements.

---

[1] B. Geelhood, "Self Cohering of a Flexible Linear Array," NUC Memo 6513. 272-77, 29 Dec 1976.

Supposedly, the data-collecting exercise included a second ship (many miles from the array) dangling two acoustic sources (at different frequencies) in the ocean as calibration points for the array. People connected with the exercise claim they were sometimes able to beamform the array on these control sources, although the control sources were abnormally weak and often absent. In the time segments analyzed for self-cohering, many strong signals were detected, but the control sources were never detected. Therefore, the location of the sources used for self-cohering is unknown, and again there is no way of cross-checking the self-cohering results to be sure that apparent improvement is not merely an artifact.

BEAMFORMING

All of the self-cohering work reported here was done in the frequency domain, which implies the following processing procedure. The time history from each array element is Fourier transformed. The frequency bins for which most of the array elements show relatively large-magnitude Fourier coefficients are designated "source frequencies." For each source frequency, the complex Fourier coefficient from each element is phase rotated according to the element's position in the array and according to the desired steering direction; the results from all the elements are summed, and the magnitude of the sum is the beam pattern response for that steering angle for that frequency. A full beam pattern for each frequency is formed by plotting the response as a function of steering angle.

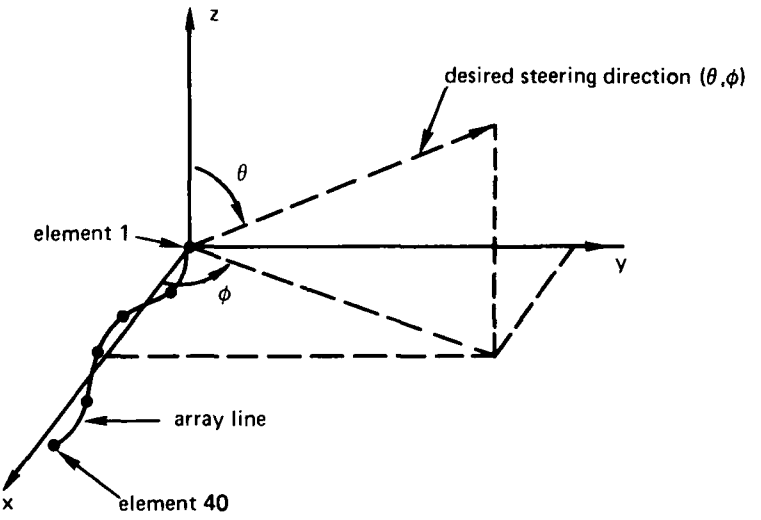

(X_n, Y_n, Z_n) = coordinates of the n^{th} array element

(θ,ϕ) = cylindrical coordinates of steering direction. Towing ship connects to element 1 and tows in negative x-direction; element 40 is "tail end" of array.

a_n = complex number representing the Fourier coefficient of the desired frequency bin for the n^{th} element

A = normalizing constant, indicating amount of energy contained in the frequency bin

$$= \sum_{n=1}^{40} |a_n|$$

$B(\theta,\phi,f)$ = beam response for frequency f

$$= 20 \log \left(\frac{\left| \sum_{n=1}^{40} a_n \exp \left[j \frac{2\pi f}{c} (X_n \sin\theta \cos\phi + Y_n \sin\theta \sin\phi + Z_n \cos\theta) \right] \right|}{A} \right) \quad (1)$$

All of this processing was done in non-real time using the Center's Univac 1110 computer. The Fourier transforms were done using a canned FFT routine. This canned routine used exp (+jωt) as the Fourier kernel, so exp (+j . . .) must be used in Eq. (1). (Otherwise, the beam would be steered in a direction conjugate to the desired direction.)

For convenience in determining how well self-cohering is working, the term "coherence" is coined. "Coherence" is equal to the value in parentheses in Eq. (1). If a signal is noise-free and consists entirely of a plane wave propagating from a single distant point source, and if the element locations are known exactly, then there is a steering angle such that the phase rotations introduced in the numerator of Eq. (1) exactly cancel the phase rotations due to signal propagation, in which case all of the rotated a_n's add in phase and the coherence is unity (ie, $|\Sigma\, a_n| = \Sigma\, |a_n|$). Thus, a "perfect" beam has unity coherence, and any degradation (such as noise or imperfect knowledge of array element locations) causes coherence to be less than unity.

The amount of integration time is an important consideration in frequency-domain beamforming. A Fourier transform is effectively a set of narrowband filters with bandwidth inversely proportional to integration time. Coherent integration can be advantageously used to discriminate against noise for only as much time as the signal is stable. If, during the coherent integration time, the signal frequency drifts due to Doppler effects or the signal phase changes because the array moves or bends, then the signal will cancel itself. An "optimum" integration time for the data used for self-cohering was determined by trial and error to be about 8 s. With less integration time, all of the frequency bins look more or less the same (ie, no frequency lines stand out as being strong sources). With 8 s integration time, it is usually possible to pick out several strong discrete-frequency sources. With more integration time, most of the previously strong discrete frequencies begin to fade, and computer costs mount rapidly. An integration time of 8 s corresponds to a frequency bandwidth of about 1/8 Hz, which is about the same as that used (by persons connected with the data-collecting exercise) in the original analysis of the line array data.

FINDING SOURCES SUITABLE FOR SELF-COHERING

Figure 1 is a sequence of plots of energy vs frequency. Each plot is a result of 8 s worth of coherent integration and 40 elements' worth of incoherent integration; that is, an 8-s block of data from each array hydrophone is Fourier transformed, and the energy from all 40 array elements is added together to produce the plotted value for each frequency bin. This incoherent average over the array elements produces a little extra processing gain (not as much as if the average could be done coherently), so that spectral lines can be seen in Fig. 1 which could not be seen by looking at one element only.

Figures 1a–1i are all normalized such that the highest value on each plot is placed at 50 dB. Rolloff at the high end of the spectrum is due to the anti-aliasing filter in the recording electronics. At the extreme right of each figure, the spectrum appears to level off again; this is the noise floor established by quantization error in the 8-bit analog-to-digital converters used in taping the data. This noise floor is an absolute constant, and therefore individual plots from Fig. 1 may be compared with each other on an absolute (not relative) scale by aligning the noise floors (instead of by aligning the 0- to 50-dB scales).

The data represented in Figs. 1a through 1h came from day 256 of the at-sea exercise. According to ship's logs for that day, at time 1255 (Fig. 1a) the array was straight, the towing ship was heading 295°, the towing speed was 3 knots, and the depth of the array was 700 ft. At time 1300 (5 min later; Fig. 1b) the towing ship began a left turn to heading 240°. The next entry in the ship's logs is for a time over an hour later and is unrelated to the turn. No mention is made in the logs as to when the towing ship straightened out on its new heading or how large was the radius of the turn. People associated with the exercise do not remember that specific turn, of course, but they say that generally when the ship turned, it did so without slowing down and without making any allowances for the fact that it was towing an array. Probably, therefore, the ship completed its turn in less than a couple of minutes. These same people also say that they think that the array tends to follow itself, so that the ship's relatively sudden turn propagates along the array as a kink moving at about the towing speed. At a towing speed of about 3 knots, it would take about 14 min for the kink to travel the 4000-ft length of the towing cable and reach the array itself. Indeed, at time 1315 (Fig. 1e) the energy-vs-frequency plots show a sudden and drastic increase in the low-frequency noise level. This extra noise is possibly flow noise caused by hydrophones in the kink region being dragged sideways.

This extra noise is a serious problem when self-cohering is attempted. It is difficult to tell whether a beam pattern is degrading because of decreasing signal-to-noise ratio or because of array curvature. Besides, the extra noise occasionally saturates the recording electronics, which upsets the phases of the desired signals in spite of the narrowband Fourier transform filters.

Note in Fig. 1 that the control-source frequencies, 57 Hz and 23 Hz, never appear as strong spectral lines. Occasionally a 56.5-Hz line appears, but subsequent beamforming shows the source of that line to be at an angle to the array which is inconsistent with the towing ship's heading and the control-source ship's location. However, data from day 251 (5 days earlier) show a 56.8-Hz source at an angle to the array only 6° different from what would be consistent with towing heading and control-source location at that time. Also on day 251, a second source ship was identified by independent means as it transited the exercise area; that source shows up clearly as a sharp spectral line and beamforms at the expected angle. This evidence for day 251 indicates that the Fourier transforming and

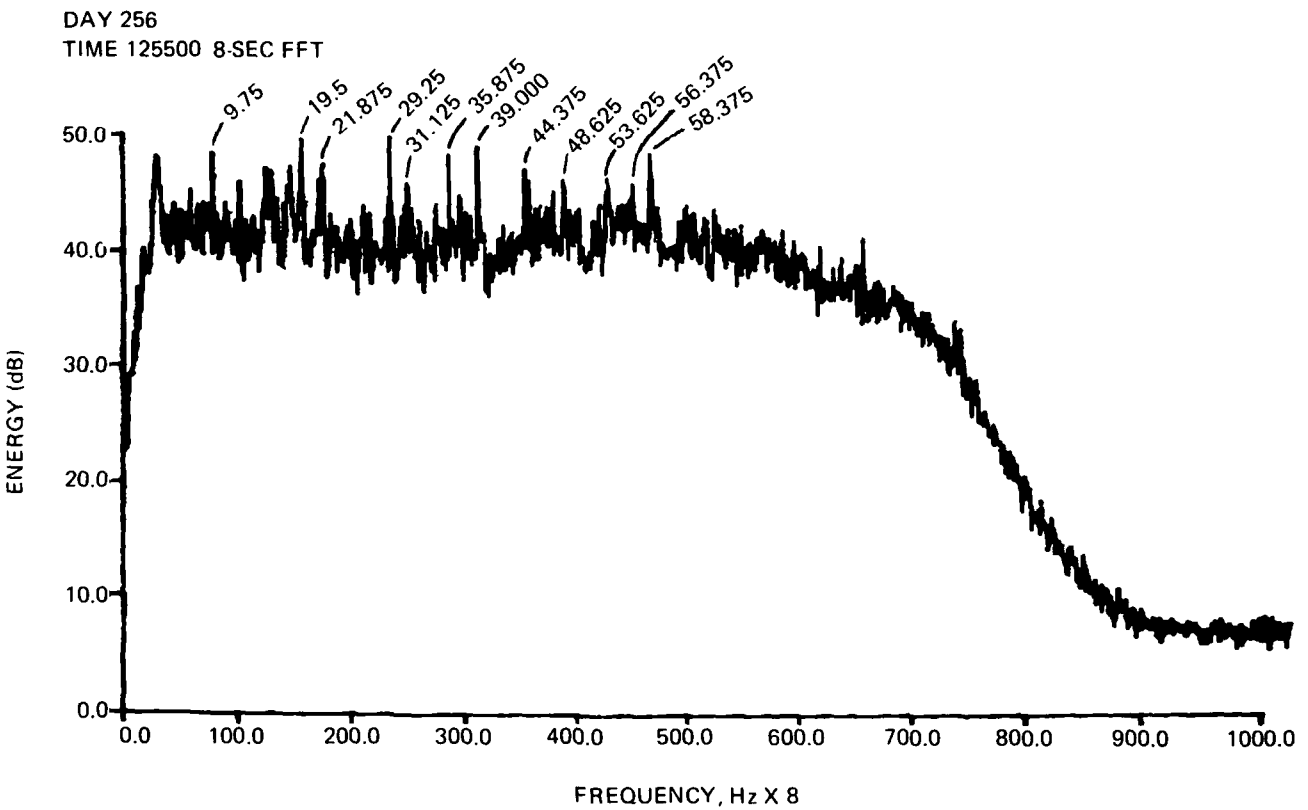

Figure 1a. Typical spectra before a turn.

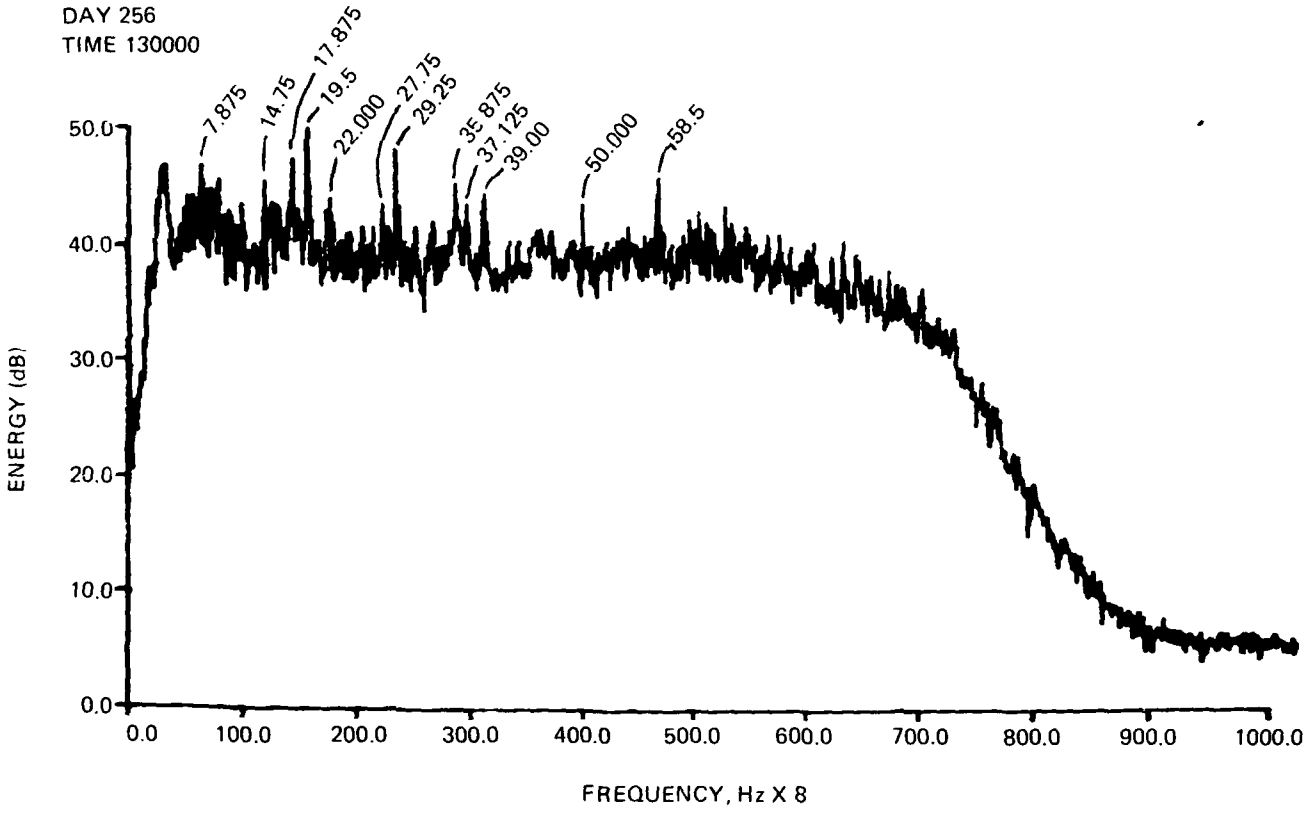

Figure 1b. Typical spectra before a turn.

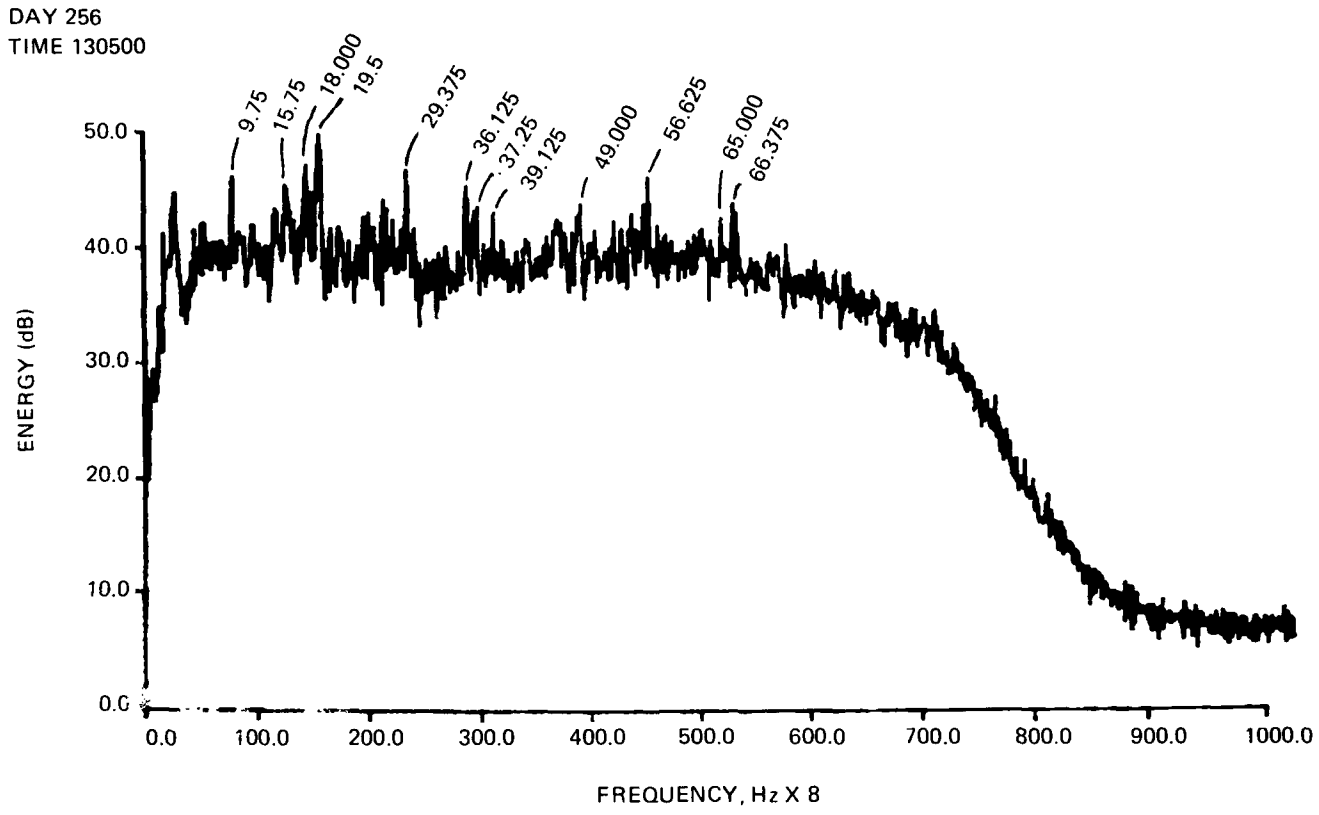

Figure 1c. Typical spectra before a turn.

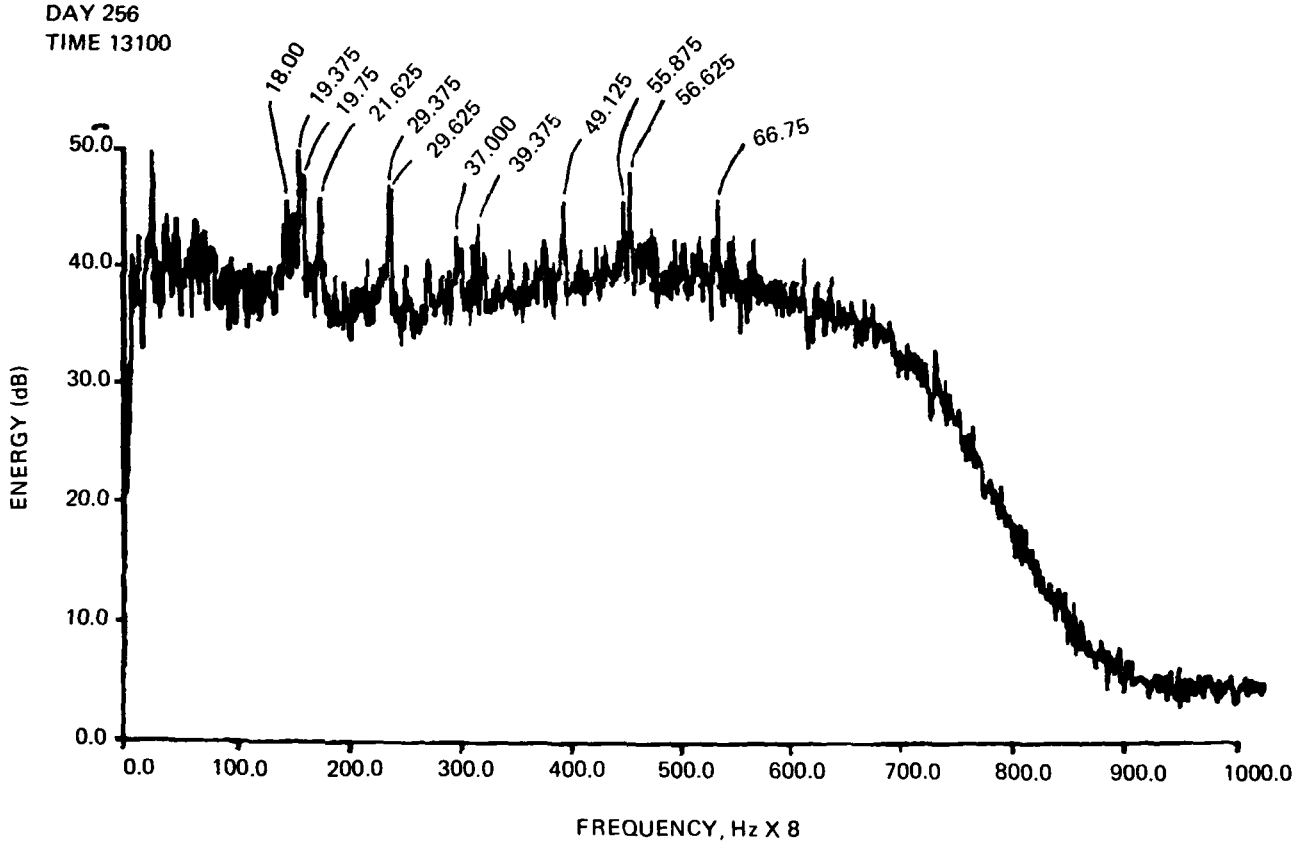

Figure 1d. Typical spectra before a turn.

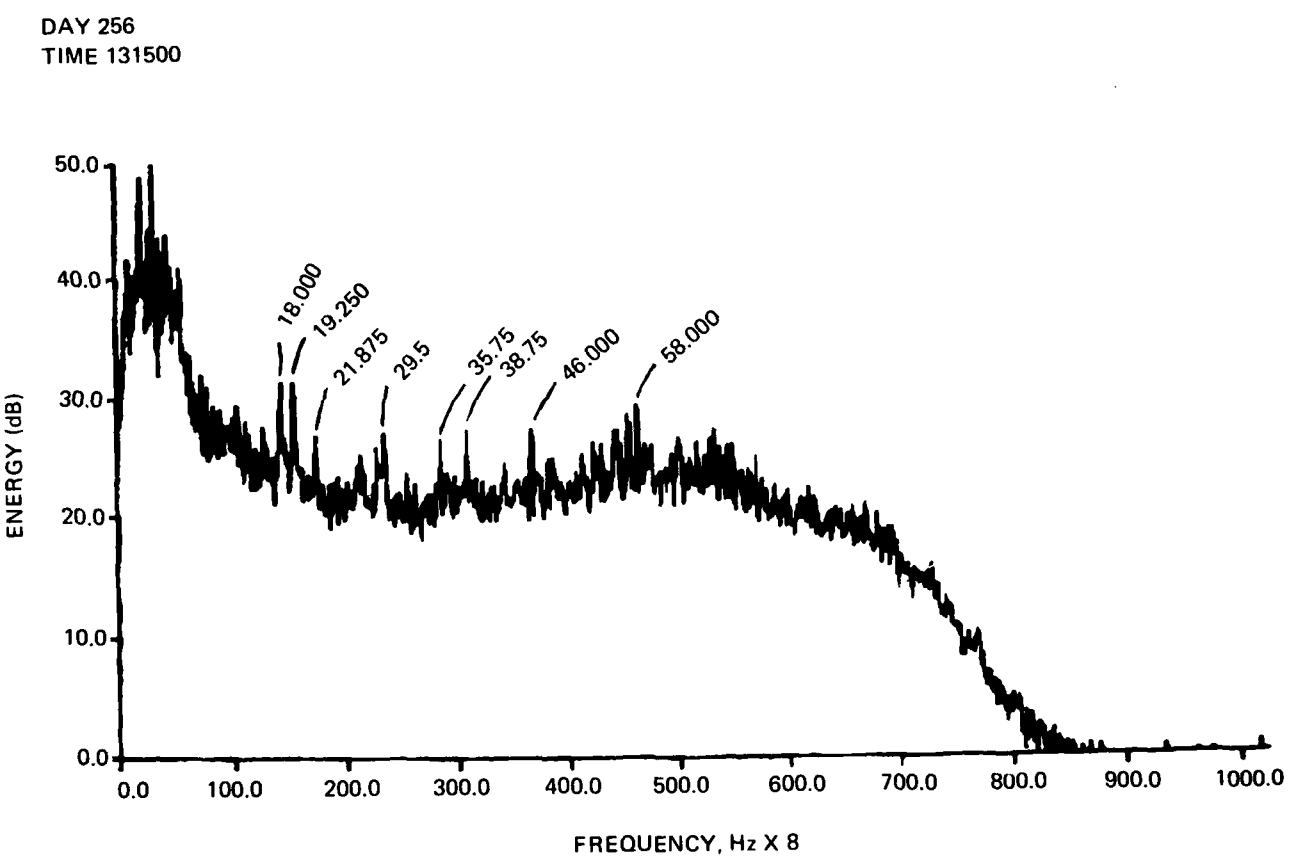

Figure 1e. Typical spectra before a turn.

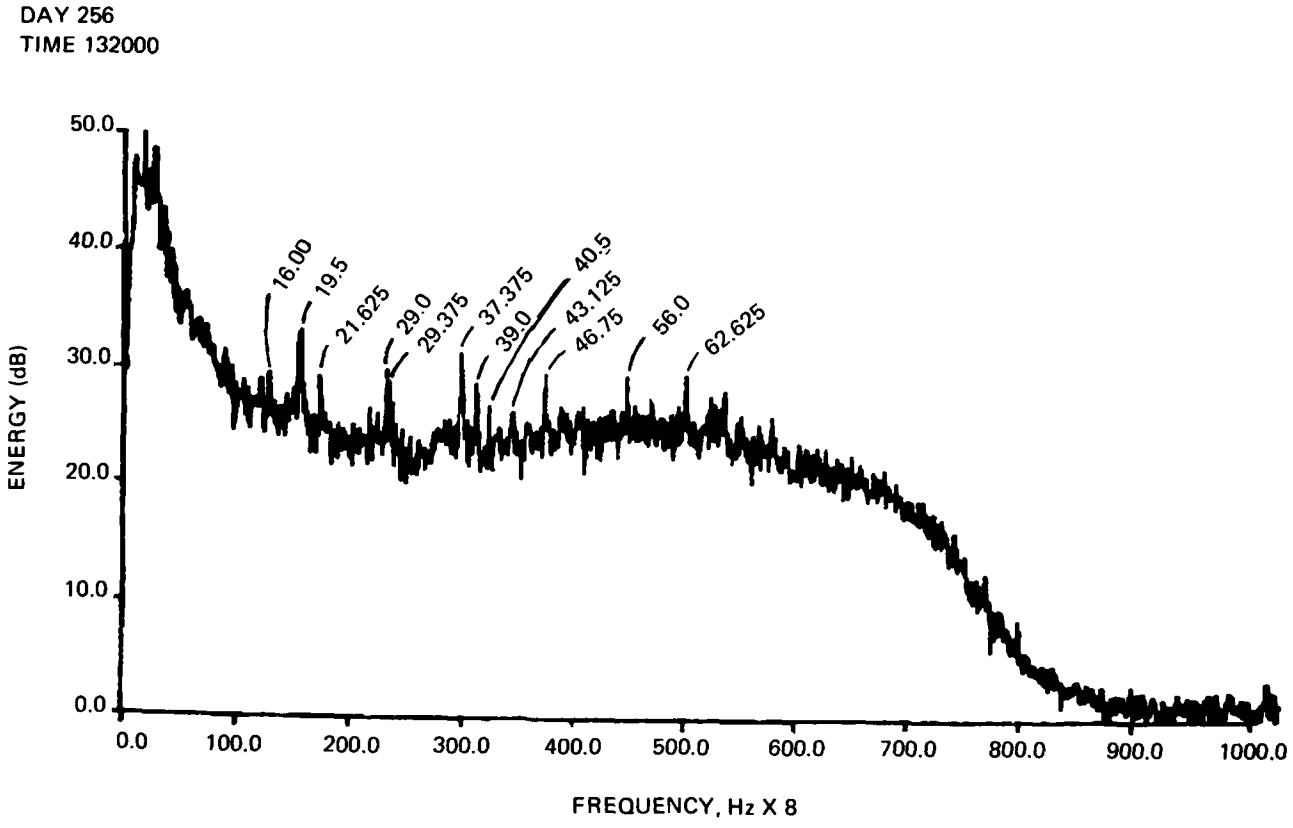

Figure 1f. Typical spectra before a turn.

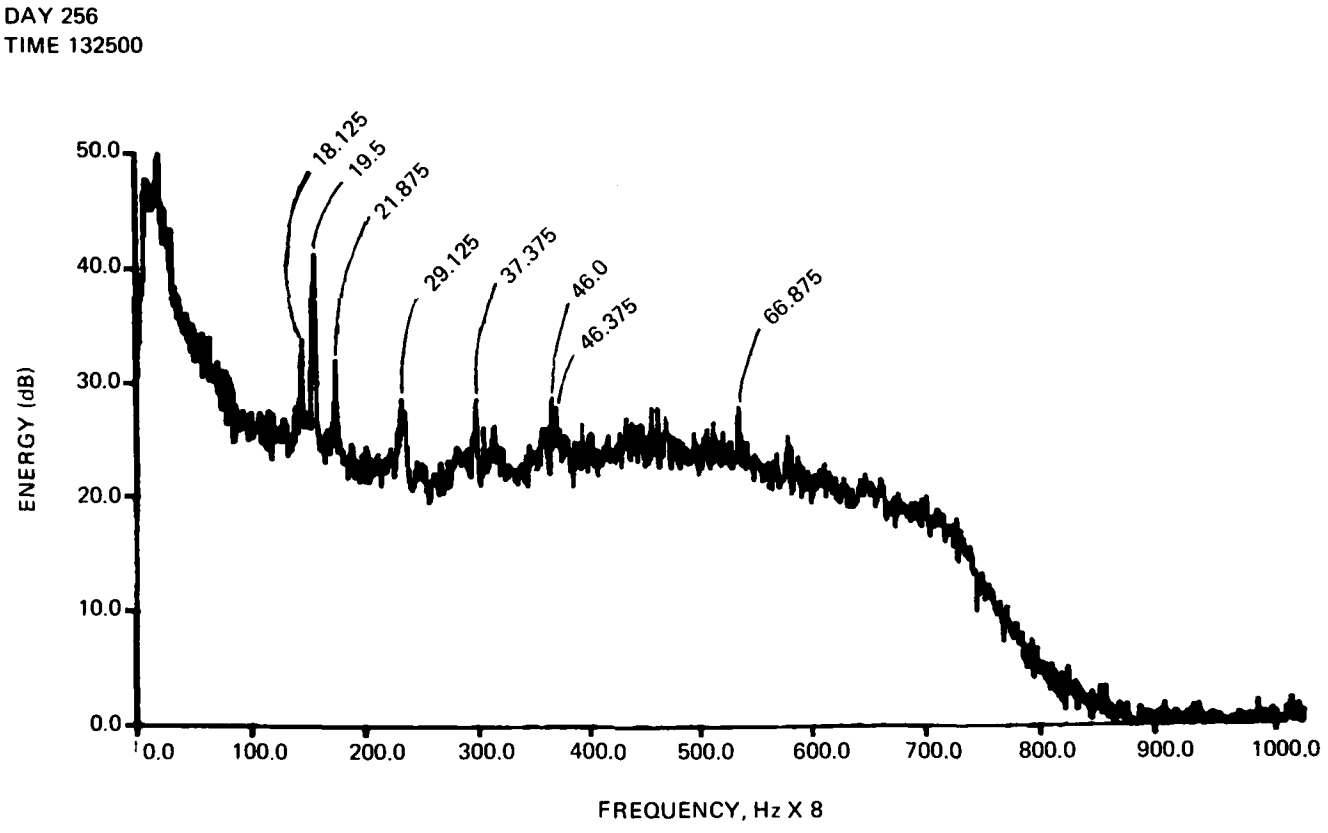

Figure 1g. Typical spectra before a turn.

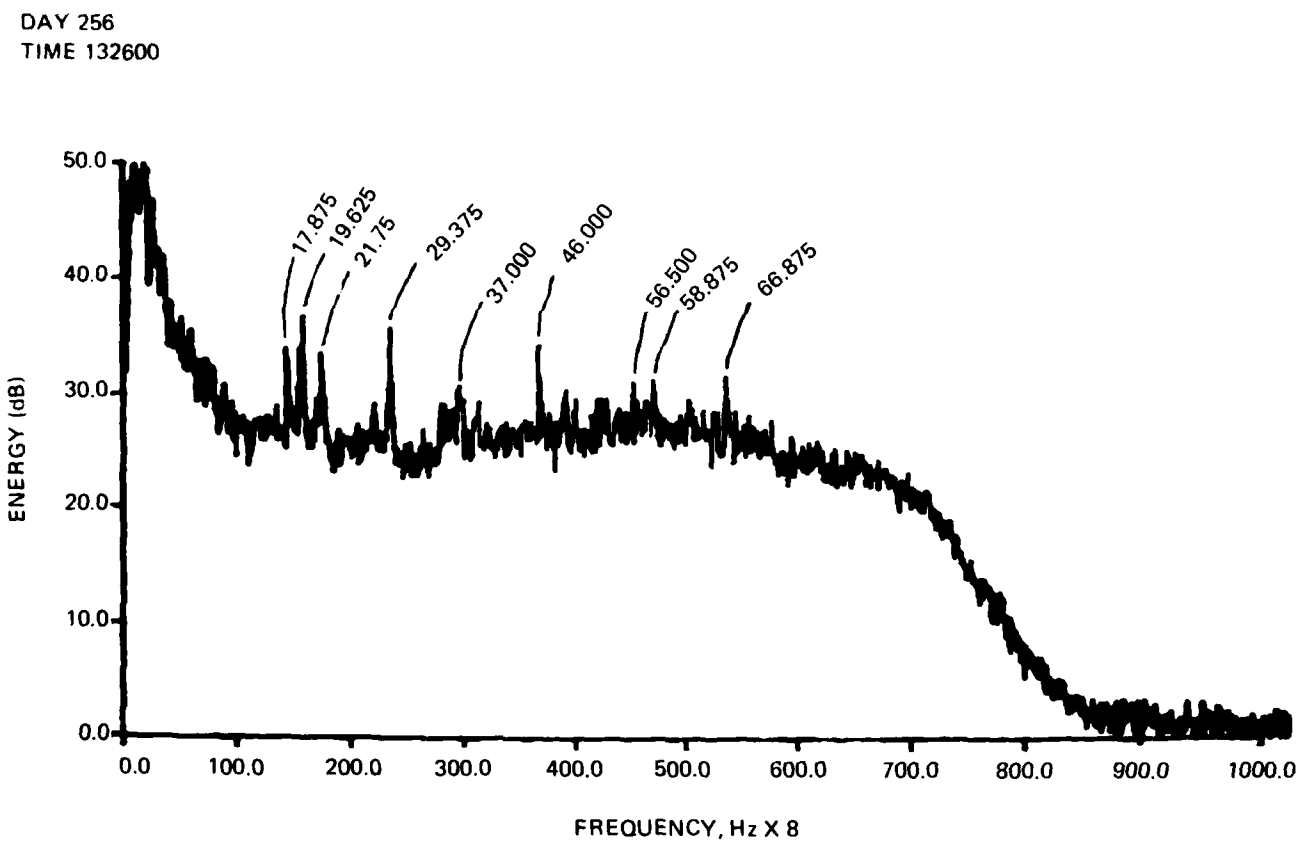

Figure 1h. Typical spectra before a turn.

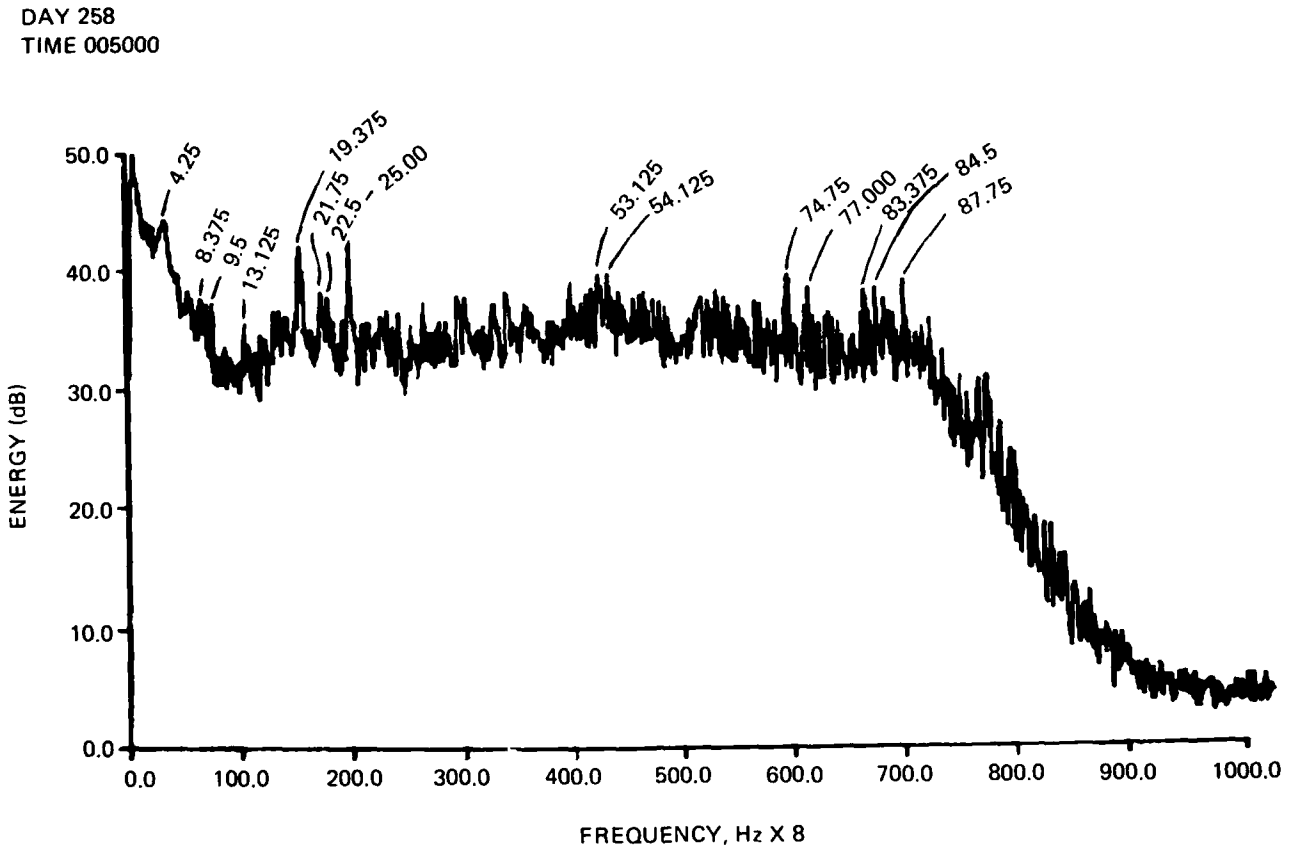

Figure 1i. Typical spectra from a straight line array.

beamforming algorithms used for the self-cohering experiment are correct (ie, free of such mistakes as end-for-end swapping of the array numbering system), and that the failure of the control-source lines to show up on day 256 is probably due to the control-source ship having drifted out of a convergence zone.

An ideal source for self-cohering would be one which shows up as a strong line at a constant frequency throughout all the plots in Fig. 1; the angle to such a source could be tracked as a function of time so as to verify that the array was indeed turning in the correct direction. Unfortunately, there is no such source. Frequency lines appear and disappear, drift back and forth in frequency, sometimes appear to split into two frequencies, and occasionally jump to different beam angles. Not being able to correlate any of these data against known target locations detracts from the credibility of self-cohering, since it is possible that a "signal" which appears out of what was pure noise prior to self-cohering may be an artifact of the algorithm.

METHODS OF SELF-COHERING

Four different self-cohering algorithms were tested. All four assume that the line array is flexible but not stretchable, and that the line array is piecewise linear (ie, that the straight-line distance from any element to either of its neighboring elements is fixed at 125 ft). All four are designed to work on results from the Fourier transform of a single 8-s block of data. Some thoughts on how to incorporate incoherent averaging over successive time blocks are included later in this report.

LEAST-SQUARES FITTING

Reference 1 describes in detail the self-cohering method of least-squares fitting to a parameterized array shape. The essence of the method is this: A single parameter is chosen to represent how far along the array's length each element is located. The x- and y-coordinates of each element are modeled by power series in that parameter, and the z-coordinate of each element is then fixed by the non-stretch requirement. Data from several different frequencies are fed to the algorithm, and the algorithm is told that the data from each frequency represent a plane wave (or a spherical wave, or a cylindrical wave, etc.) from a source at a specified angle to the array. The algorithm is also told an "initial guess" for the array shape. The algorithm calculates what the phases of signals coming from those sources ought to be at each element (assuming the elements are located at the positions stated by the initial guess), and then calculates an error function given by the sum of the squares of the differences between the actual phases of the data and the calculated phases based upon assumed element positions. (The sum is taken over all data points; there is one data point per array element per frequency.) An iterative technique seeks to minimize this error function by changing the values of the coefficients of the power series. Once a minimum is found, the "self-cohered" array shape is found by plugging the final coefficient values into the power series and evaluating x, y, and z for each element. This new array shape is then used to beamform on targets other than those used to perform the self-cohering.

The process of minimizing the error function for this least-squares method is mathematically complicated. First derivatives of the error function relative to each power series coefficient are set to zero; this gives a set of n equations in n unknowns (coefficients). Unfortunately, the equations are nonlinear and cannot be solved exactly in closed form;

so the second derivatives of the error function are used as linear approximations valid for a small region around the true error function minimum. The matrix of equations is inverted by diagonalizing (using an eigenvector transformation), inverting, and re-transforming to get a trial solution.

No example of successful self-cohering by means of the least-squares fitting method has yet been found. It is uncertain whether the problem is in the concept or the implementation. The method is so complex and abstract that it is virtually impossible to trace it through step by step to see where it goes wrong. In nearly every attempt to use this method, the algorithm produces a "final" array shape nearly identical to the "initial guess" array shape and indicates little, if any, improvement in any of the beam patterns.

There are three possible explanations for the difficulty experienced with the least-squares fitting method. First, the error function may be ill behaved with respect to the coefficients (ie, the error surface may have saddles, peaks, and valleys, causing the algorithm to get trapped in a relative minimum instead of at the absolute minimum). Second, the model for x- and y-coordinates (each a power series in the parameter representing fractional distance along the array length) may be inappropriate to shapes the array is likely to assume (eg, it can easily be shown that even a simple parabolic shape cannot be exactly matched by such a model). Third, the method tries to average over several targets at different arrival angles; the true arrival angles are unknown, and the input estimates of the angles may be so inaccurate that array shape changes which appear to improve one target may cancel array shape changes which appear to improve a second target. These possibilities have not yet been thoroughly investigated.

MAXIMIZING SHARPNESS

Reference 2 describes in detail the self-cohering method of maximizing the sharpness of the beam pattern. The essence of the method is this: The array shape is modeled by a Fourier series whose coefficients are the variables for the algorithm. For any set of coefficients, the x- and y-coordinates of element locations are found by integrating for the appropriate lengths along the array shape's arc. A beam pattern is calculated using data from a single frequency and an assumed "initial guess" for the array shape. The square of the intensity in the beam pattern is integrated over all steering angles in the beam pattern to get a sharpness value. An iterative technique seeks to maximize this sharpness value by changing the coefficients of the Fourier series. Once a maximum is found, the "self-cohered" array shape is found by plugging the final coefficient values into the Fourier series and evaluating x and y for each element. (The array is assumed two-dimensional; no attempt is made to calculate z.) This new array shape is then used to beamform on targets other than the one used to perform the self-cohering.

The process of maximizing the sharpness value for this self-cohering method is mathematically simple: change one of the coefficients, and recalculate sharpness. If sharpness is bigger than before, keep the change. If sharpness is less than before, return the coefficient to its original value and try changing the next coefficient. Loop through all the coefficients until sharpness no longer increases. The convergence characteristics of this simple iteration are improved by increasing the rate of change of a coefficient whenever sharpness increases, and vice versa (so that convergence is rapid when far from the solution and slows down at the end to "zero-in" on the solution).

[2]H. Bucker, "Beamforming a Towed Line Array of Unknown Shape," J. Acoust. Soc. Am., 63 (5), May 1978, 1451-1454.

It is not completely clear why maximizing sharpness should necessarily produce the correct array shape. The technique was originally proposed for an optical implementation to compensate telescope images for aberrations due to atmospheric inhomogeneities. In that context, it was shown that the maximum-sharpness criterion produces the correct solution regardless of the image being corrected, but the proof is incomprehensible. Later work takes issue with that proof by showing that the maximum-sharpness criterion cannot produce the correct solution, although in a statistical sense over the ensemble of all possible images it should come pretty close (Ref. 3).

An intuitive feel for why maximizing sharpness should tend toward the correct solution can be obtained from the following simple argument. If the intensity of the beam pattern were integrated over all arrival angles, the result would be simply equal to the total energy incident on the array, and would, therefore, be independent of array shape. However, if the intensity is squared before integrating, then array shapes are favored which tend to concentrate beamformed energy into narrow-angle, high-intensity spikes instead of broad-angle, low-intensity background (a rectangle 1 unit wide and 1 unit tall has the same area as a rectangle 1/2 unit wide and 2 units tall; but if the height is squared first, the tall and narrow rectangle has greater sharpness). Most acoustic energy of interest comes from "point source" targets, just the type of beam pattern favored by the sharpness criterion.

Regardless of whether the sharpness criterion produces the correct solution in the optics case, it is evident that it does not always produce the correct solution in the acoustics case. The maximum-sharpness self-cohering method has been tested in certain simulated cases (where the "true" array shape and "perfect" beam pattern are known initially, and the test of the self-cohering algorithm is to see if it can reveal the true array shape starting with a wrong initial guess), and has been found to produce "wrong" array shapes for which beam pattern sharpness was greater than for the "perfect" beam pattern! The problem appears to be related to aperture sampling. An optical aperture is infinitely sampled, so its "beam pattern" (optical transfer function) differs from a perfect delta function only because of imperfect knowledge of arriving wavefront shape (atmospheric aberrations). On the other hand, the acoustical array is very sparsely sampled (in fact, the array is undersampled for all frequencies above 20 Hz), so much of the detail (sidelobes) of the beam pattern is due to sampling statistics and has nothing to do with phase errors caused by imperfect knowledge of the array shape. Hence, when the sharpness criterion is applied in the acoustic case, the algorithm is apt to find an array shape unrelated to the true shape, which nevertheless improves the beam pattern sharpness by changing the array sampling statistics to lower the beam pattern sidelobes.

In spite of this possibility of converging on the wrong answer, Ref. 2 indicated success in using the maximum-sharpness self-cohering method to improve the beam pattern for an actual acoustic array. Reference 2 had no way of checking whether or not the self-cohered array shape was the "correct" shape, and did not attempt to use the self-cohered shape to improve the beam patterns of any frequencies other than the cohering frequency.

For this report, the maximum-sharpness criterion in its pure form was not much used because of excessive computer time demands. Each time a coefficient in the Fourier series is changed, the x-y coordinates of all the array elements change, so that the number of calculations in the beam pattern is proportional to the product of the number of beams and the number of elements.

[3]T. Brown, "Performance of Image-Plane Sharpness Criteria in Image Reconstruction," J. Opt. Soc. Am., 68 (7), July 1978, 890-892.

A shortcut for the maximum-sharpness technique is to vary the x- and y-coordinates themselves, instead of varying the coefficients of a Fourier series. When only a single x- or y-coordinate is changed, the beam pattern can be recomputed by subtracting the contribution of the new element location, reducing the number of calculations (after initially finding the beam pattern) to be proportional to the number of beams only.

This shortcut form for the maximum-sharpness method is much faster than the pure form, but it suffers from not taking full advantage of the shape characteristics of a towed array. The pure form, with its Fourier series array shape model, has a built-in low-pass spatial filter due to the finite length of the series. The shortcut form has no such filter, and self-cohering by the shortcut tends to respond to noise in the element data by putting too many zigs and zags into the array shape. The shortcut form has produced some dramatic improvements in the beam pattern at the self-cohering frequency, but its ability to produce improvement in beam patterns at other frequencies has not been extensively tested.

MAXIMIZING COHERENCE

The essence of this method is: The array shape is again modeled in two dimensions by a Fourier series whose coefficients are the variables for the algorithm. For any set of coefficients, the y-coordinate of the n^{th} element is found by evaluating the Fourier series in the x-coordinate of the n^{th} element:

$$Y_n = \sum_{m=1}^{7} \left[A_m \sin\left(\frac{m\pi x_n}{L}\right) + A_{m+7} \cos\left(\frac{m\pi x_n}{L}\right) \right] ,$$

where

the A_m's are the coefficients of the Fourier series

L is the array length.

Then the slope of the array shape curve is found at the n^{th} element, and the x-coordinate of the $(n + 1)^{th}$ element is derived from this slope with a linear approximation designed to keep the interelement distance constant at ΔL:

$$\frac{dy}{dx} = \frac{\pi}{L} \sum_{m=1}^{7} \left[mA_m \cos\left(\frac{m\pi x_n}{L}\right) - mA_{m+7} \sin\left(\frac{m\pi x_n}{L}\right) \right]$$

$$x_{n+1} = x_n + \frac{\Delta L}{\sqrt{1 + (dy/dx)^2}} .$$

(The array element locations are found one at a time: y_n is found from x_n, then x_{n+1} is found from dy_n/dx_n, then y_{n+1} is found from x_{n+1}, etc.). Data from one frequency are fed to the algorithm, and the algorithm is told that these data represent a plane wave from a source at a specified steering angle. The algorithm calculates the coherence (as prescribed in the section on "Beamforming") of the data, using the specified steering angle and the calculated element locations. An iterative technique seeks to maximize the coherence by changing the coefficients of the Fourier series. This latter technique is the same as that used in the maximum-sharpness method.

Coherence is really nothing more than the normalized beam pattern for one steering angle. Thus, this method combines the good features from both the pure and shortcut forms of the maximum-sharpness method: the Fourier series array shape model has the appropriate low-pass spatial filter characteristics; but even though all of the element locations change whenever a single Fourier coefficient changes, the recalculation of coherence does not require much computer time because the calculation need be done at only one steering angle.

Simulations indicate that the maximum-coherence method can find the correct array shape even when shape errors (difference between correct shape and "initial guess") are on the order of ± a wavelength at the cohering frequency. For shape errors greater than one wavelength, the iterative algorithm tends to get confused at some false relative maximum (the same trouble as the "saddles, peaks, valleys" problem mentioned in the section on "Least-Squares Fitting"). For frequency domain beamforming with only one cohering source, this is a fundamental problem. If more than one cohering source is available, the array could be "rough-tuned" by first cohering at the lowest frequency (longest wavelength), then "fine-tuned" by using the rough array shape as an initial guess for cohering at the higher frequencies.

One further difficulty with the maximum-coherence method appears to be related to the problem of nonuniform array-element amplitude response. The plots in Fig. 2 demonstrate the severity of the problem. The amplitude of the complex data from each array element acts as a weight in the sums used to calculate coherence, so the maximum-coherence self-cohering method tends to favor high-amplitude elements and to produce array shapes with extra contortions added to fine-tune the high-amplitude elements without regard to the phase errors consequently produced at the low-amplitude elements.

The plots in Fig. 2 show normalized amplitude versus position along the array. The time histories of data from each element are first Fourier transformed, and the plots of Fig. 2 are taken from only those frequency bins which show strong spectral lines in Fig. 1. The element responses are obviously very nonuniform, but the cause has not been investigated. Some possibilities are signal fading, anomalous noise, dead array elements, and multiple interfering sources.

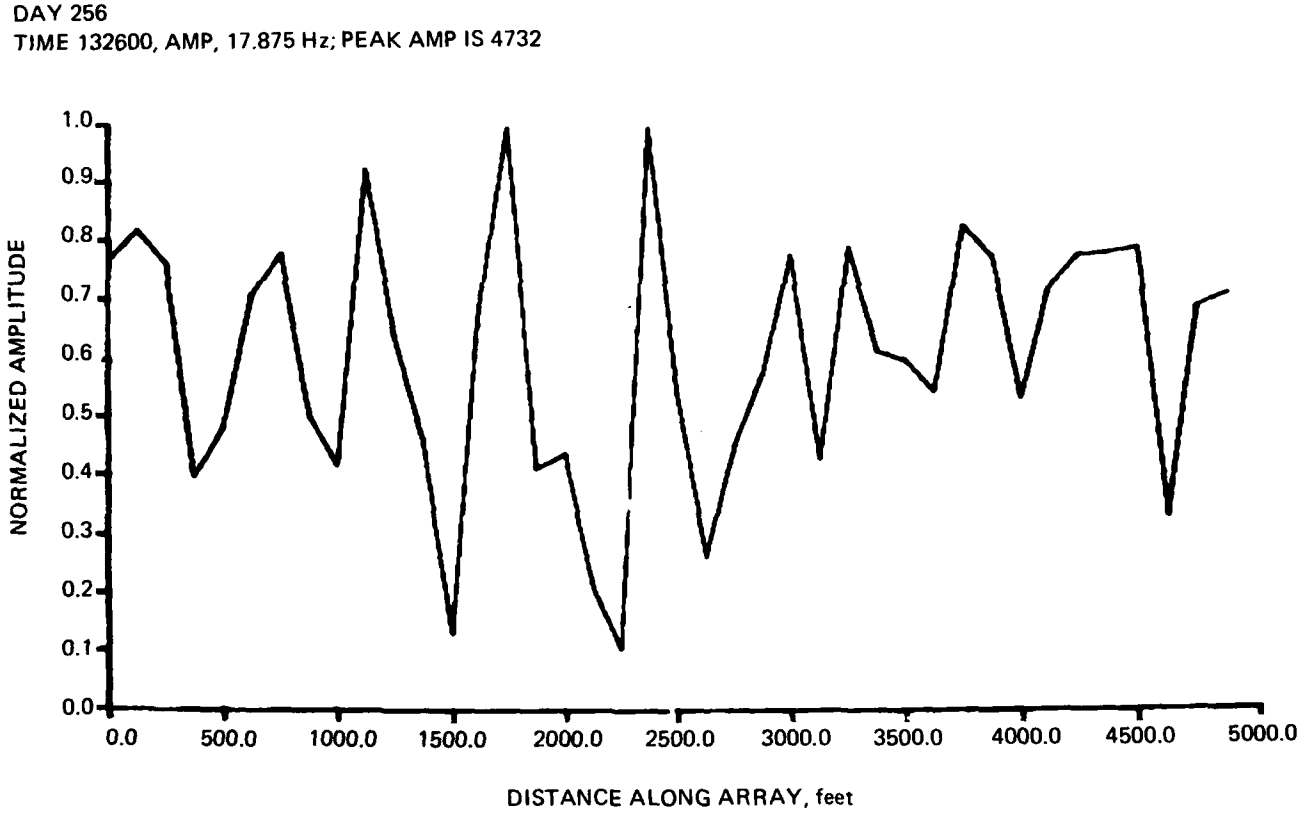

Figure 2a. Typical single-element amplitude response.

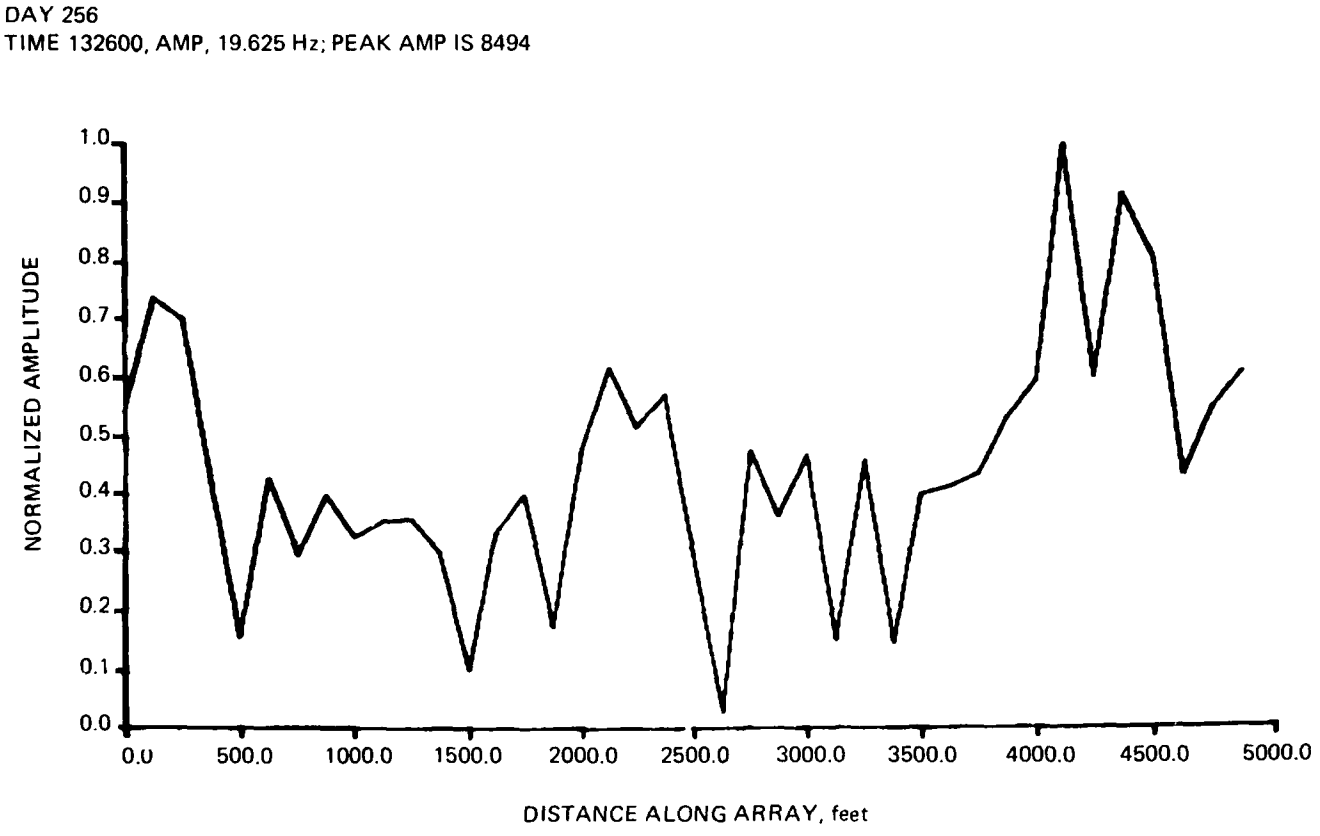

Figure 2b. Typical single-element amplitude response.

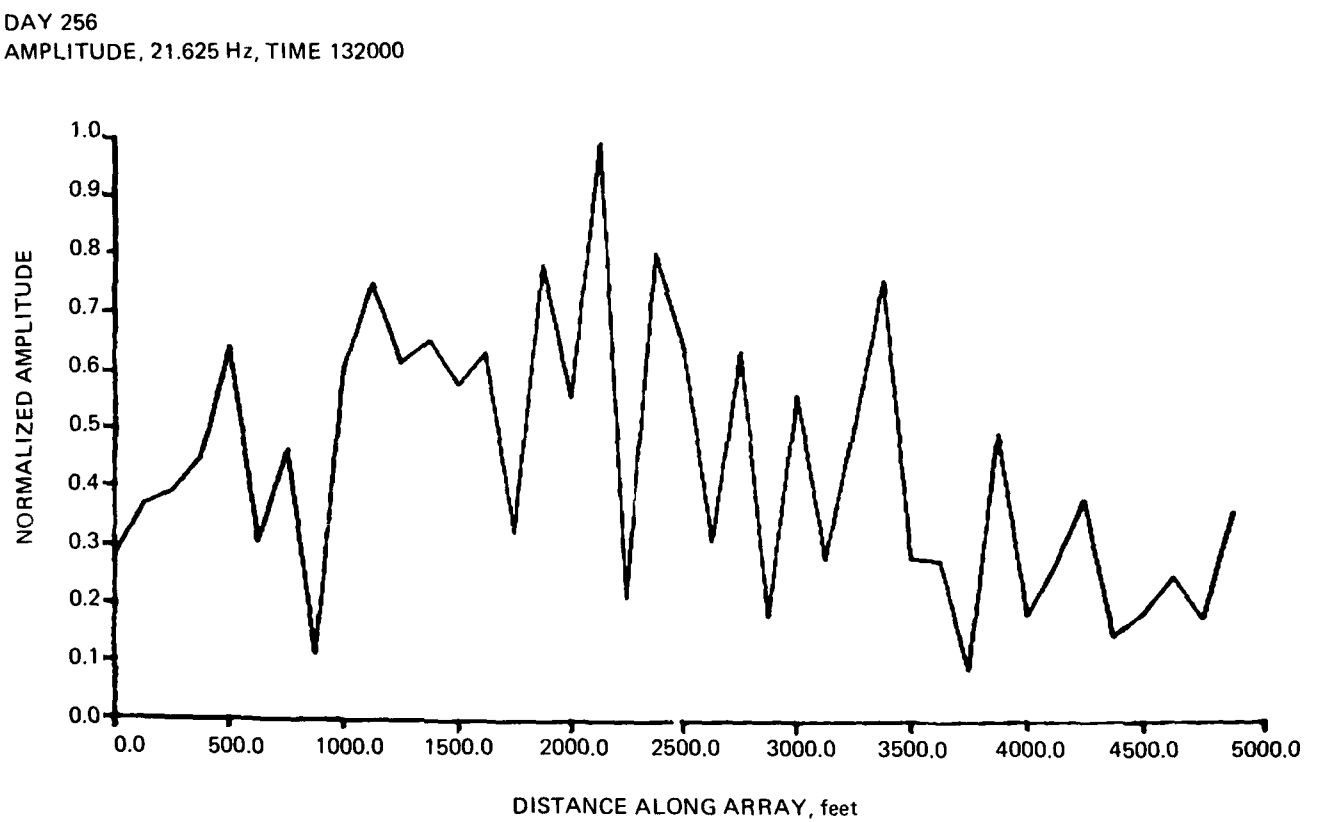

Figure 2c. Typical single-element amplitude response.

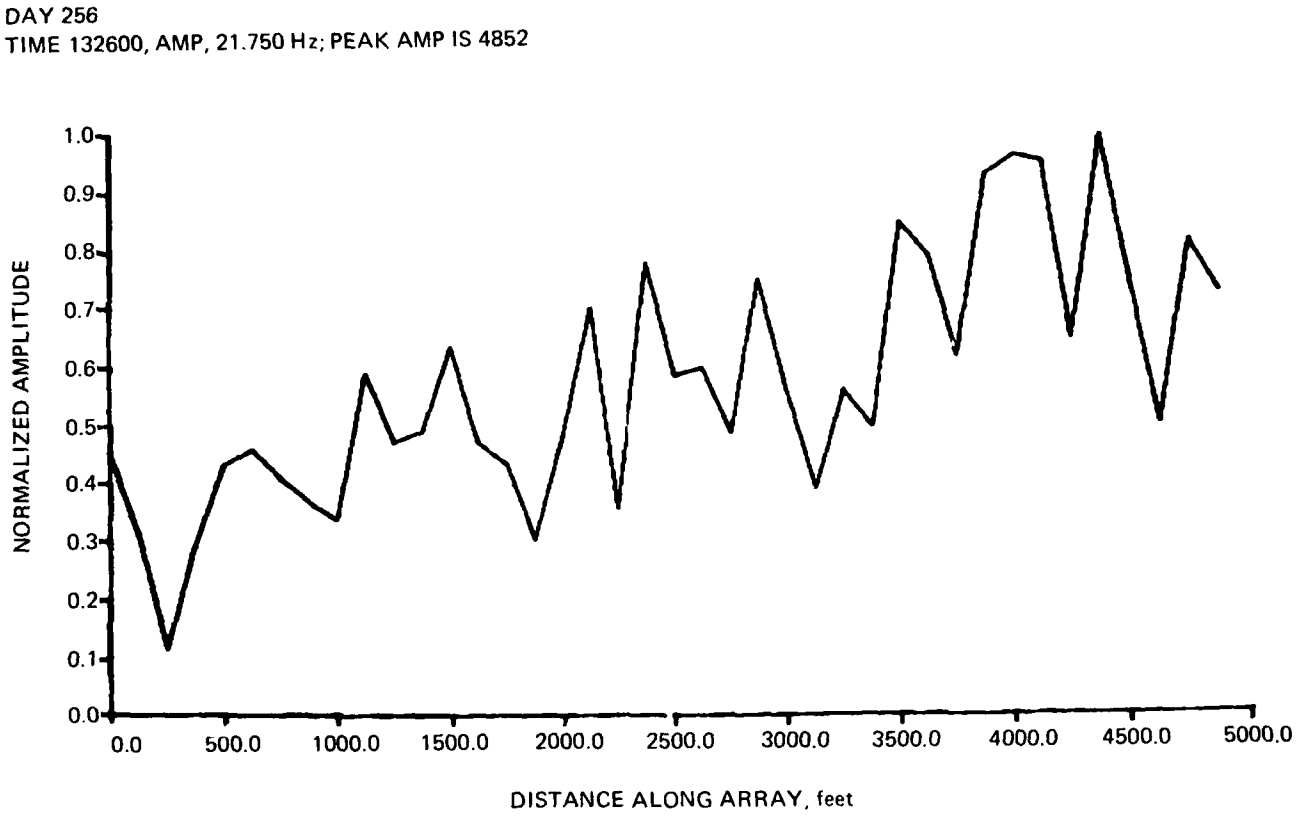

Figure 2d. Typical single-element amplitude response.

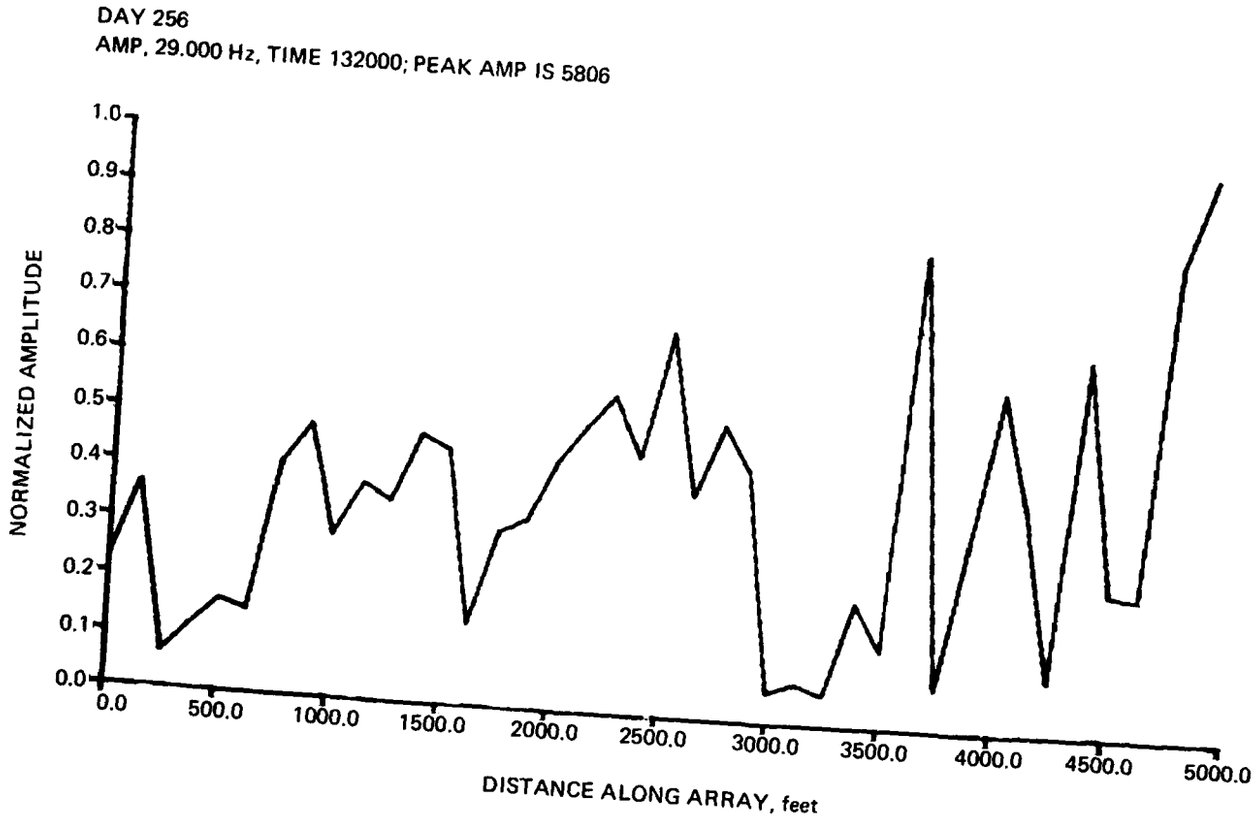

Figure 2e. Typical single-element amplitude response.

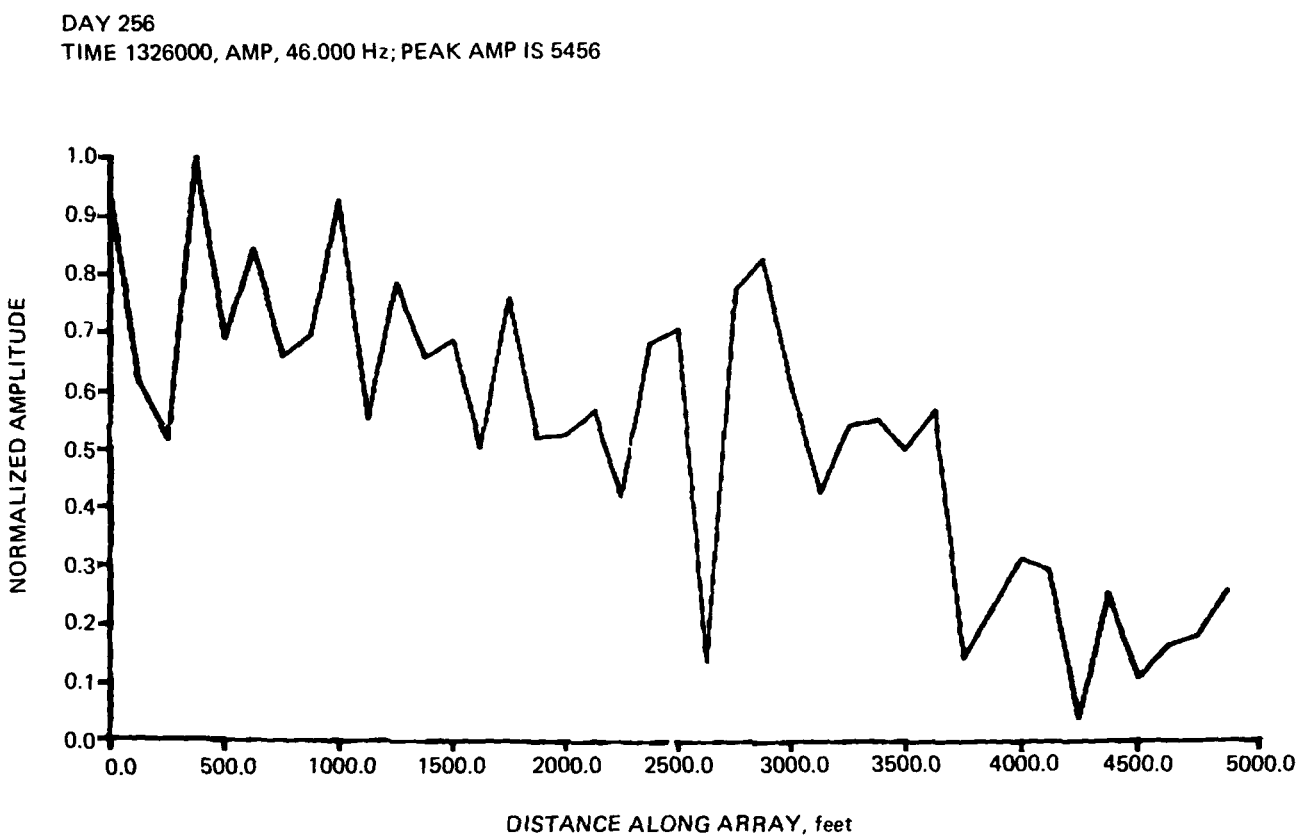

Figure 2f. Typical single-element amplitude response.

COMPENSATING RESIDUAL PHASES

The final self-cohering method involves the low-pass spatial filtering of residual phases and adjusting array element locations to cancel the results for a given steering direction. Once again, the array is assumed to lie in the x-y plane.

The data are first beamformed in the ordinary manner, using the assumption that the array is straight. The beam pattern is scanned to find the steering angle with the greatest coherence. This must be the angle for which the signal phases at the array elements are most nearly perfectly aligned. The phase angle by which each element, when steered in the appropriate direction, fails to align with the general trend of the other elements is called the residual phase. Residual phase is due partly to noise corrupting the signal and partly to errors in the assumed array shape. Noise is uncorrelated between elements and, hence, changes rapidly along the array. Array shapes assumed by a towed array are not likely to zig-zag much from element to element. Therefore, much of the noise can be removed from the residual phases by low-pass spatial filtering.

This filtering is performed simply by averaging together the residual phases from adjacent elements. The number of adjacent elements used determines the "bandwidth" of the filter. Phases themselves, being modulo 2π, are hard to work with because of a discontinuity at $\pm\pi$. So the actual filtering is done using the complex-number representations of rotating phasors (ie, average $e^{j\phi}$, not ϕ).

After filtering, the residual phases are converted to lengths by dividing by the wavenumber (for example, a residual phase of 90° represents a distance of a quarter of a wavelength). The array elements are then located as follows. Element 1 is placed at (0,0). A circle is drawn about the n^{th} element with a radius equal to the fixed interelement distance of 125 ft. Two parallel straight lines are drawn at an angle to the x-axis given by the desired steering direction, as shown below.

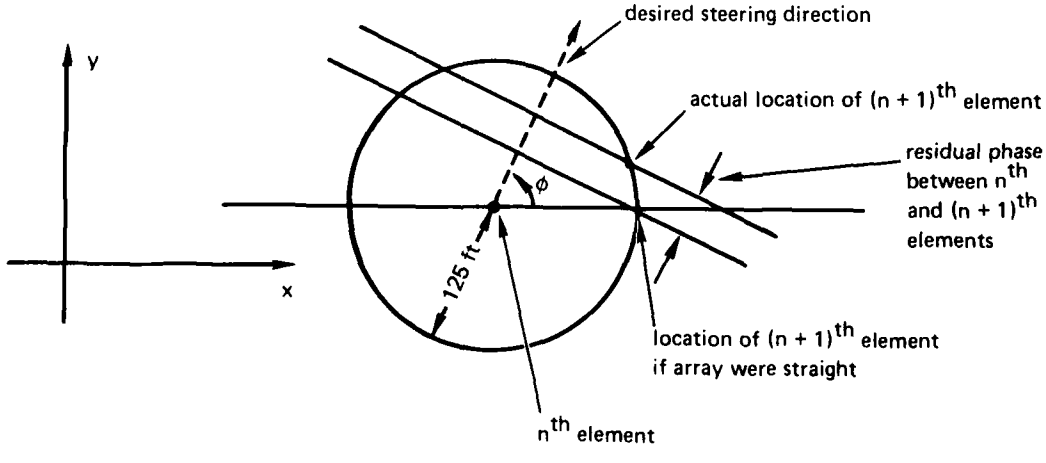

These two lines represent plane wavefronts. The first line represents the phase that the $(n + 1)^{th}$ element would have (relative to the n^{th} element) if the array were straight. The second line represents the actual phase at the $(n + 1)^{th}$ element. The point of intersection of this second line with the circle is taken to be the location of the $(n + 1)^{th}$ element.

(If the line intersects the circle at two points, the point more nearly in the positive x- direction and nearest the x-axis is chosen to prevent the array shape from folding back on itself. If the line does not intersect the circle, because of noise, the point on the circle horizontally from the n^{th} element is chosen for want of a better choice.)

Most of the good self-cohering results presented in this report were obtained using this residual-phase method. The method is so simple and so fast (no iterations required) that it is very easily tailored to meet the idiosyncracies of each particular situation. However, simplicity is also the method's biggest problem: success requires constant attention. The width of the spatial filter seems to require readjustment to meet different noise conditions, and the cohered array shape often has glitches and sudden jumps, apparently due to abnormally large phase errors or modulo-2π problems.

Perhaps the spatial filtering of residual phases would be unnecessary if noise could be reduced to a low enough level by time integration. Incoherent time integration is usually done by computing a covariance matrix. (The mn^{th} entry in the covariance matrix for one frequency is the time average of the product of the spectral component of the m^{th} array element and the complex conjugate of the spectral component of the n^{th} array element. The spectral components are found by a Fourier transform over a block of time, and the time average is taken over successive blocks.) The entries in the covariance matrix actually represent residual phases $\left(e^{j\phi_m} e^{-j\phi_n} = e^{j(\phi_m - \phi_n)}\right)$, so the covariance matrix may be utilized directly in the residual-phase self-cohering method.

RESULTS OF SELF-COHERING ON HIGH-FREQUENCY TARGETS

Figure 3 shows beam pattern plots from time 0050, day 258 of the sea-test exercise. (The energy-vs-frequency plot for this time is Fig. 1i.) According to ship's logs, this time is 20 min after the towing ship began a right-hand turn from heading 270° to heading 004°. The horizontal axis of the Fig. 3 plots is beam steering angle relative to the tail end of the array; 180° points toward the towing ship. The array is 2000 ft deep.

Beam aliasing occurs in an equally spaced line array whenever element spacing is greater than half wavelength. The wavelength at 75 Hz is about 70 ft, considerably less than twice the 125-ft element spacing for this array, so beam aliasing occurs in all the Fig. 3 plots.

Note that the beam patterns in Fig. 3 are <u>not</u> theoretical shapes of sidelobes due to particular array sampling densities, but rather are actual array responses when steered through the true sound field.

Figure 3a shows the beam pattern at 77 Hz (it is assumed that the array is straight). The peak coherence is 0.57. Because of aliasing, this peak occurs at three different angles; and because of right-for-left ambiguity (a straight line is symmetric), each of the three peaks also appears folded about 180°.

The data for 77 Hz were subjected to self-cohering , using the maximum-coherence method with a specified steering angle of 56°. Figure 3b shows the resulting array shape. (The towing ship is at the left, towing in the negative x-direction.) Figure 3c shows the beam pattern recalculated using the new array shape. The coherence has increased to 0.913, the peaks have become sharper, and (because the array is no longer symmetric) the beams folded around 180° have been significantly suppressed.

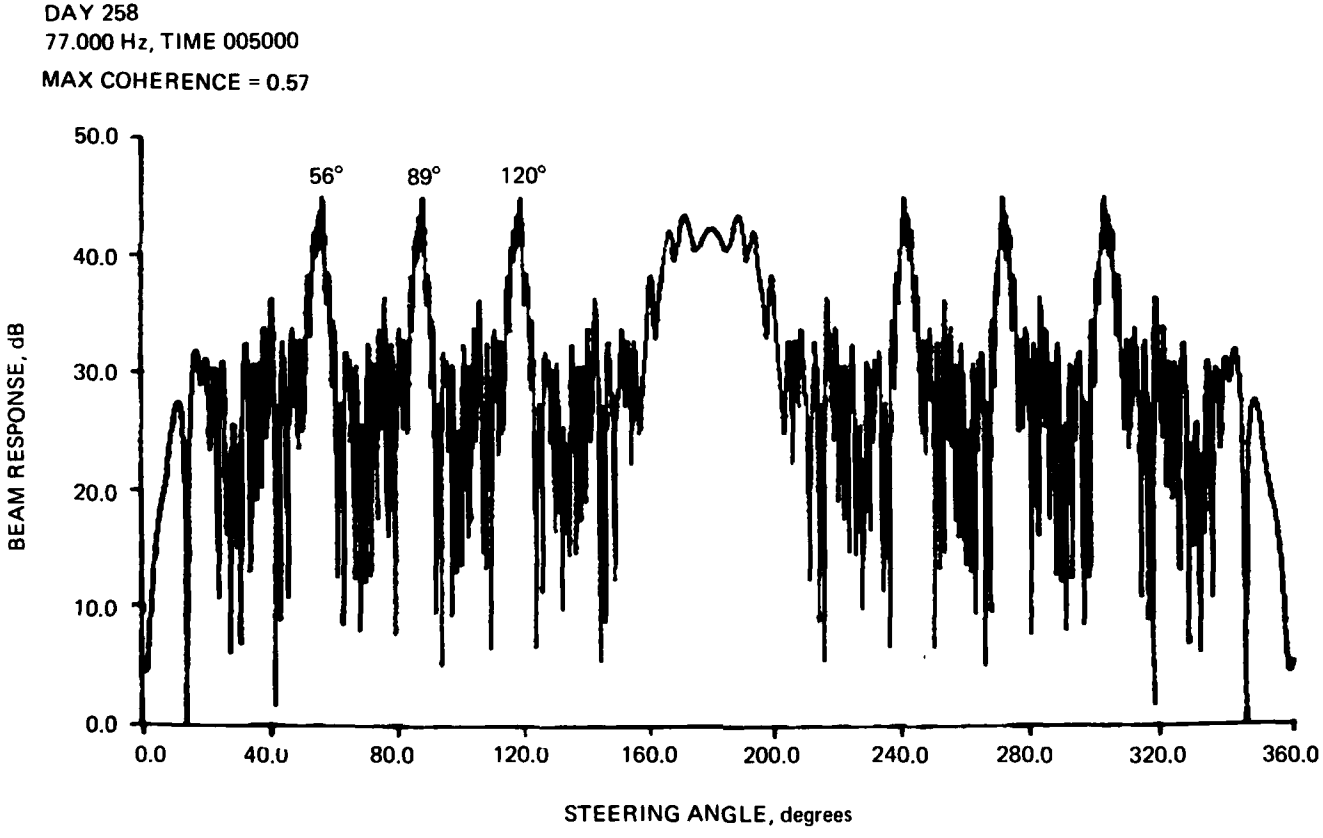

Figure 3a. Beam pattern at 77 Hz (straight array assumed).

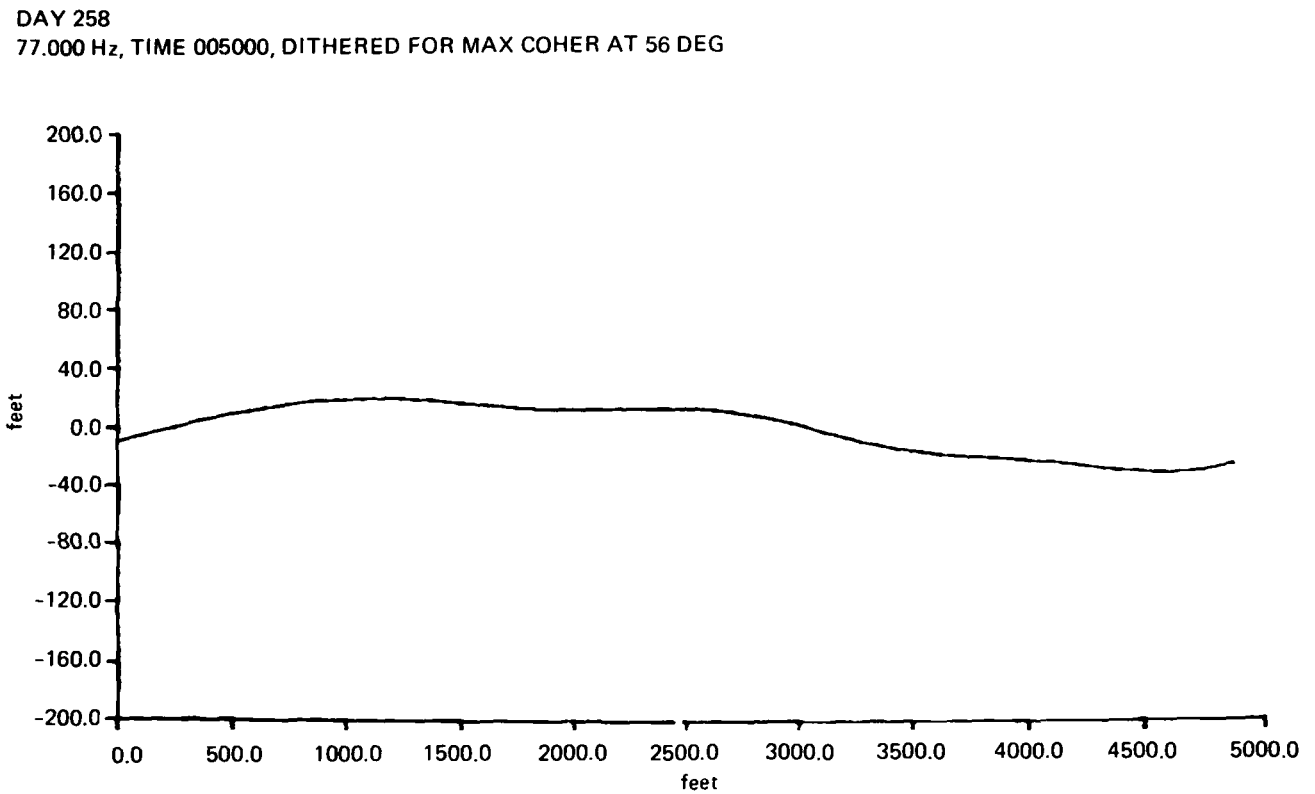

Figure 3b. Array shape after self-cohering.

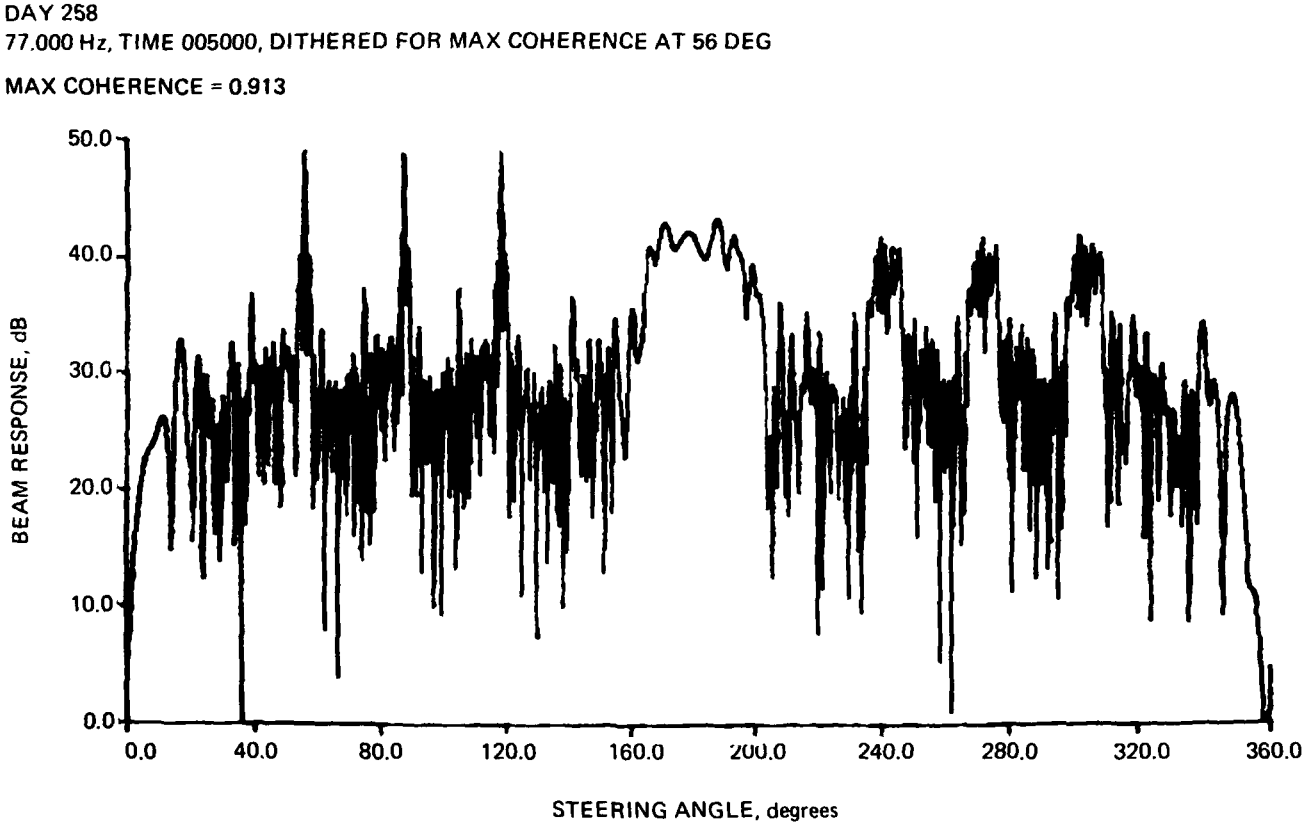

Figure 3c. Beam pattern at 77 Hz after self-cohering.

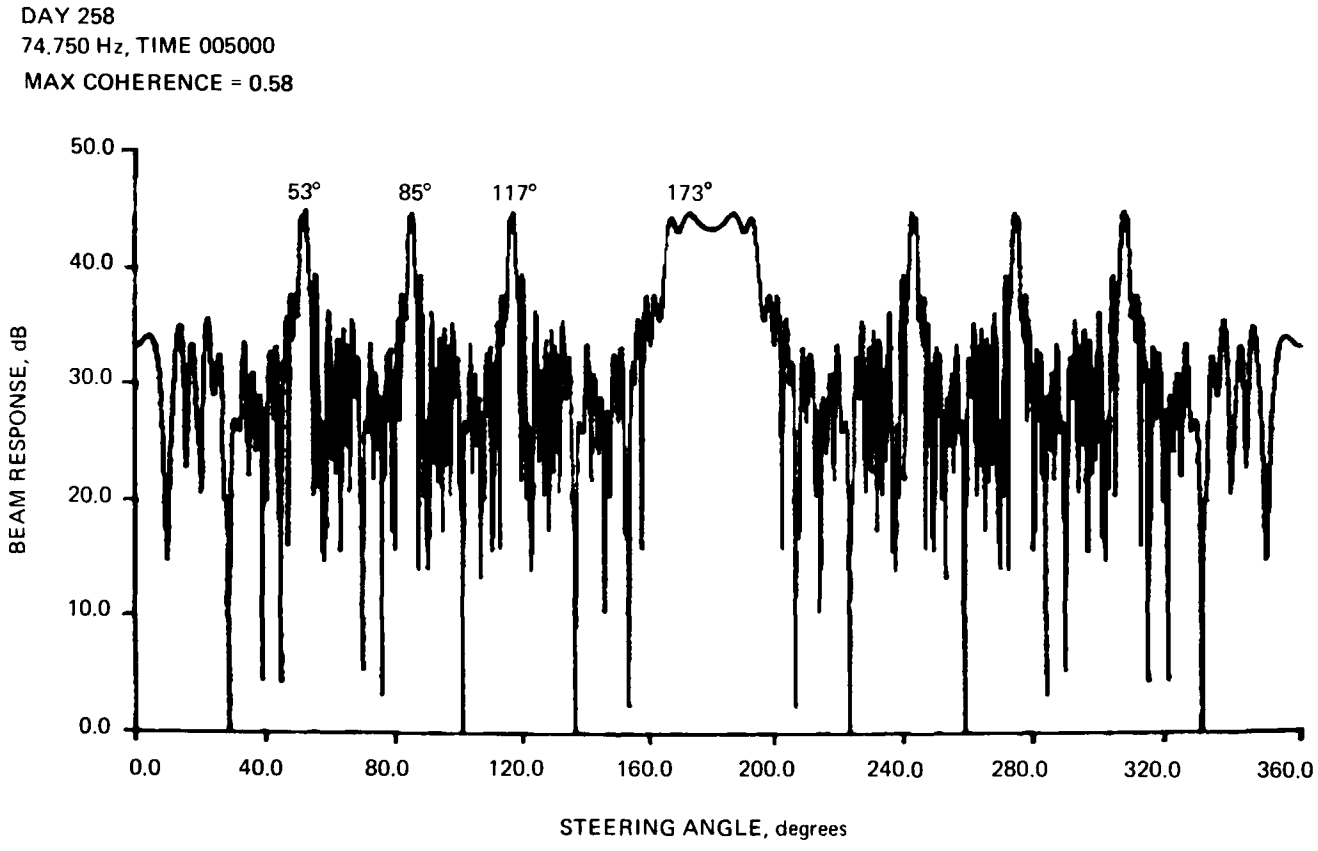

Figure 3d. Beam pattern at 74.75 Hz (straight array assumed).

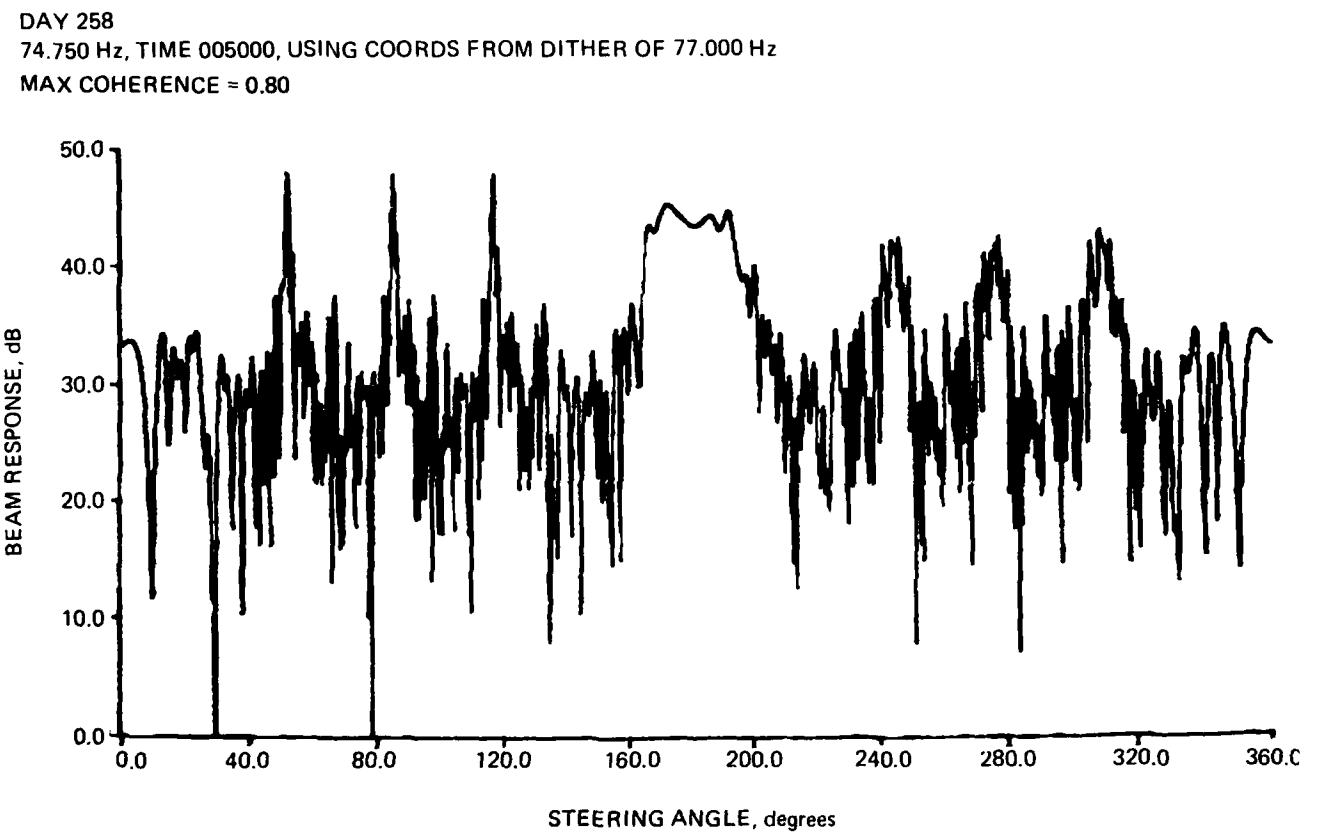

Figure 3e. Beam pattern at 74.75 Hz recomputed using array shape of Fig. 3b.

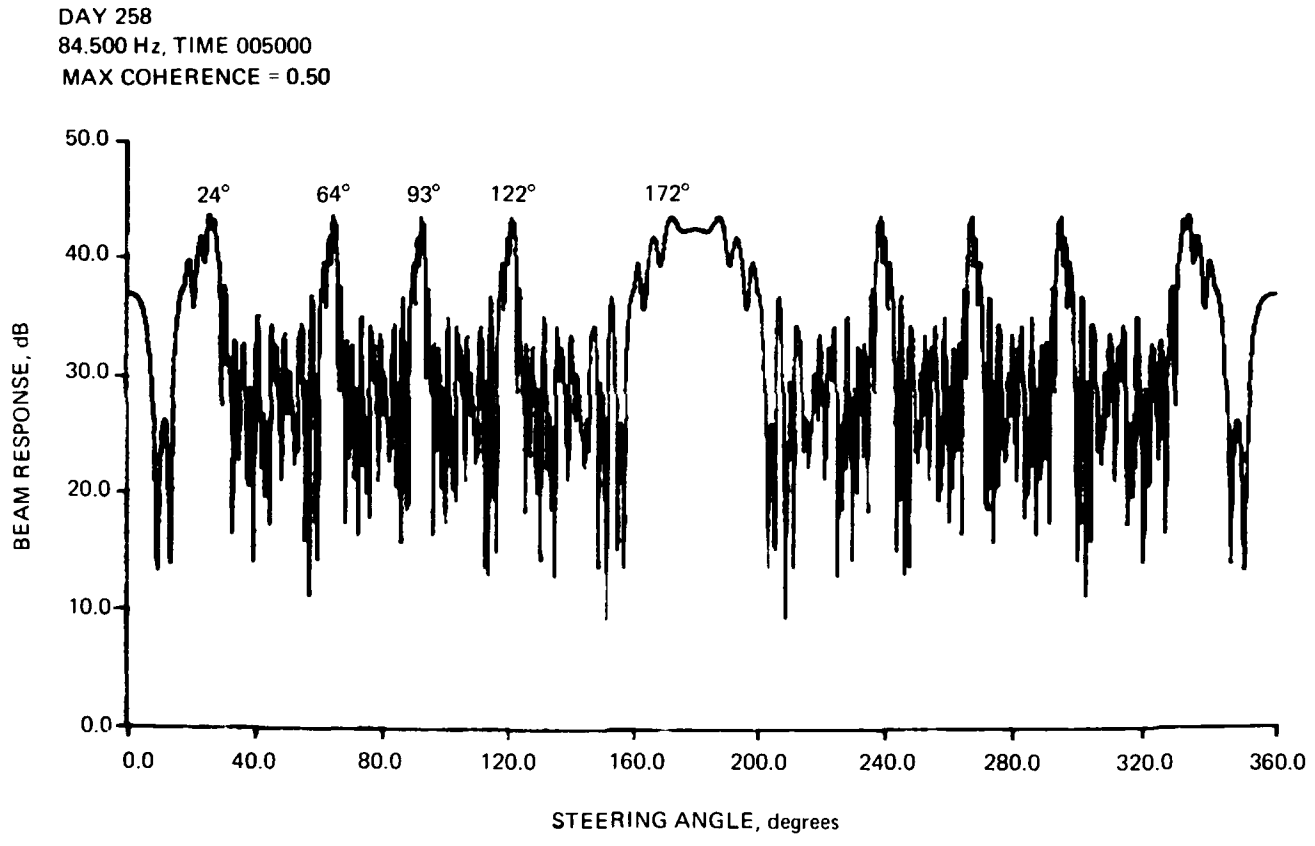

Figure 3f. Beam pattern at 84.5 Hz (straight array assumed).

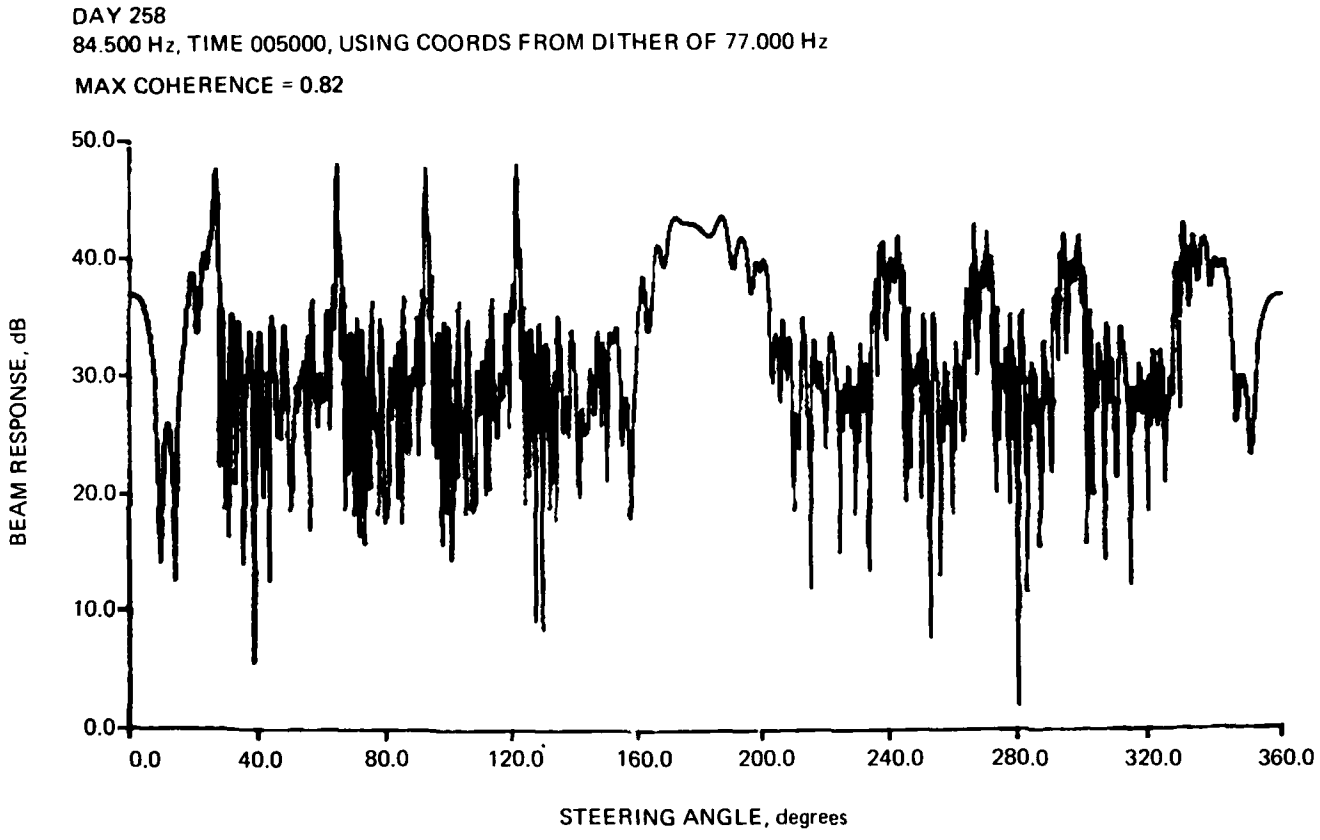

Figure 3g. Beam pattern at 84.5 Hz recomputed using array shape of Fig. 3b.

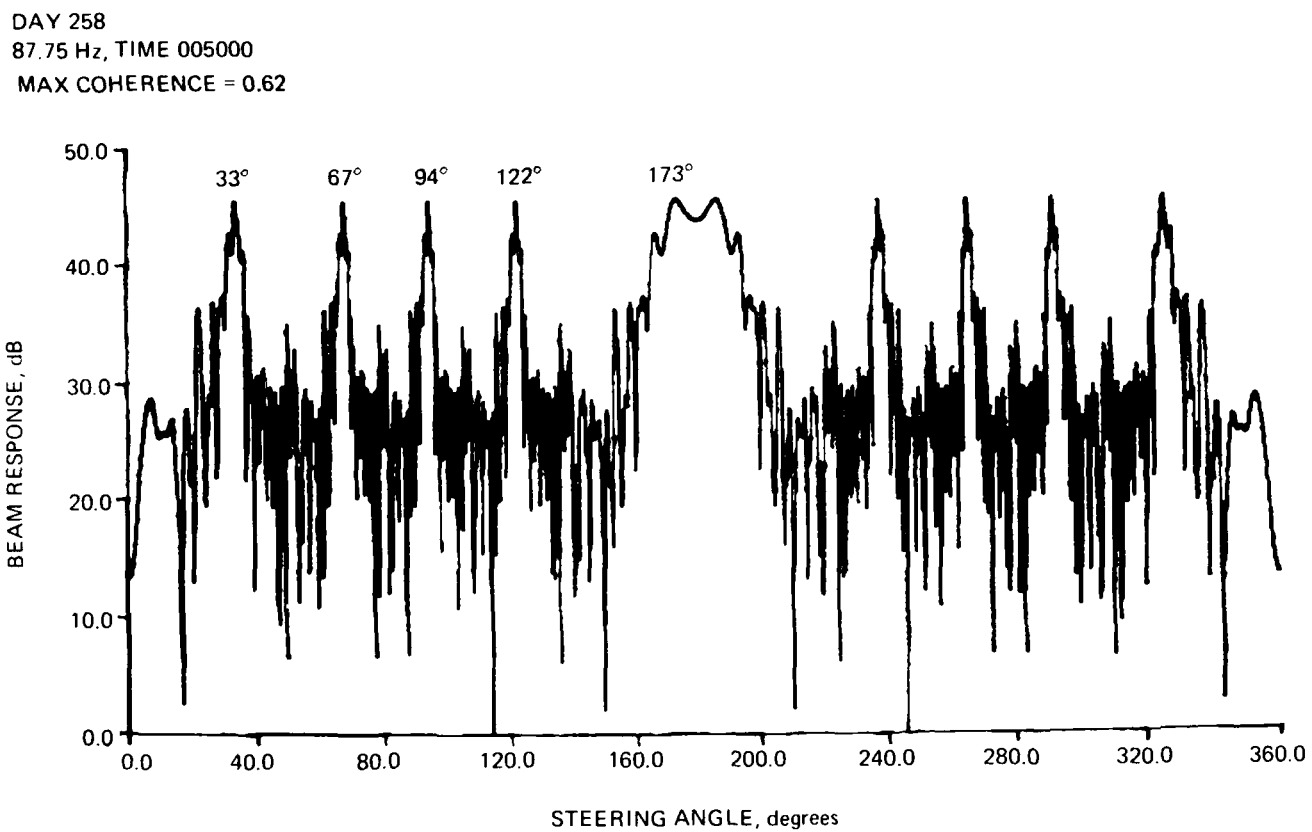

Figure 3h. Beam pattern at 87.75 Hz (straight array assumed).

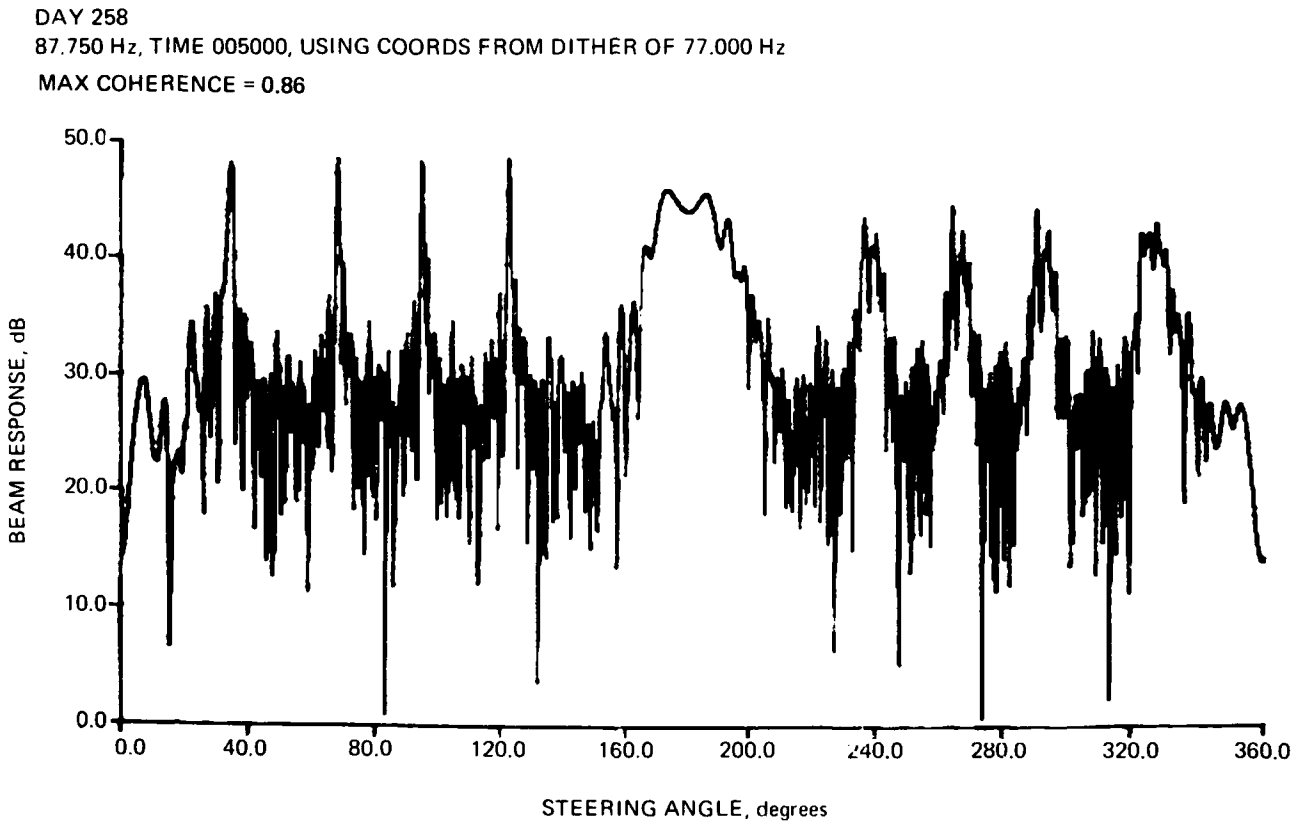

Figure 3i. Beam pattern at 87.75 Hz recomputed using array shape of Fig. 3b.

Figures 3d, 3f, and 3h show beam patterns for three different frequencies at this same time of day. A straight line array is assumed in each case. Figures 3e, 3g, and 3i are recomputed beam patterns using the array shape of Fig. 3b. In all cases, these beam patterns show significant increase in coherence, sharpening of main peaks, and suppression of foldover peaks; this improvement accrues in spite of the fact that the array shape came from cohering a different frequency.

There are problems with these data. Although the beam patterns look much better after self-cohering, there is no guarantee that the improved peaks are the true peaks. Figure 3a has six peaks, of which the one at 56° was arbitrarily chosen for self-cohering. Presumably, any of the remaining five peaks would have worked as well.

Presumably, also, if one of the peaks at an angle greater than 180° had been used for self-cohering, the resulting array shape would have curved the other way. Furthermore, the curve shown in Fig. 3b as being in the x-y plane because of a turn by the towing ship might actually be in the x-z plane because of array sag. The self-cohering algorithm sees only the phases of the signals at the elements, and cannot tell from that information which way the array curves, only that it does curve. This might be a problem with the least-squares fitting method, which tries to include z in its array-shape model, when in fact there may not be enough information to determine z.

In fact, the curve in Fig. 3b may not even represent array curvature at all. Perhaps the source of the signals used in Fig. 3 is the towing ship itself, which is so close to the array that the wavefronts don't look planar. The curve in Fig. 3b may be the self-cohering algorithm's attempt to compensate for near-field wavefront curvature. There is some evidence to support this possibility. Figure 4a shows the straight-array beam pattern of still another spectral line from Fig. 1i. Peak coherence for this frequency is 0.63, which is better than any of the pre-cohering coherences in Fig. 3, in spite of the fact that the Fig. 4 frequency has a shorter wavelength (hence more severe degradation from array curvature) and a poorer signal-to-noise ratio (as seen by the height of the spectral line in Fig. 1i) than most of the Fig. 3 frequencies. When the cohered array shape of Fig. 3b is used on the Fig. 4 frequency (Fig. 4b), there is very little improvement in coherence (from 0.63 to 0.69). Nevertheless, when the Fig. 4 frequency itself is self-cohered, coherence improves to 0.81. Evidently, the Fig. 4 frequency is seeing an apparent array shape that is straighter than the apparent array shape seen by the Fig. 3 frequencies. The only obvious explanation for this is that the Fig. 4 frequency comes from a distant source, and that the array really is as straight as the Fig. 4 frequency thinks it is, that the Fig. 3 frequencies come from a near-field source, and that the shape in Fig. 3b is an artifact of near-field wavefront curvature.

Figure 5 is an attempt to determine whether or not the amount of curvature observed in Fig. 3b could logically be explained by assuming the towing ship to be the signal source. Figure 5 shows a scale drawing of the array at the end of the towing cable at the proper depth. The array is curved so as to produce a constant angle between it and a line drawn from the towing ship, which seems to be a reasonable approximation of what the self-cohering algorithms would attempt to do. The resulting curve deviates from a straight line by about 250 ft, which is considerably more curvature than what is shown in Fig. 3b (which deviates by less than 50 ft). Perhaps there is another ship in the area, a little more distant than the towing ship but still in the near field.

The results of this analysis indicate that self-cohering can significantly improve the array's ability to discriminate targets from noise, even at aliased frequencies, but that target angles and array shapes remain uncertain.

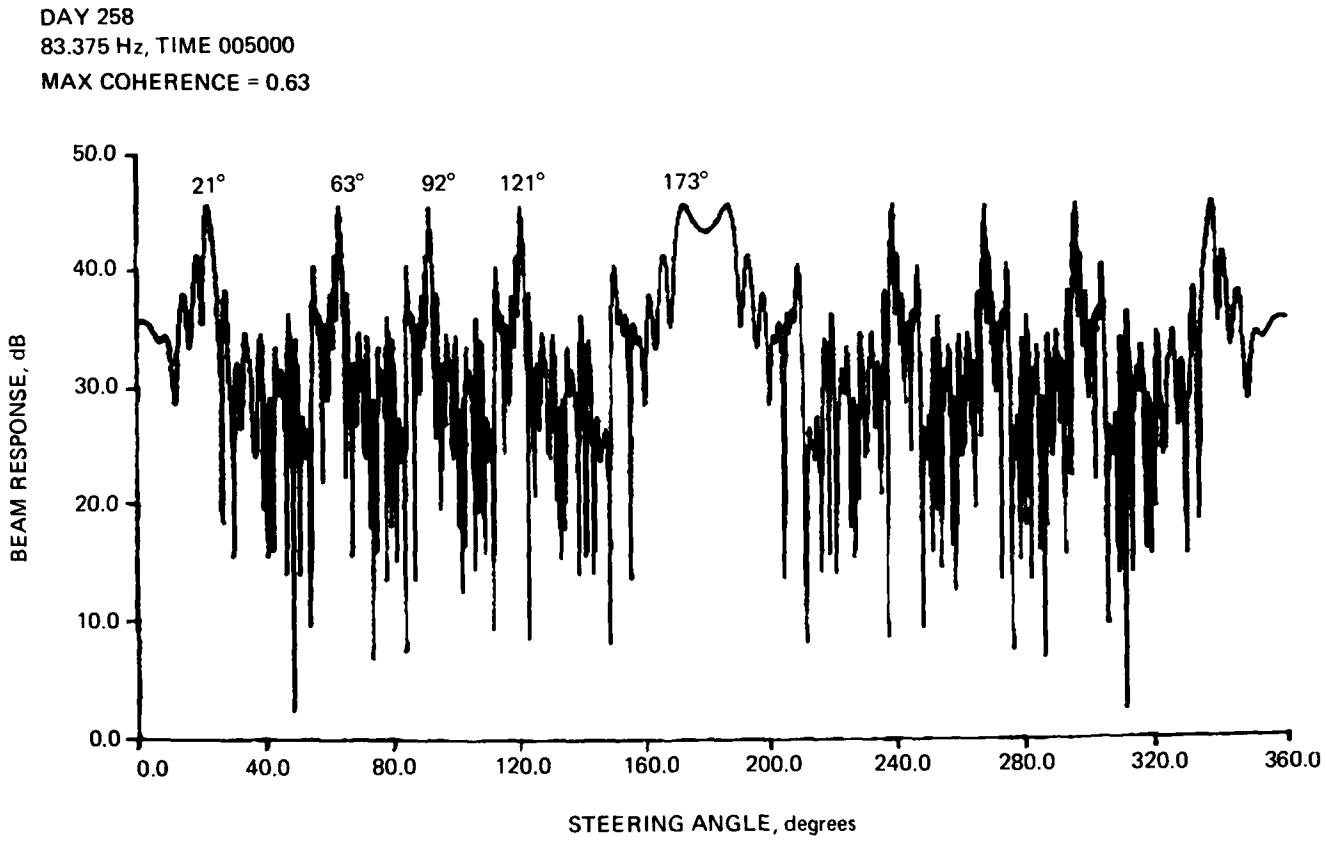

Figure 4a. Beam pattern at 83.375 Hz (straight array assumed).

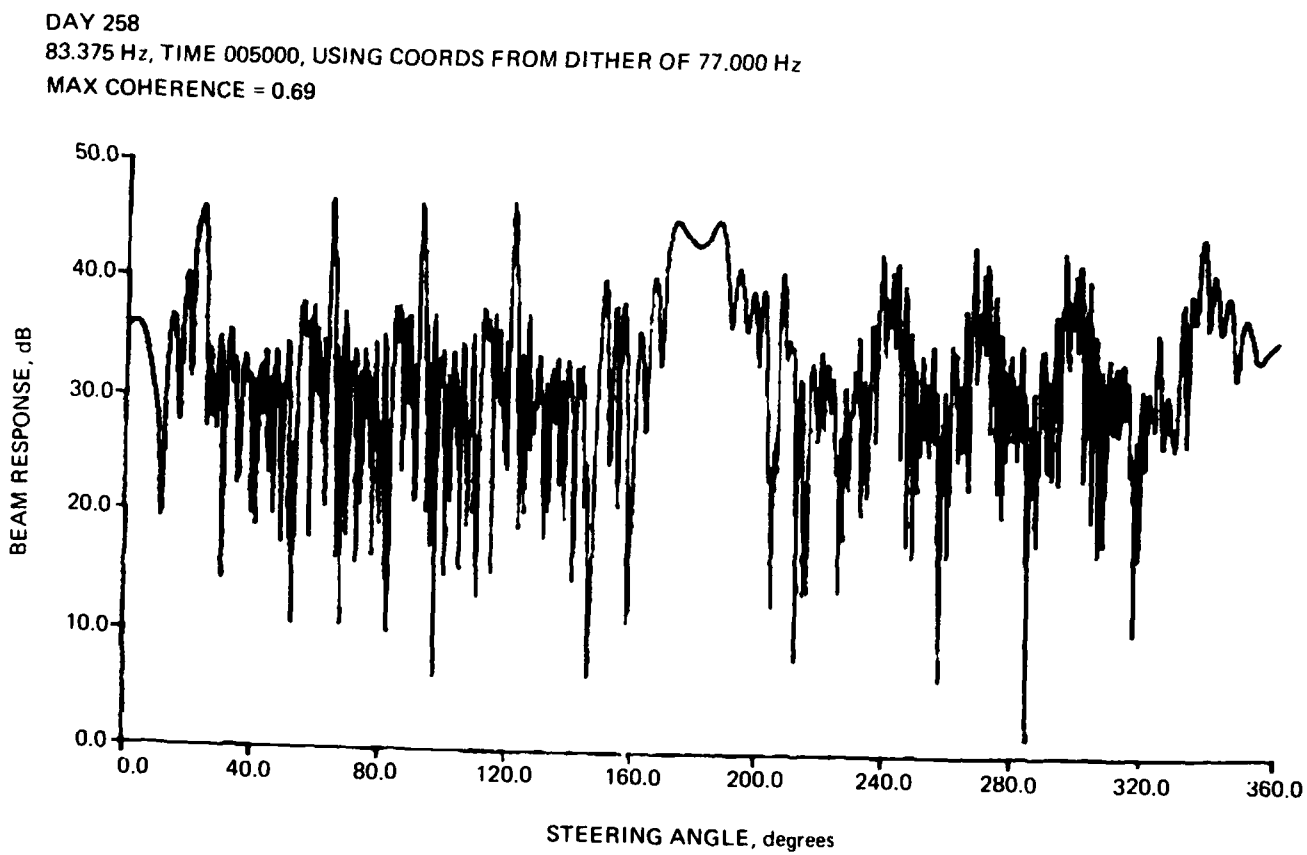

Figure 4b. Beam pattern at 83.375 Hz recomputed using array shape of Fig. 3b.

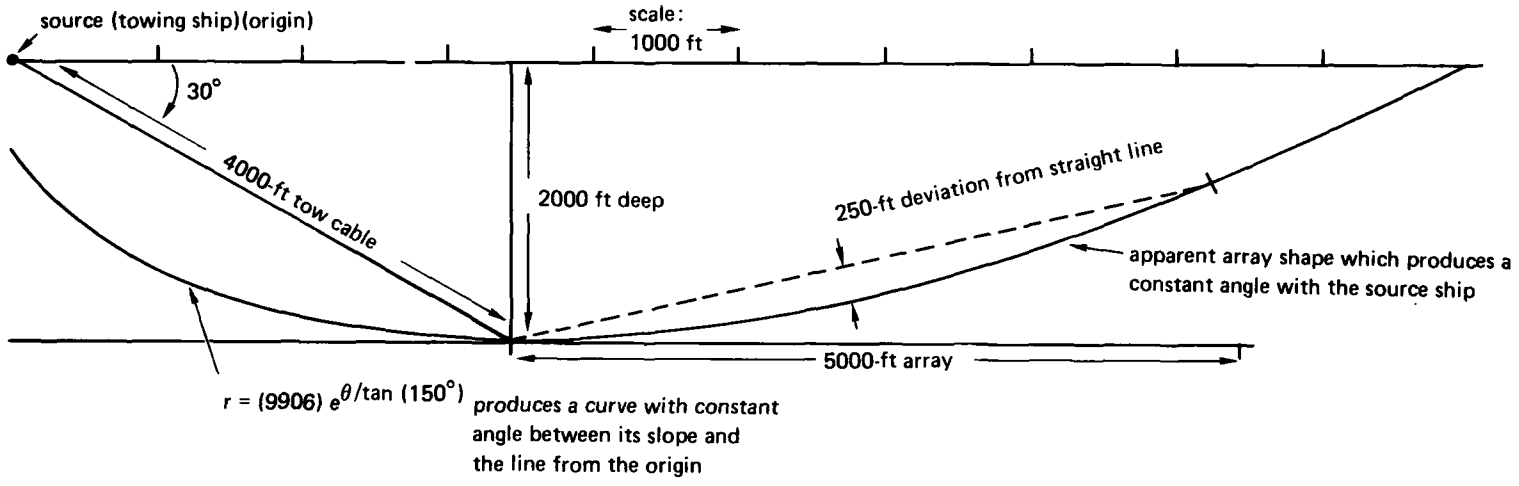

Figure 5. Apparent array shape due to wavefront curvature.

RESULTS OF SELF-COHERING ON LOW-FREQUENCY TARGETS

Self-cohering was attempted for much of the data from day 256 (as described in the section "Finding Sources Suitable for Self-Cohering" and shown in Figs. 1a through 1h). From time 1255 until time 1310, good-quality beam patterns (coherence >0.8) could almost always be obtained without any self-cohering at all. Figure 6 shows some examples of beam patterns on the assumption of a straight array. Figure 6c shows 58.5 Hz beamformed to a peak coherence of 0.87, which is only about 1 dB (take 20 log of coherence) less than perfect. By rule of thumb, coherence this good cannot be obtained unless array-element positions are known to an accuracy of a tenth of a wavelength, which at 58.5 Hz is 8.5 ft. Very likely, therefore, the array deviates from a straight line by less than 9 ft during this time.

Often, during this time, a frequency which showed up on Fig. 1 plots as being a very strong spectral line would beamform poorly under the straight-line assumption, even though higher frequencies with weaker spectral lines would beamform well. Self-cohering algorithms would effect no improvement. The problem appears to be that several different targets radiate nearly coherent signals. For example, the frequency 19.5 ± 1/8 Hz shows up as a strong spectral line (usually the strongest) on each of the Fig. 1 plots; even on day 251 (1 week earlier than Fig. 1i), 19.5 Hz is strongly present. Yet, 19.5 Hz usually beamforms poorly. By chance, it was noticed that at time 1310 (Fig. 1d), frequency 19.375 Hz appears to have a sidelobe of 19.750 Hz. Indeed, Figs. 7a and 7b strongly suggest the presence of two targets separated by almost 70° in arrival angle. It is suspected that two targets have been present all along, spoiling self-cohering efforts with constructive and destructive phase interference. (This in itself is an enigma. The peaks in Figs. 7a and 7b are at completely the wrong angles to be coming from the towing ship; yet, what other ship targets would have lingered for over a week?) Similarly, frequency 21.625 Hz certainly looks like a single target in Fig. 1d, but was shown to be at least two (maybe four) separate targets 15 min earlier (at time 1255). Figure 7c is an example of the unusual shapes that result from attempts to self-cohere multiple targets: the jog in the center is apparently the result of a single null caused by destructive interference between signals from different arrival angles.

At about time 1315 (Fig. 1e), the turn (begun by the towing ship at time 1300) reaches the array. The noise level at this time is the worst of all the times shown in Fig. 1, and some clipping was noted at the analog-to-digital converters when the magnetic tapes were being digitized. Nevertheless, self-cohering by the compensate-residual-phase method was able to effect some minor improvement. Self-cohering applied to 58.0 Hz improved coherence from 0.63 to 0.72; and when the array shape resulting from self-cohering (Fig. 8a) was used to beamform frequency 29.5 Hz, coherence increased from 0.668 (Fig. 8b) to 0.768 (Fig. 8c). The self-cohering algorithm was also applied to 29.5 Hz, and, as expected, the resulting array shape (Fig. 8d) looks very similar to the array shape from 58.0 Hz. Both these frequencies are from sources nearly at right angles to the array. More difficulty is encountered trying to self-cohere on a signal arriving more nearly endfire. Frequency 18.0 Hz would not self-cohere at all unless the low-pass spatial filter was removed completely from the self-cohering algorithm. The resulting array shape (Fig. 8e) is irregular, but in general exhibits the same slow curving trend as Figs. 8a and 8d. Evidently, the combination of lots of noise, a few bad hydrophones, a long wavelength, and a steering angle near endfire makes self-cohering difficult.

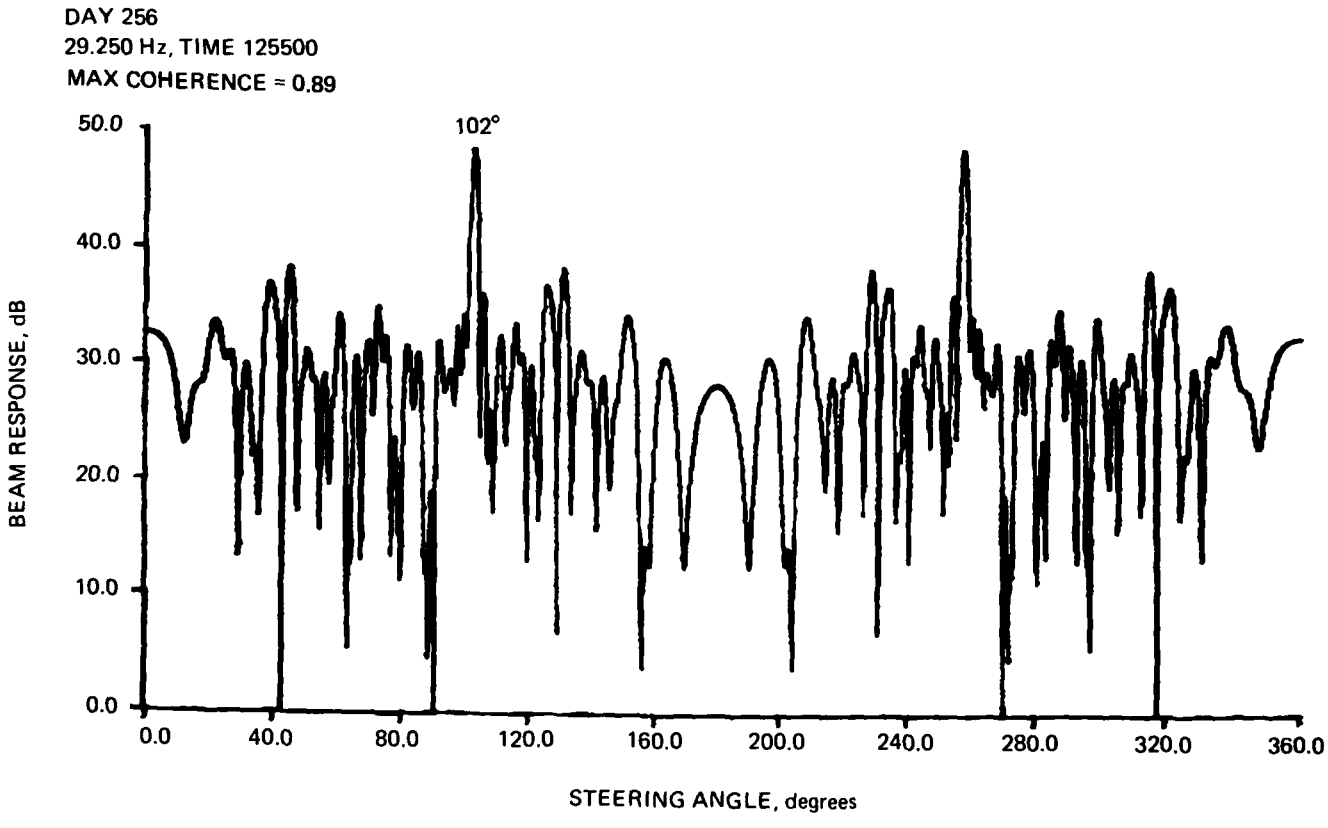

Figure 6a. Beam pattern at 29.25 Hz (straight array assumed).

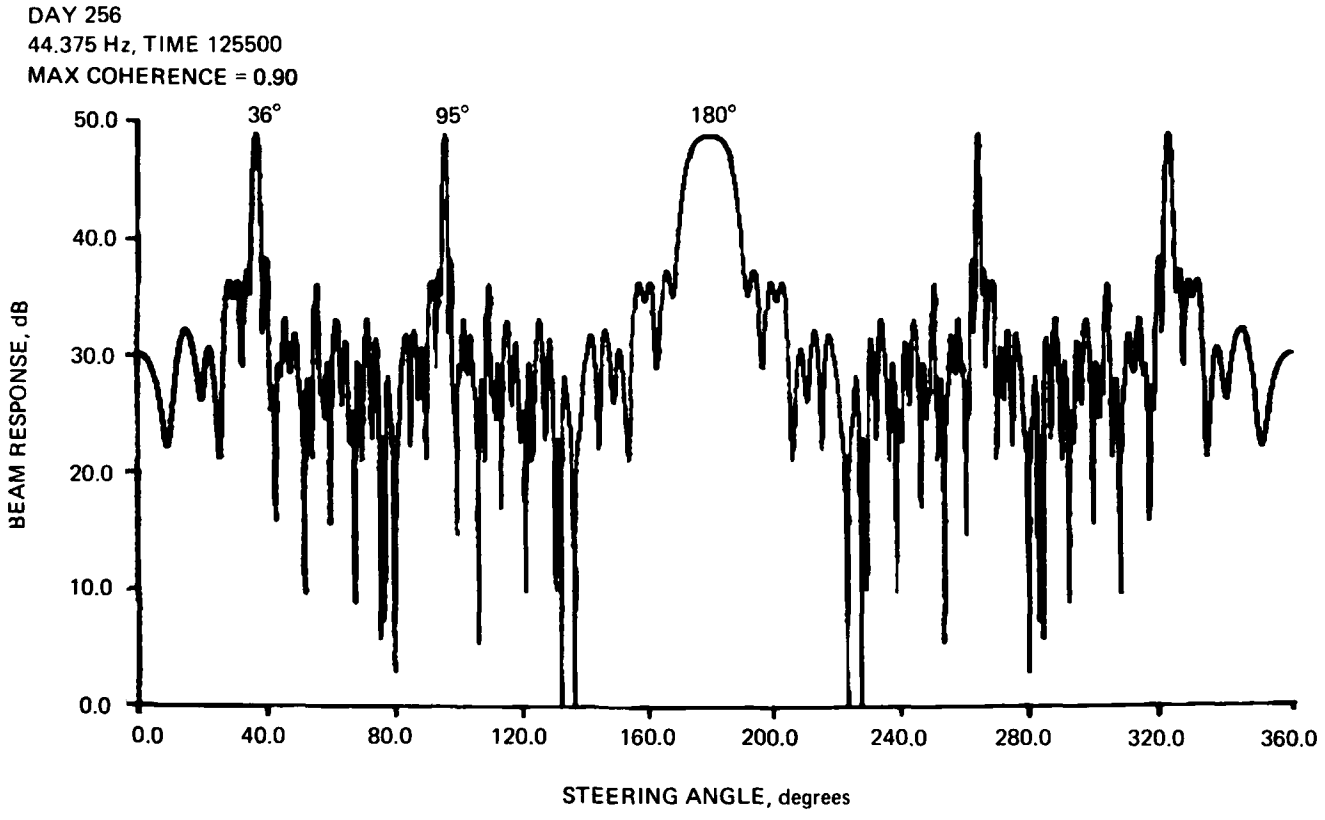

Figure 6b. Beam pattern at 44.375 Hz (straight array assumed).

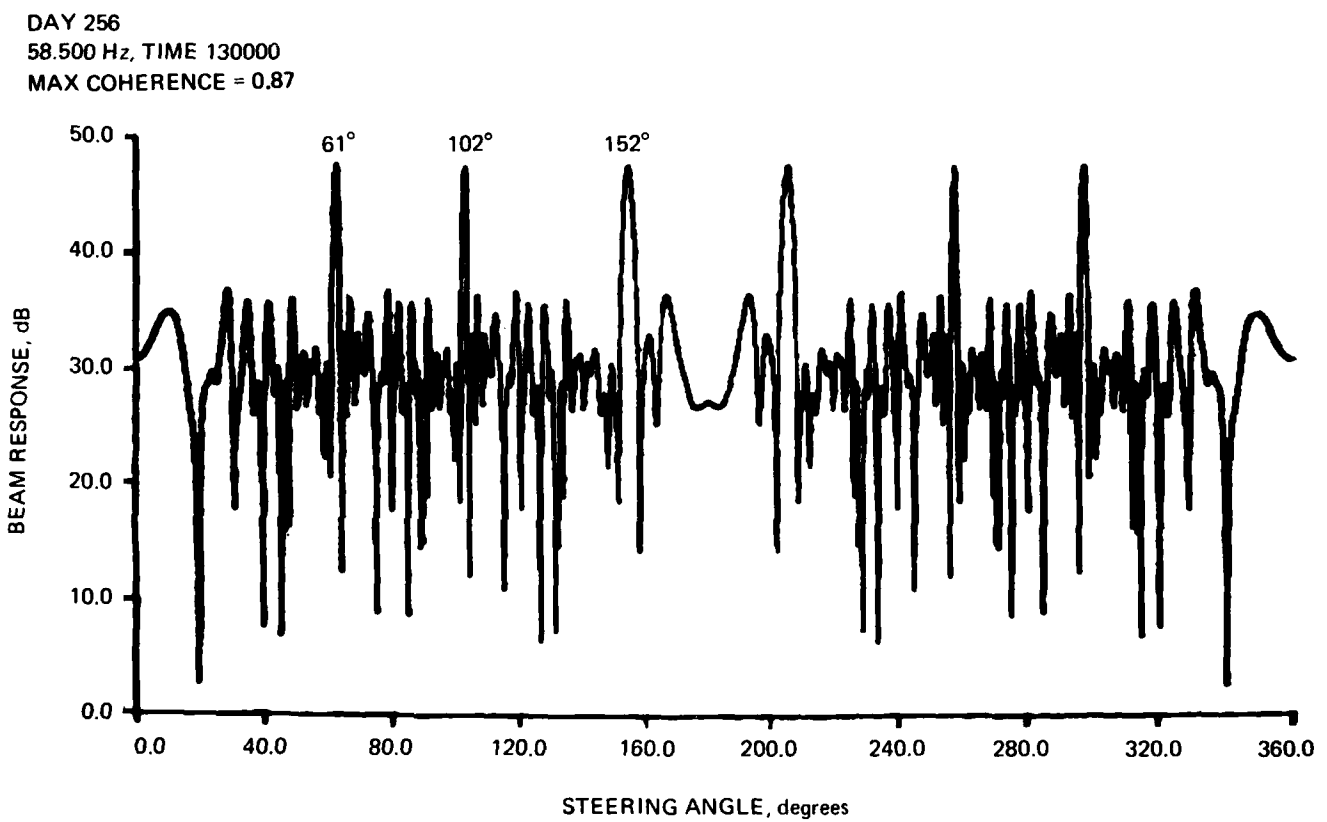

Figure 6c. Beam pattern at 58.5 Hz (straight array assumed).

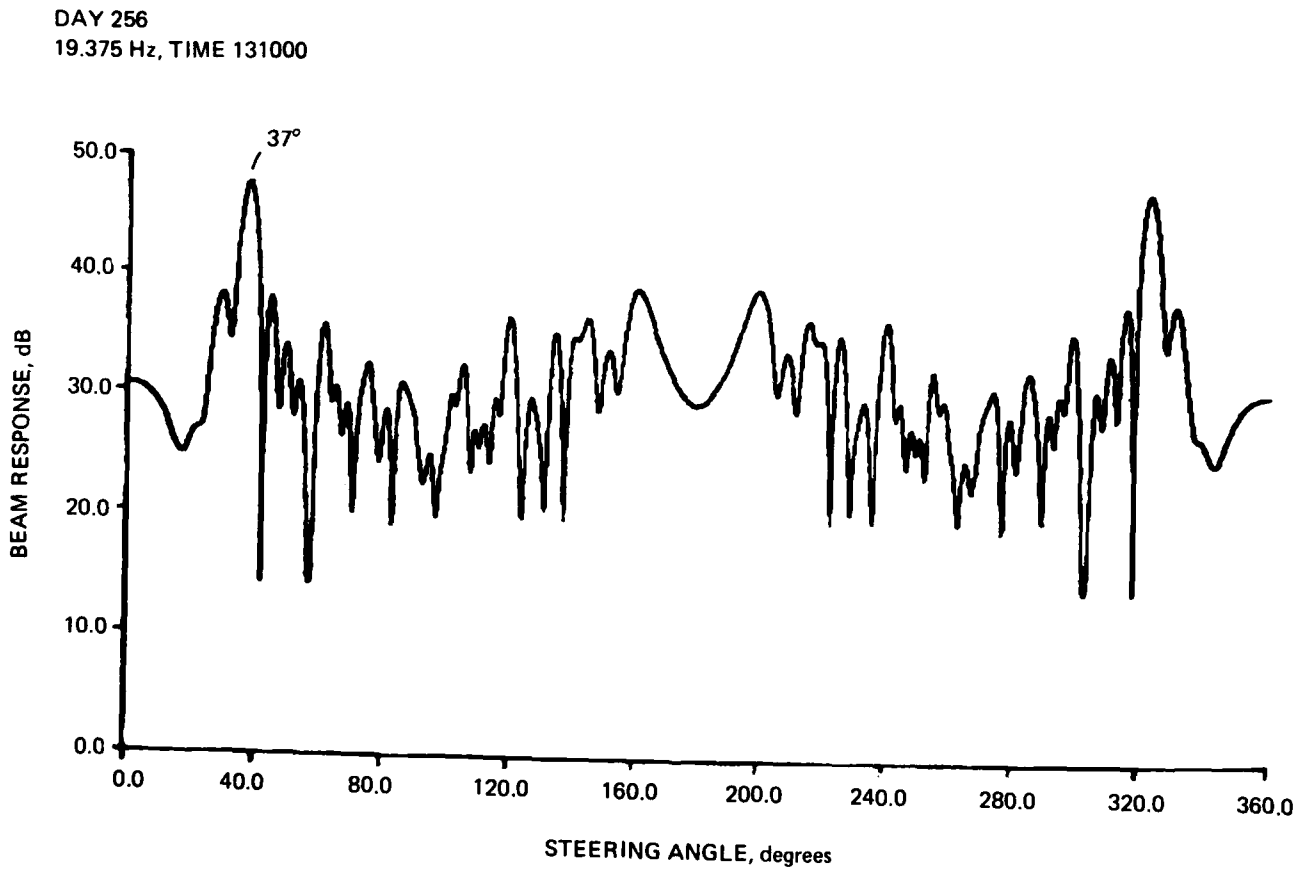

Figure 7a. Arrival-angle separation of nearly identical frequencies.

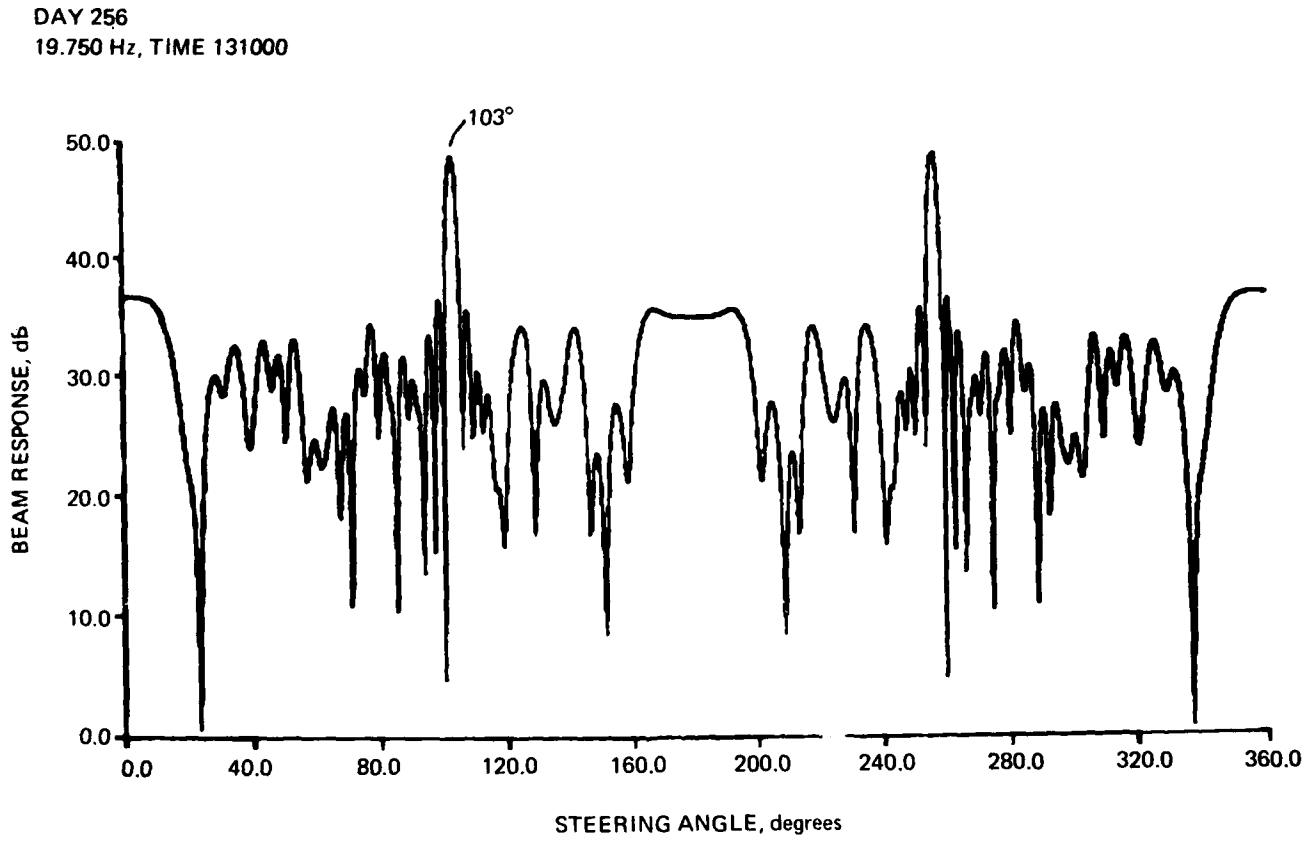

Figure 7b. Arrival-angle separation of nearly identical frequencies.

Figure 7c. Array-shape distortion due to interfering sources.

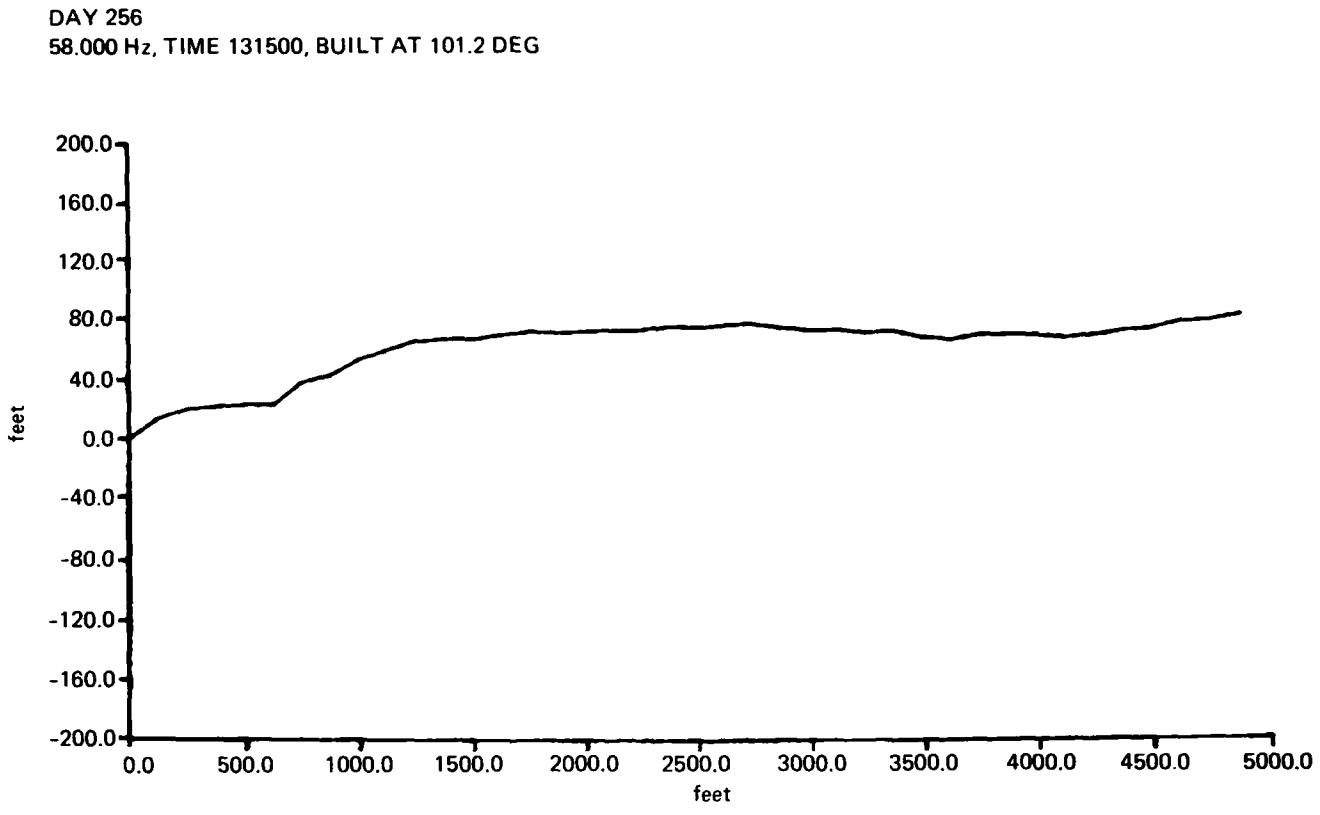

Figure 8a. Array shape, self-cohering 58 Hz near broadside.

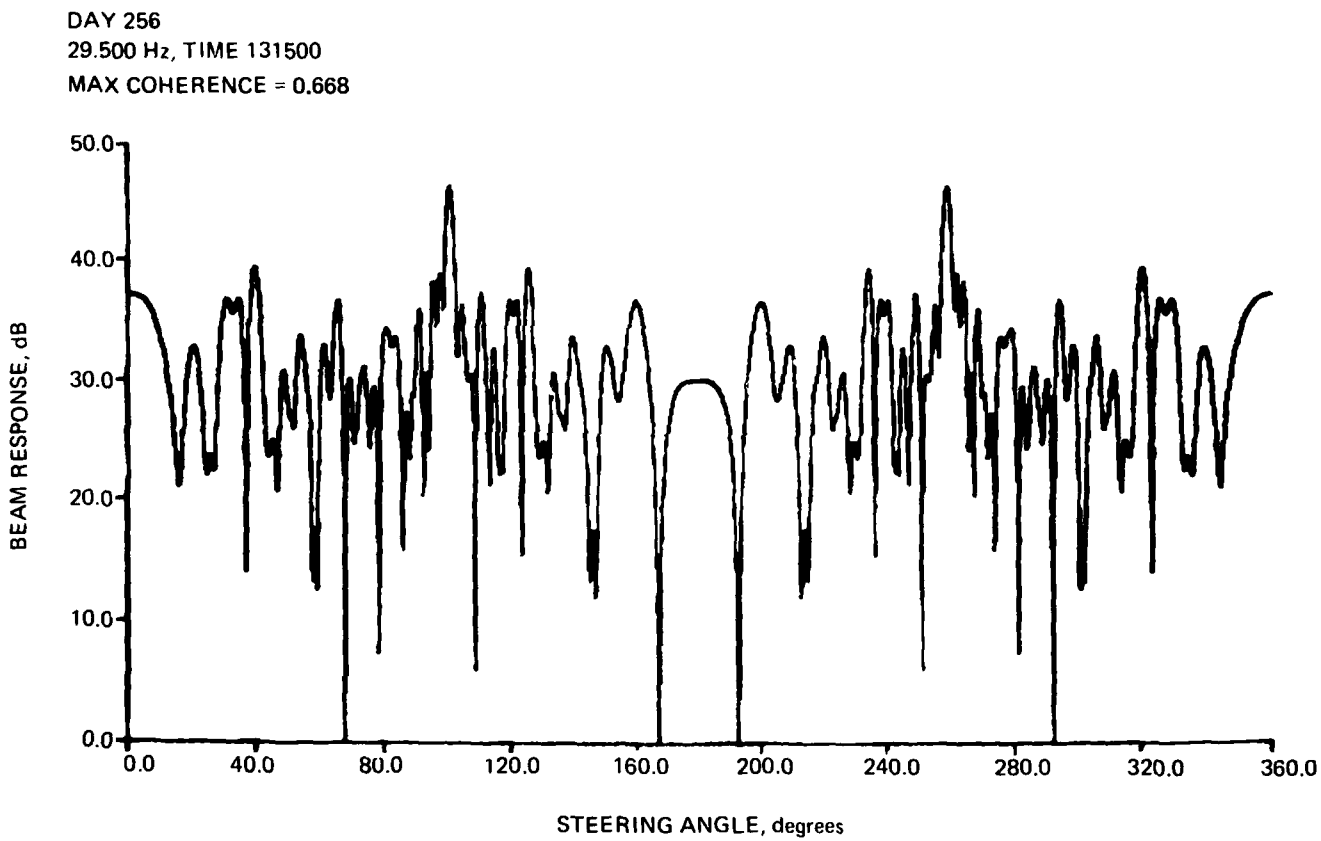

Figure 8b. Beam pattern at 29.5 Hz (straight array assumed).

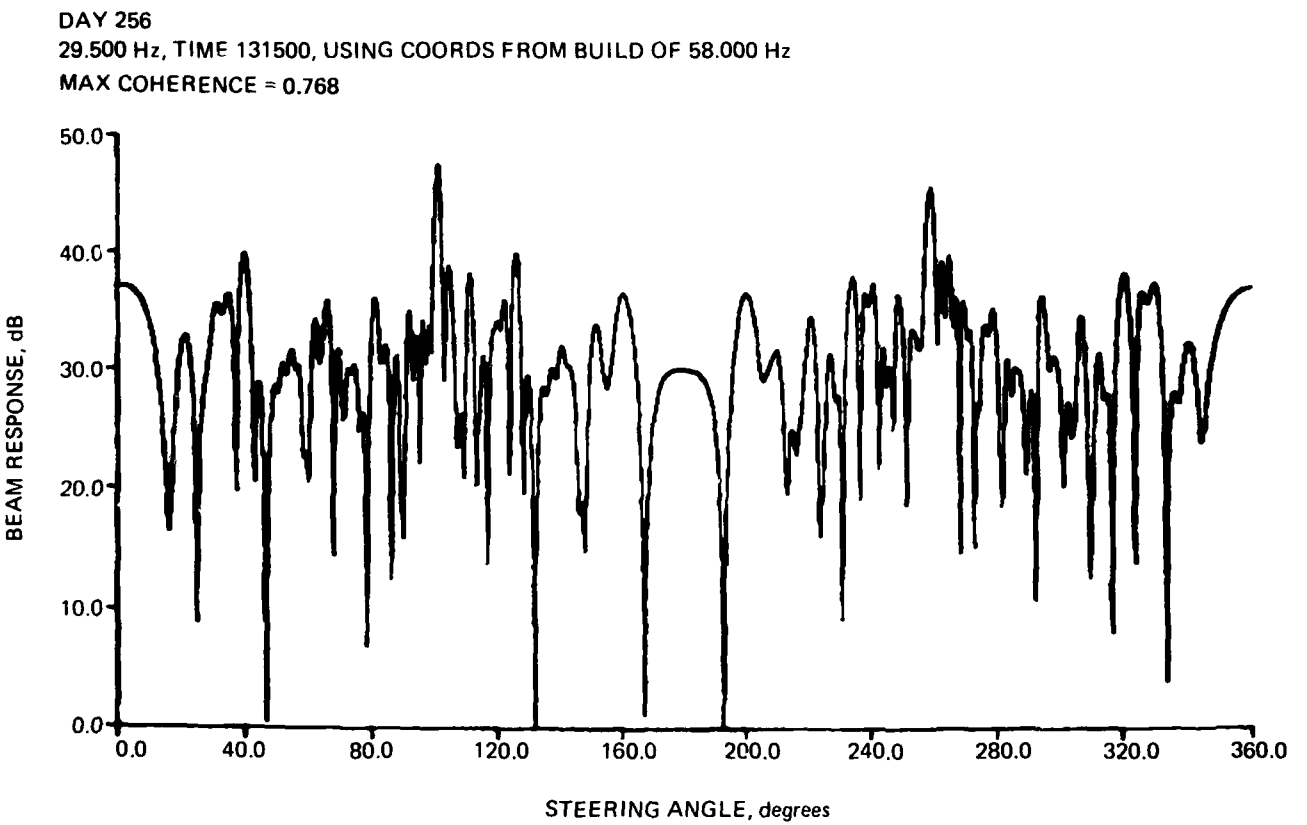

Figure 8c. Beam pattern at 29.5 Hz recomputed using array shape of Fig. 8a.

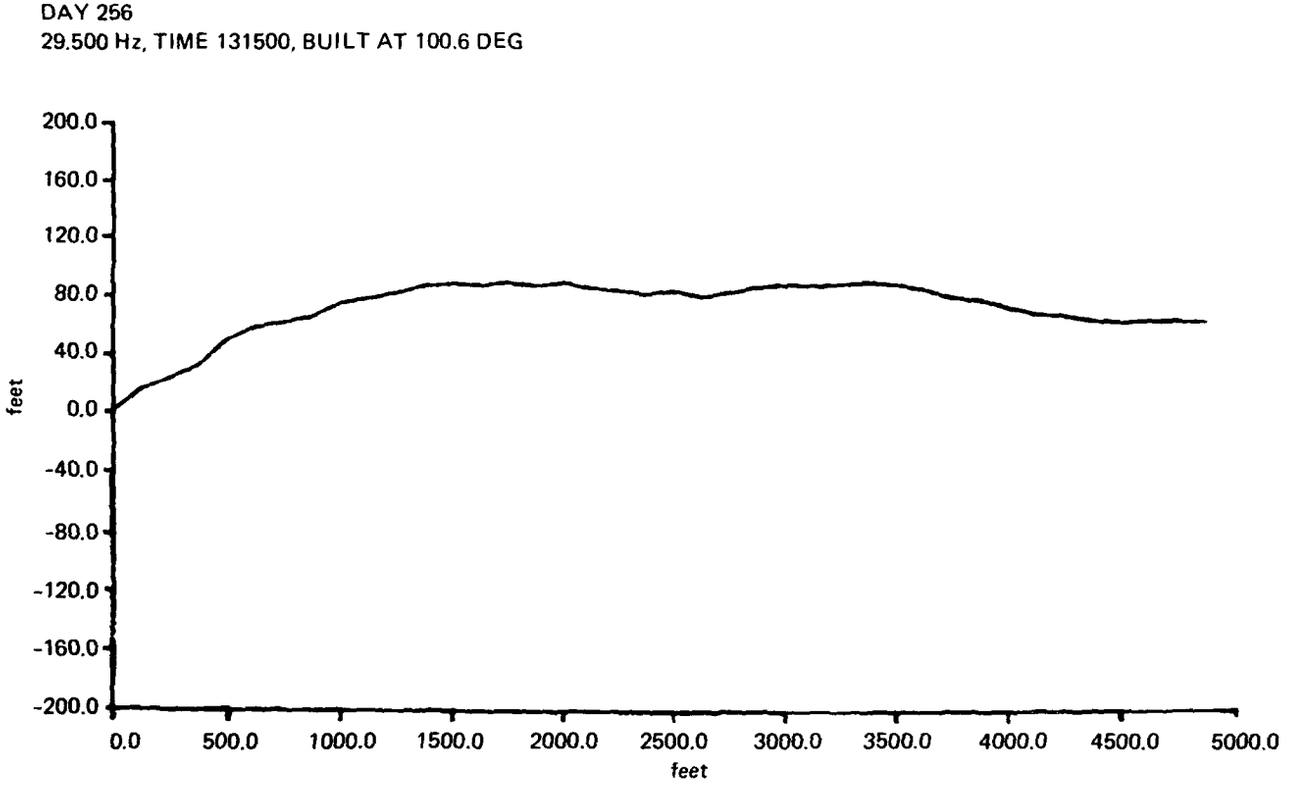

Figure 8d. Array shape, self-cohering 29.5 Hz near broadside.

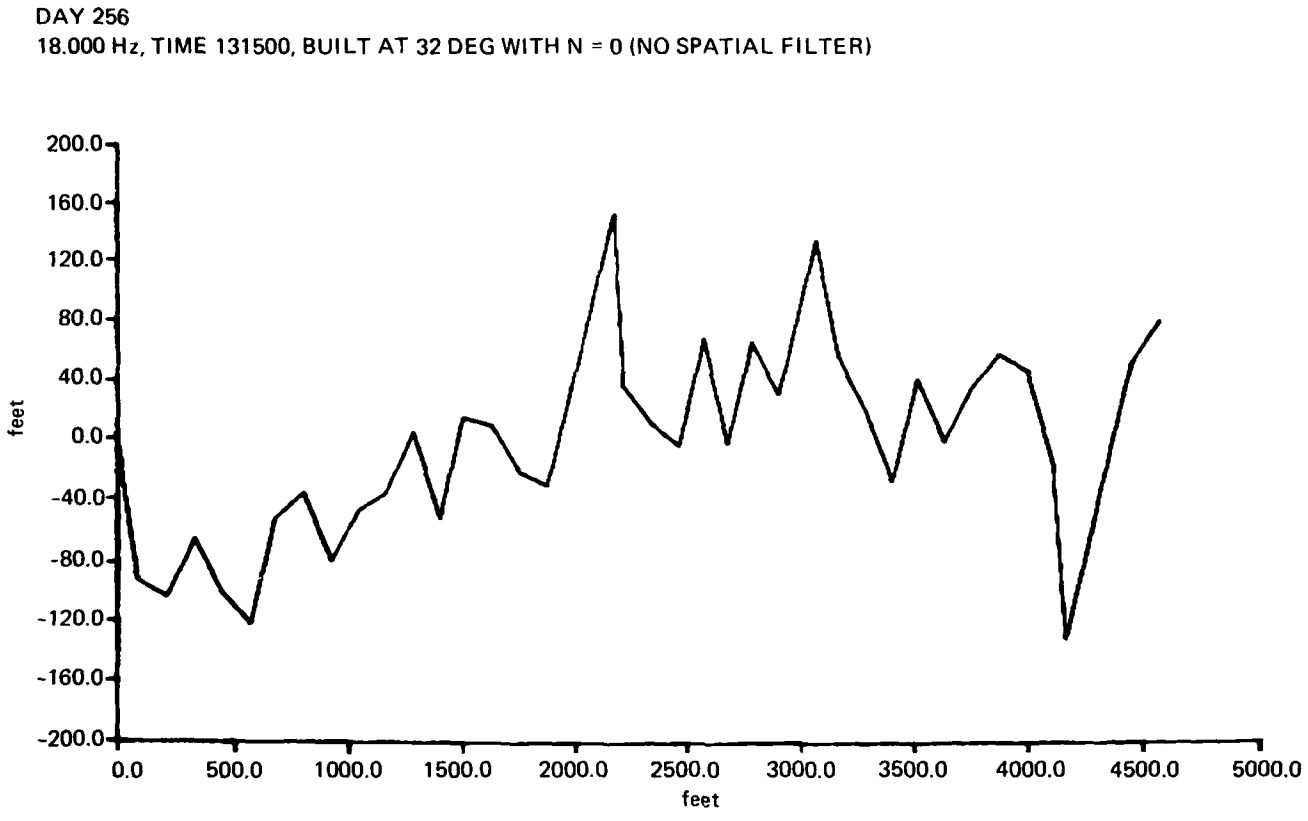

Figure 8e. Array shape, self-cohering 18 Hz near endfire.

At time 1320, self cohering was not too successful for some unknown reason. Several frequencies could be self-cohered to yield very good beam patterns at frequencies other than the self-cohering frequencies. Figures 9a and 9b are examples of these array shapes. There is agreement as to how much the array deviates from straight, but very little agreement as to specific shape details. Possibly this is due to poor element-amplitude uniformity, as seen in Figs. 2c and 2e.

At time 1325, frequency 18.125 Hz, when subjected to self-cohering, increased in coherence from 0.542 to 0.793. When the resulting array shape (Fig. 10) was used to beamform 19.5 Hz, coherence increased from 0.625 to 0.844. Both these frequencies are from sources very nearly endfire to the array.

At time 1326, when self-cohering was first applied, none of the beam patterns showed any improvement at all. In fact, the beam patterns were so bad that it was difficult to say whether or not targets were present. Figure 11a is typical. The problem (discovered by accident) was that the array curvature was many times greater than had previously been encountered. This is dramatically shown in the residual phase plot of Fig. 11b. In the absence of any element location error, if the array is correctly steered, all element phases should line up, and the residual-phase plot should be a straight horizontal line. If the array is really straight but is steered in slightly the wrong direction, the residual-phase plot should be a straight slanted line. In Fig. 11b, the residual phase is really parabola shaped (vertex at right, opening upward), but the sides slant so much that they are forced to zig-zag because phase is modulo-2π. The original width of the low-pass spatial filter in the compensate-residual-phase self-coherence was seven elements (ie, to estimate the phase at one array element, the phases from the three elements on either side are averaged together). Obviously, from Fig. 11b, the phase is changing so rapidly near the left end of the array that such an average will almost surely be zero.

When the width of the spatial filter was decreased to three elements (one element on either side), the self-cohering algorithm worked well. The coherence of 19.625 Hz increased from 0.44 (Fig. 11a) to 0.882 (Fig. 11d). The resulting array shape (Fig. 11c) shows more than 600 ft of deviation from straight (nearly three wavelengths)! When the array shape from self-cohering 19.625 Hz was used to beamform other frequencies, the following improvements resulted:

Summary of Self-Cohering Improvements

frequency, Hz	coherence assuming straight array	coherence using array shape from 19.625 Hz	steering angle, deg
19.625	0.440	0.882	77
21.75	0.460	0.771	142
29.375	0.515	0.738	78
46.000	0.374 (Fig. 11e)	0.617 (Fig. 11f)	70
56.500	0.487 (Fig. 11g)	0.571 (Fig. 11h)	120

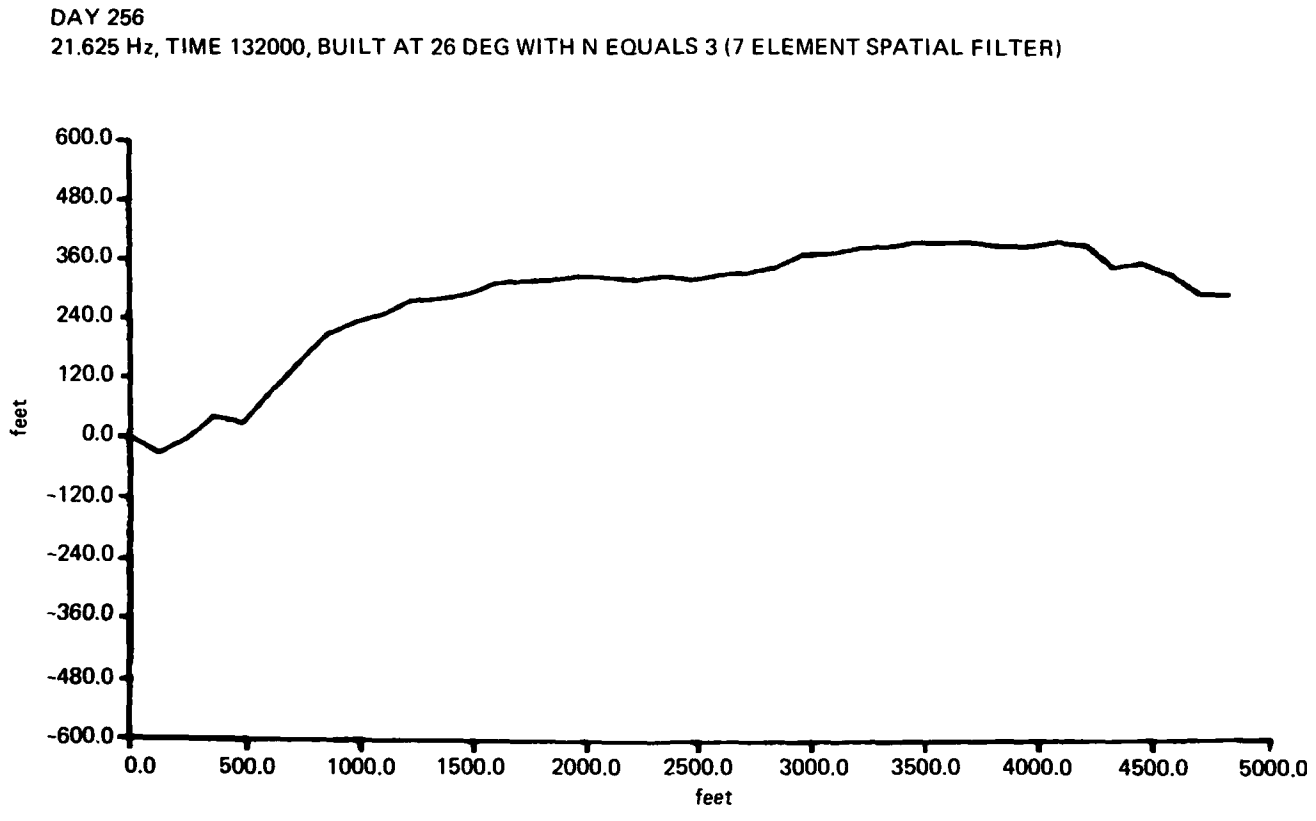

Figure 9a. Array shape (not at self-cohering frequency).

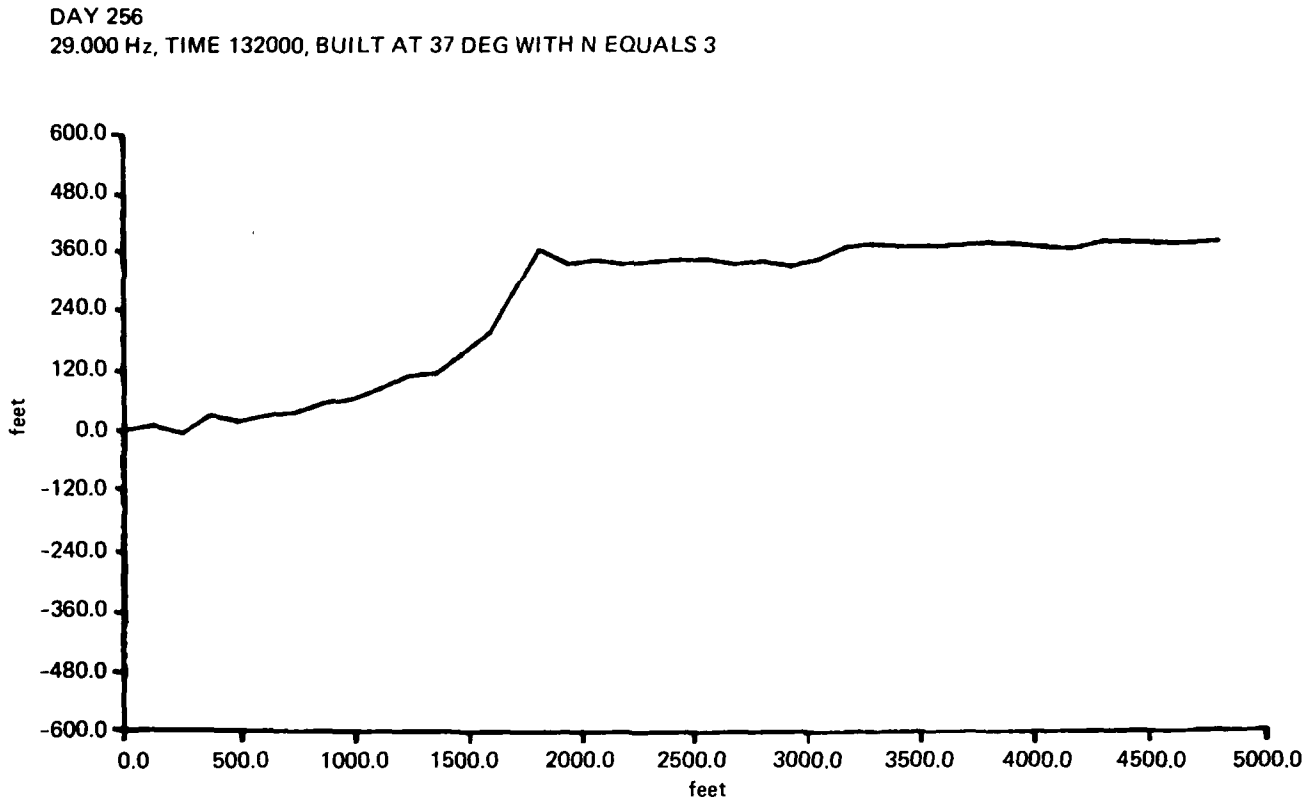

Figure 9b. Array shape (not at self-cohering frequency).

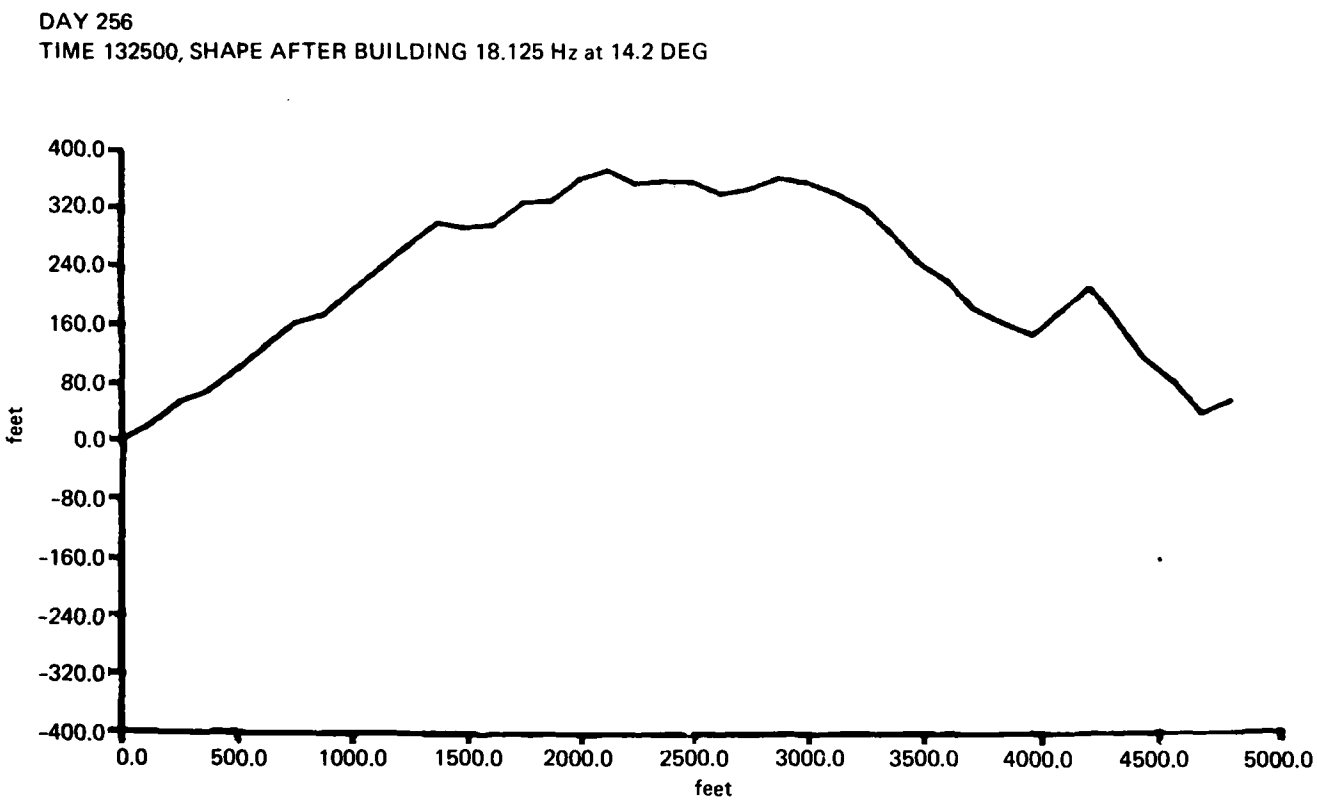

Figure 10. Array shape (self-cohered 18.125 Hz).

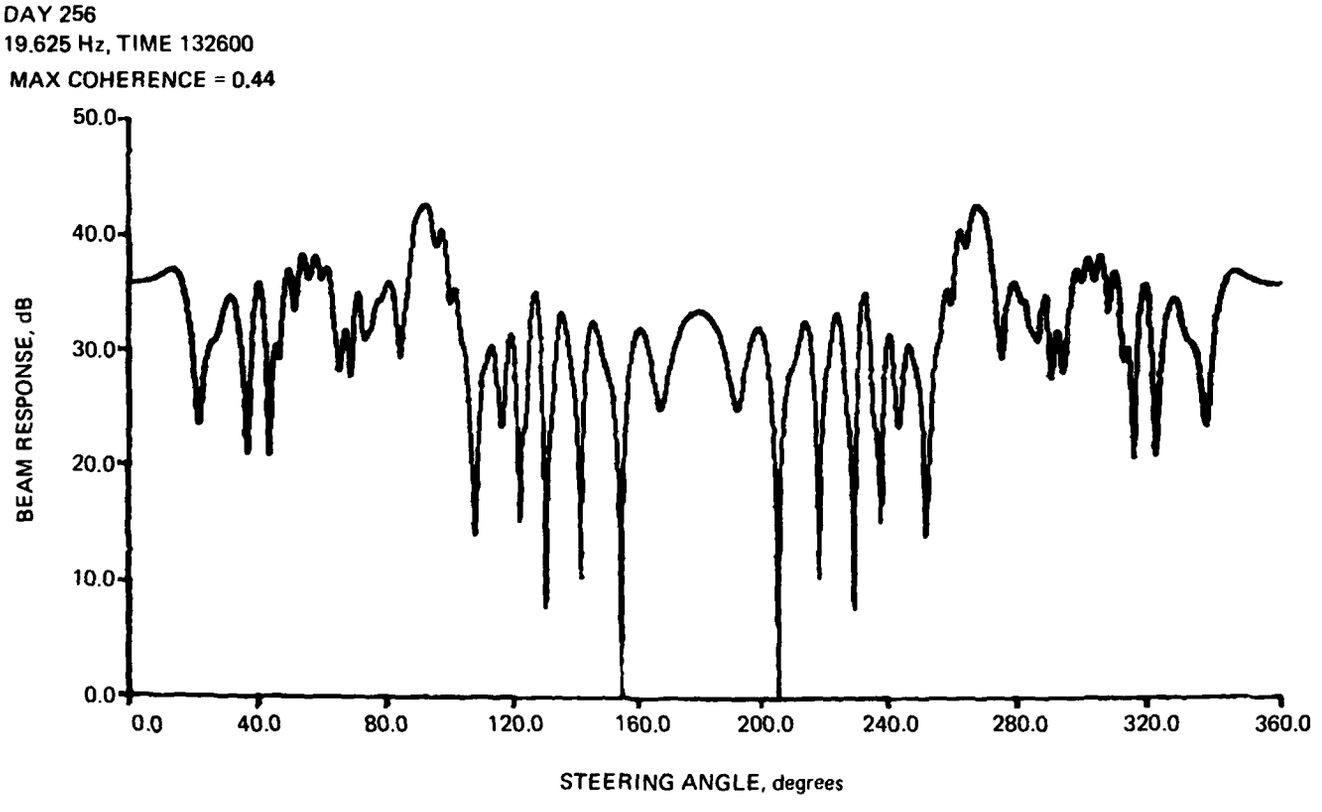

Figure 11a. Beam pattern at 19.625 Hz (straight array assumed).

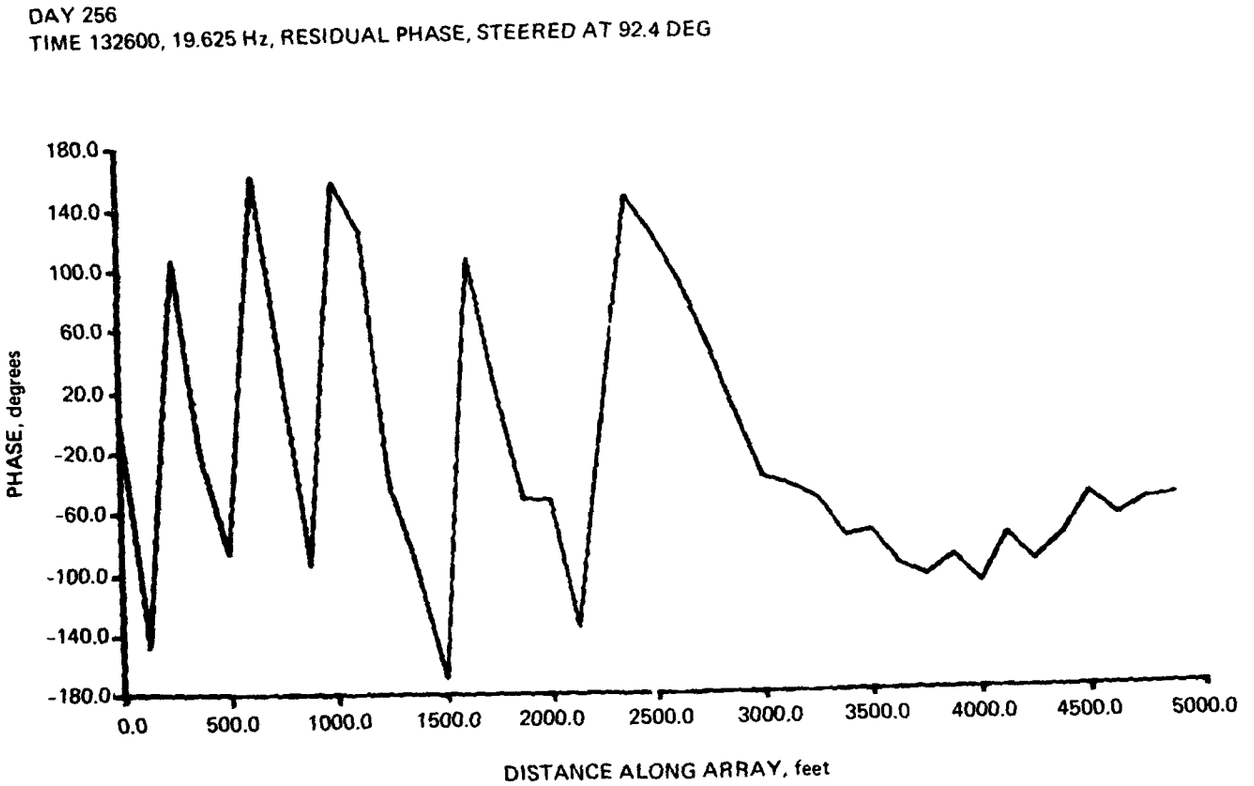

Figure 11b. Residual-phase plot showing severe array curvature.

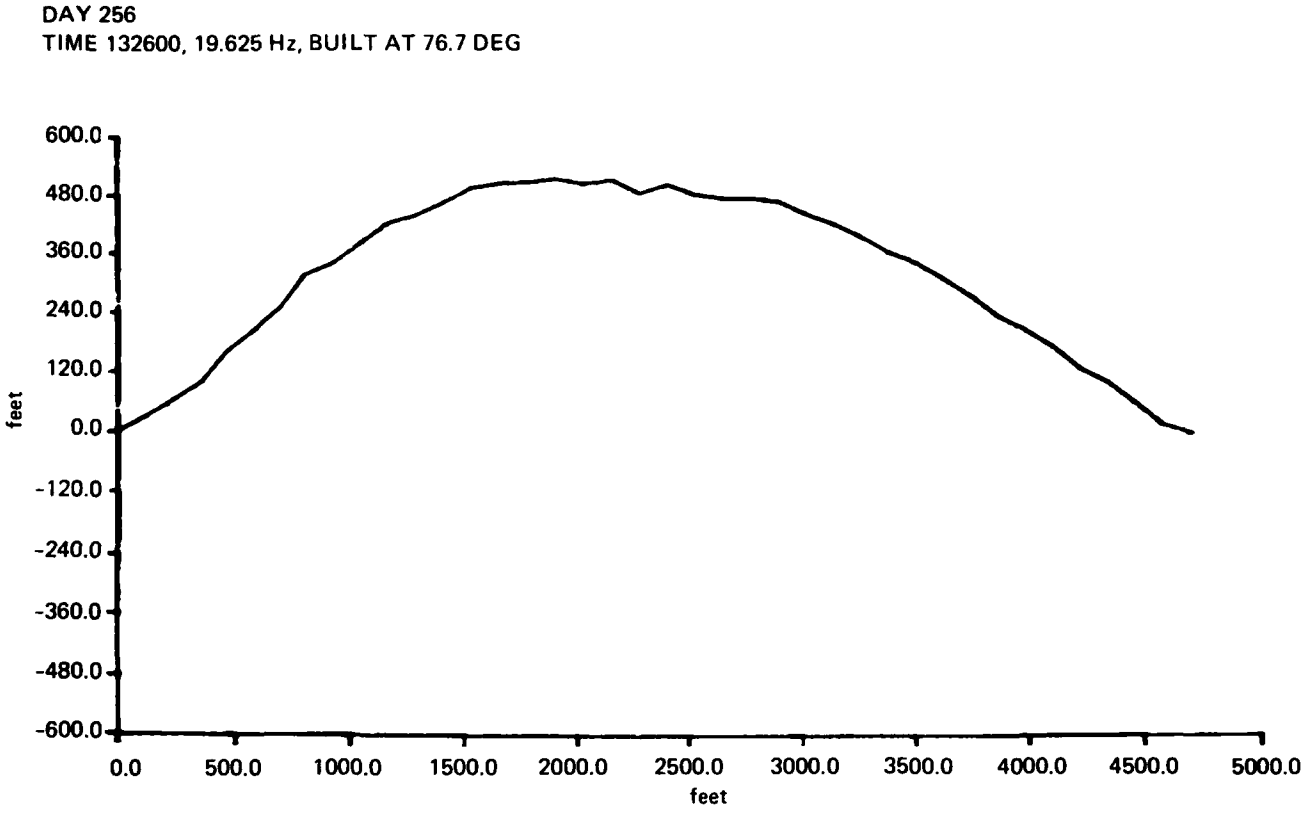

Figure 11c. Array shape, self-cohering 19.625 Hz.

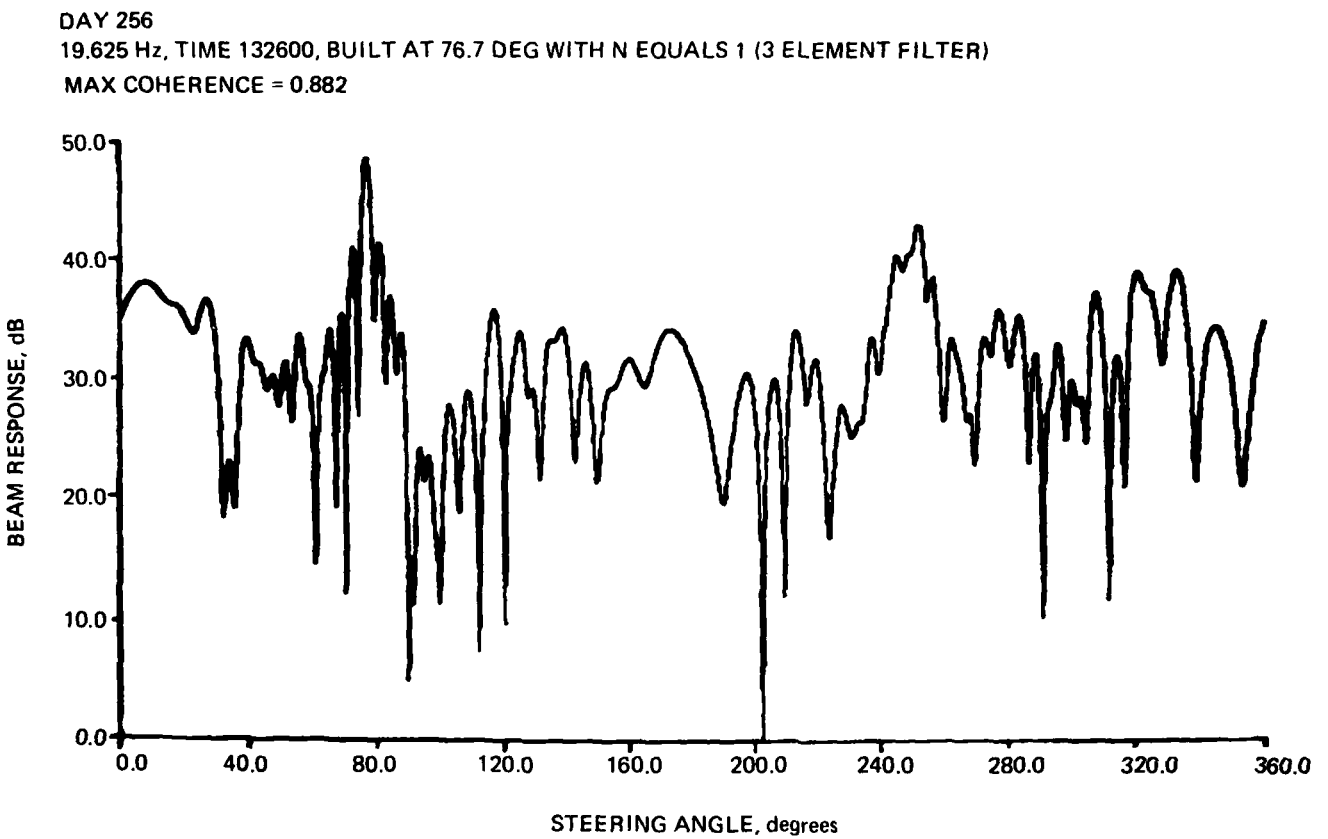

Figure 11d. Beam pattern at 19.625 Hz after self-cohering.

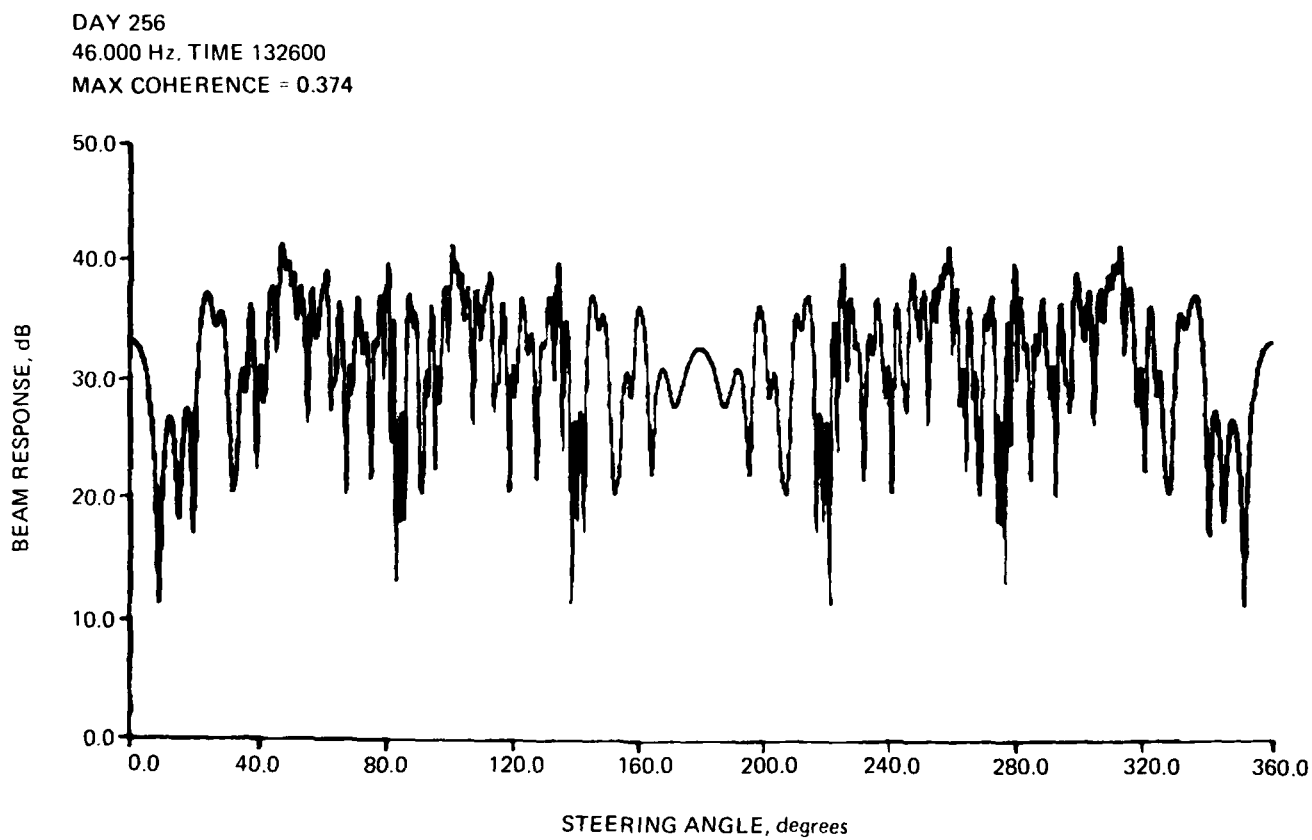

Figure 11e. Beam pattern at 46.0 Hz (straight array assumed).

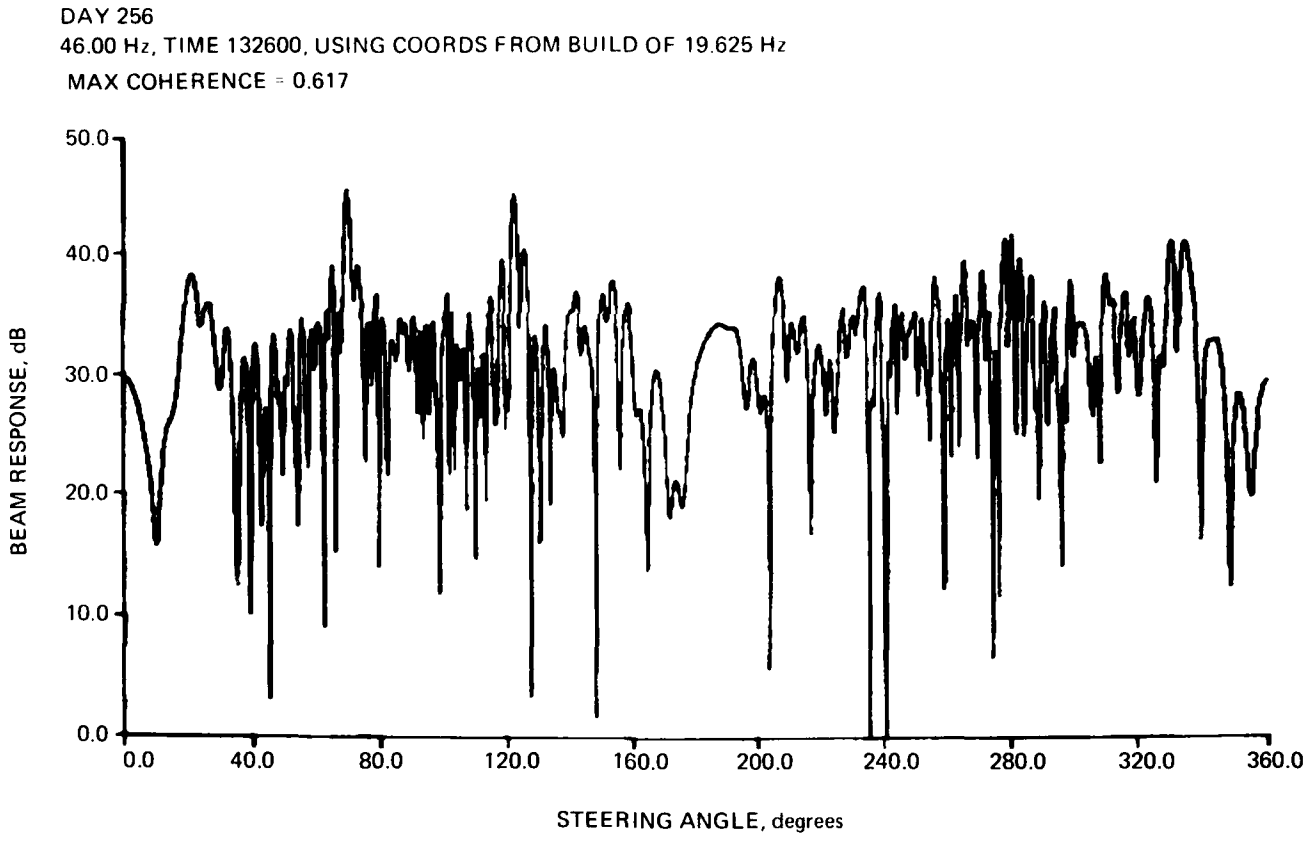

Figure 11f. Beam pattern at 46.0 Hz recomputed using array shape of Fig. 11c.

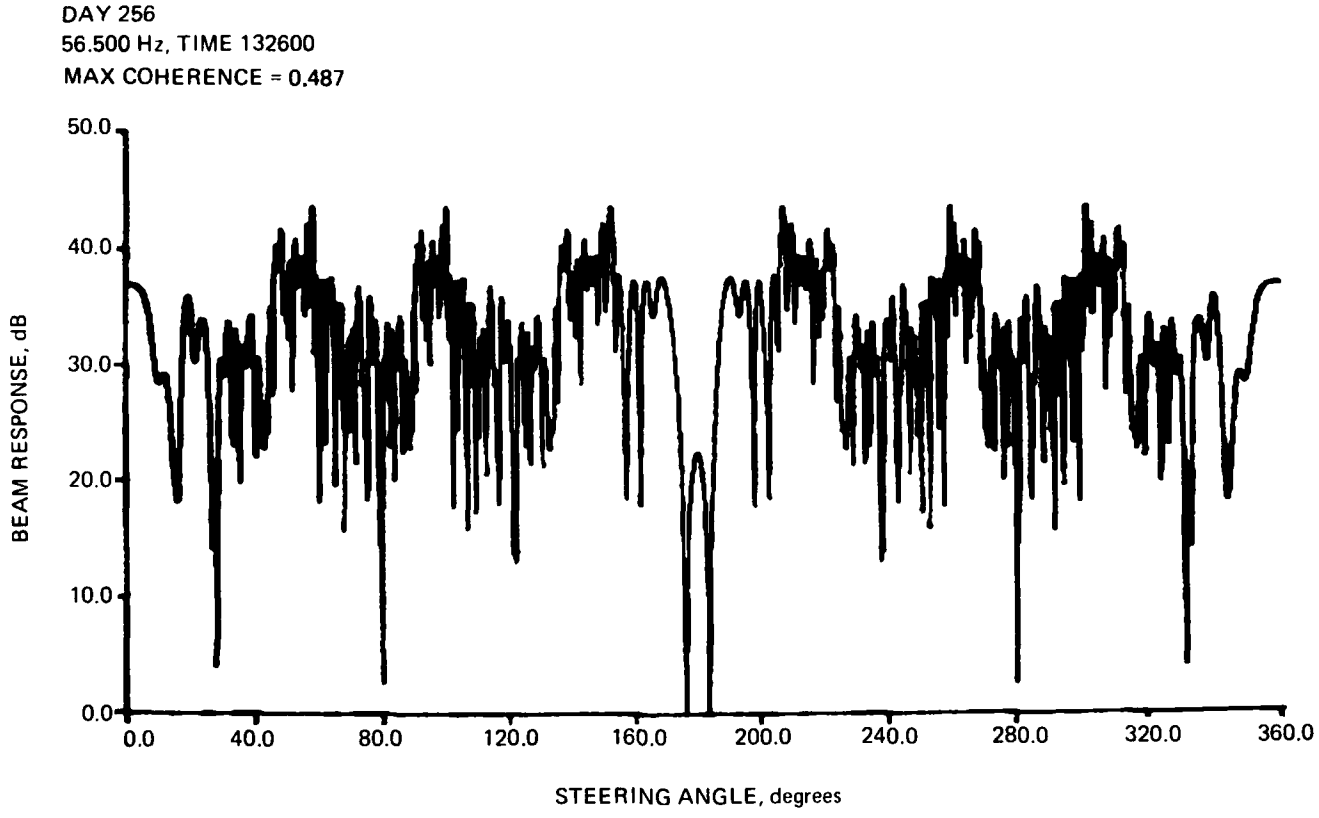

Figure 11g. Beam pattern at 56.5 Hz (straight array assumed).

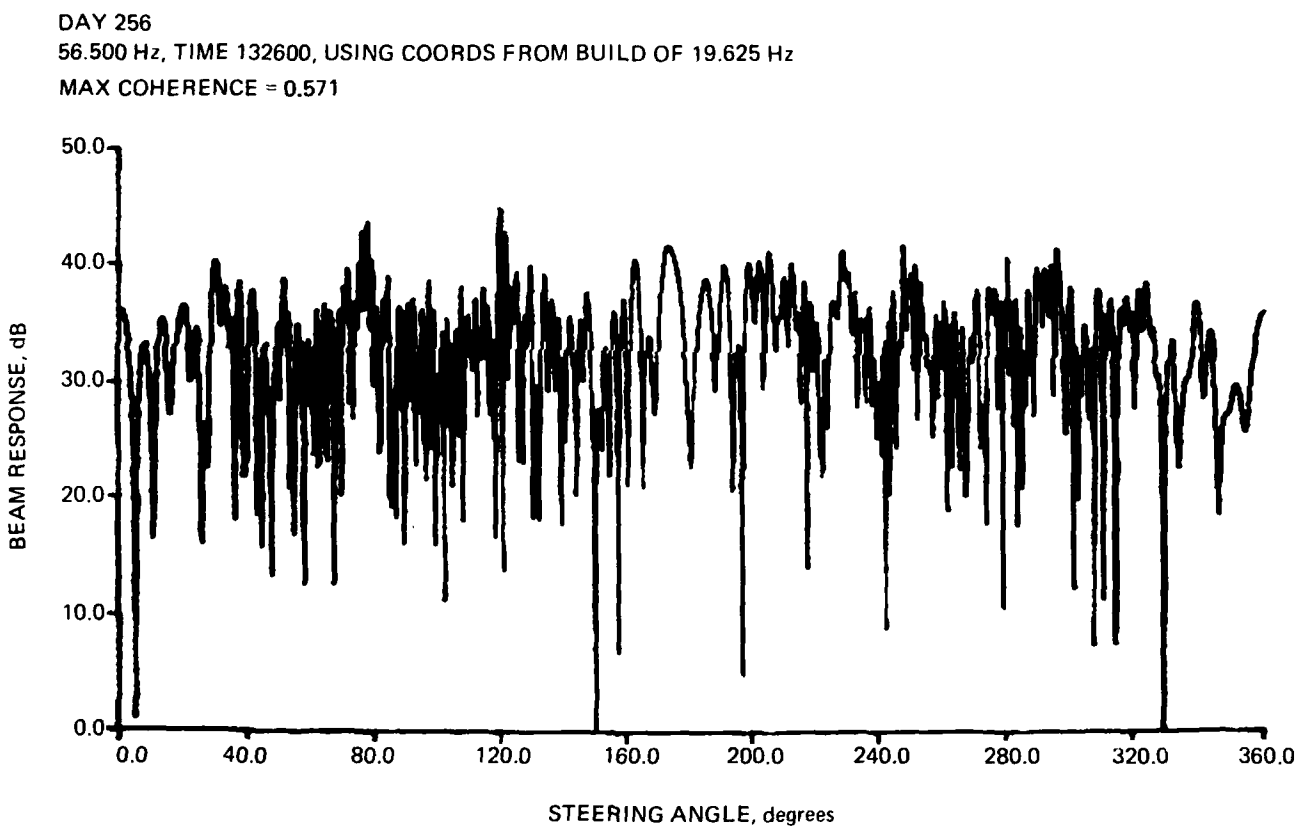

Figure 11h. Beam pattern at 56.5 Hz recomputed using array shape of Fig. 11c.

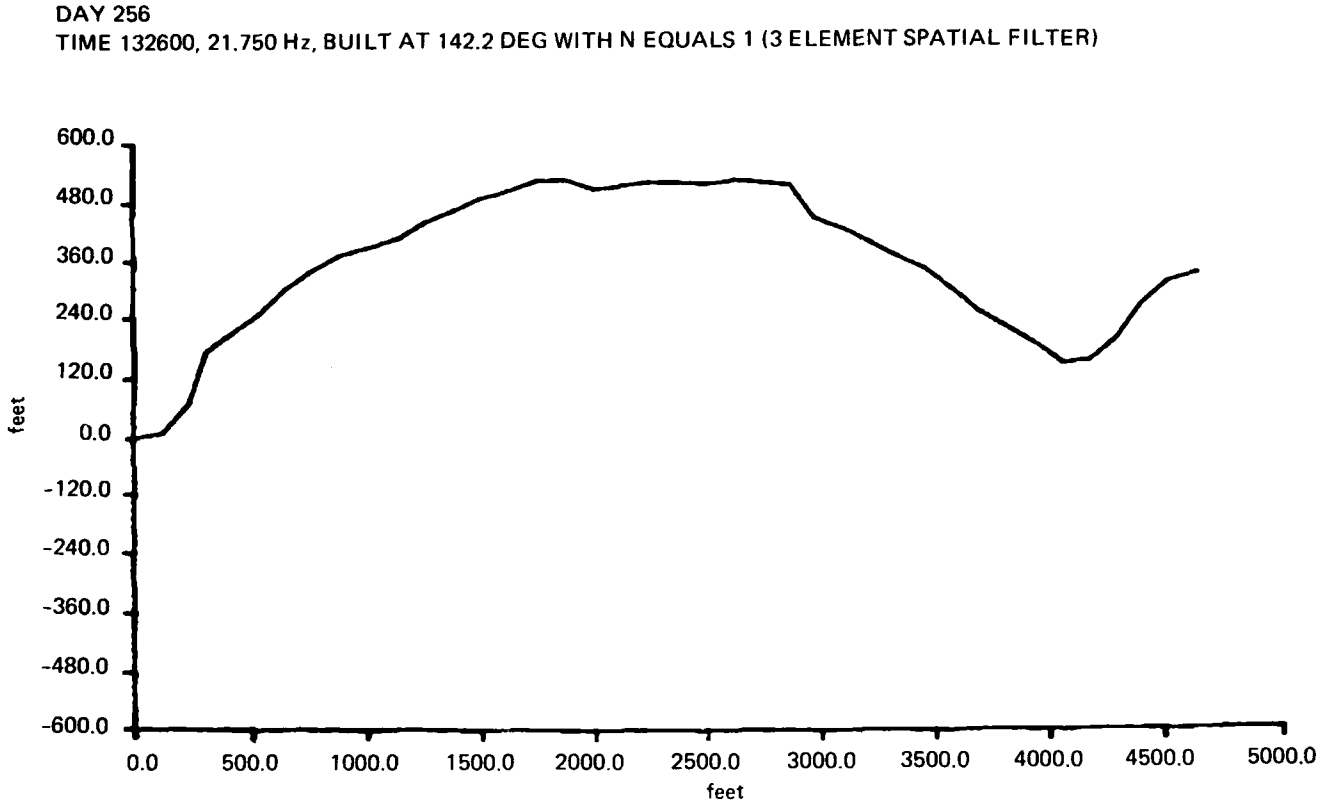

Figure 11i. Array shape, self-cohering 21.75 Hz.

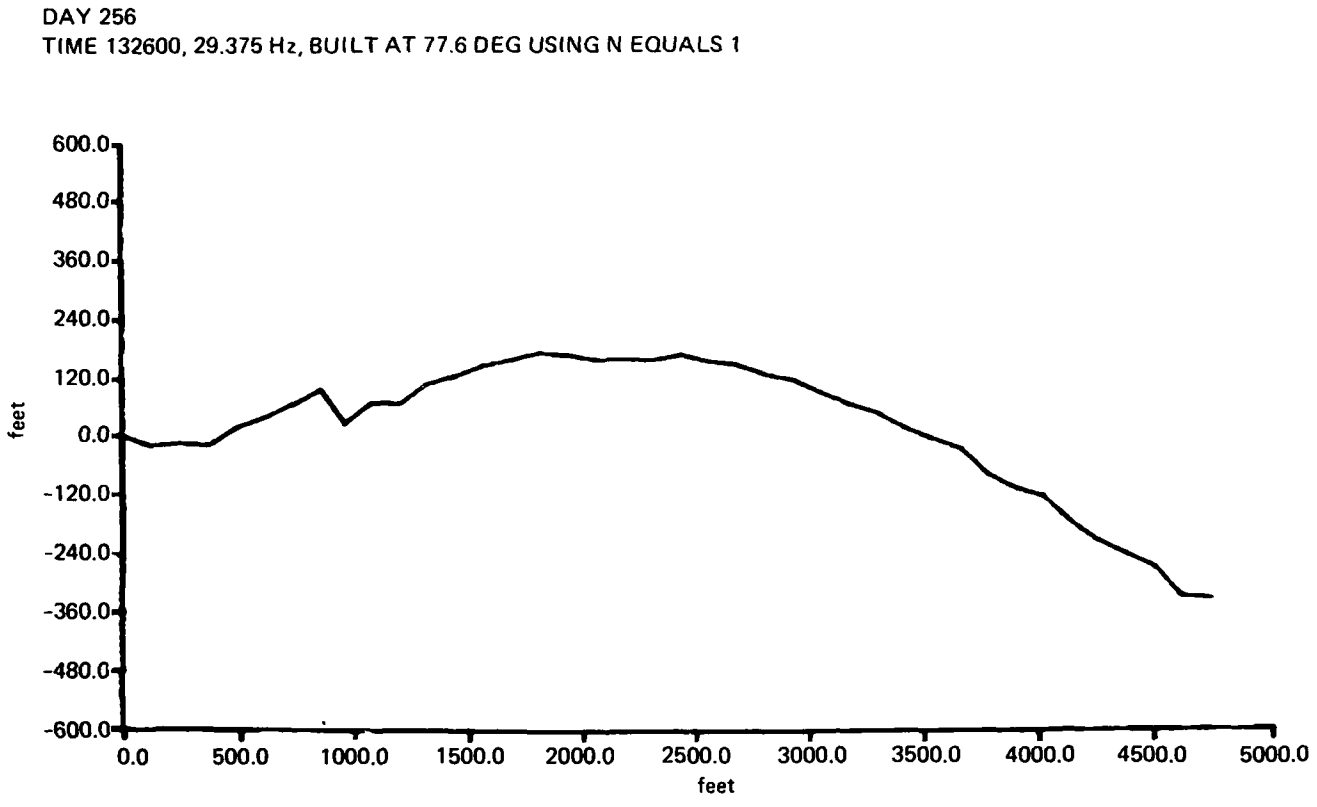

Figure 11j. Array shape, self-cohering 29.375 Hz.

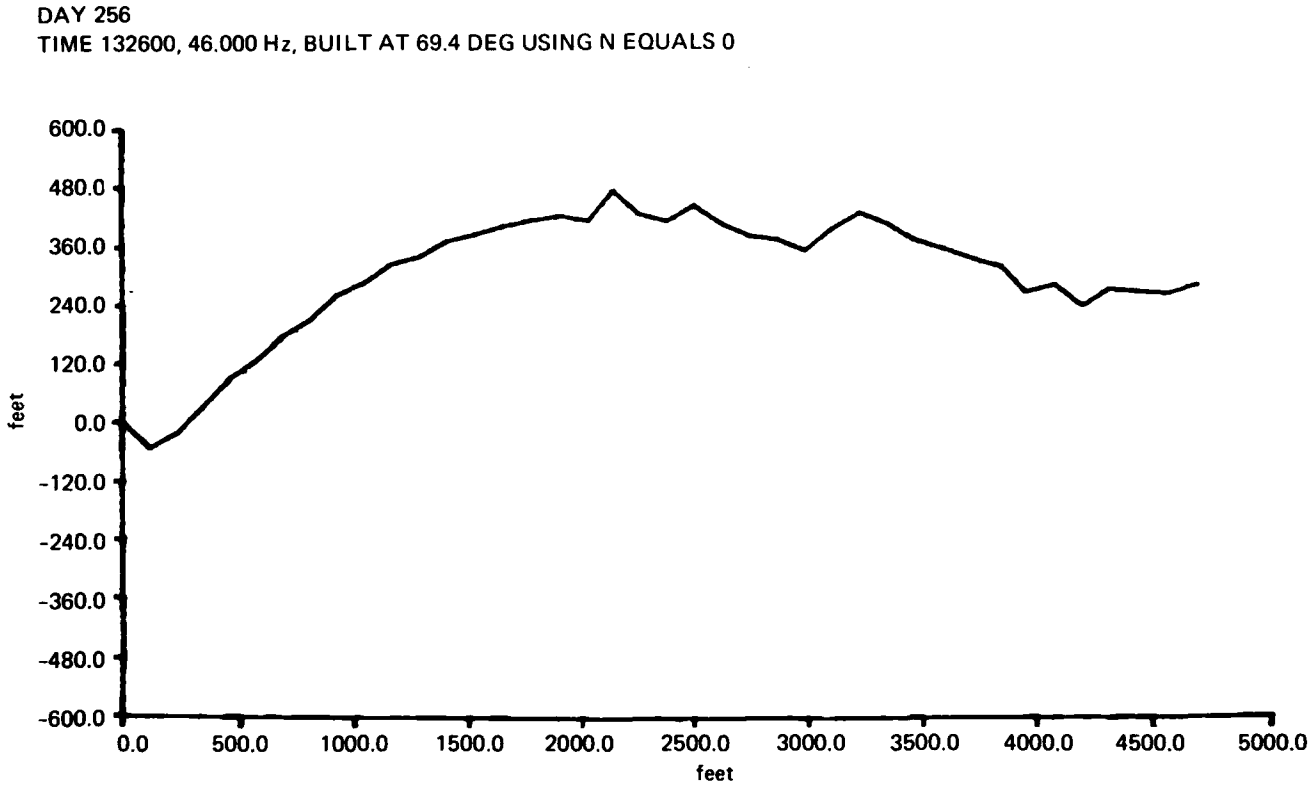

Figure 11k. Array shape, self-cohering 46 Hz.

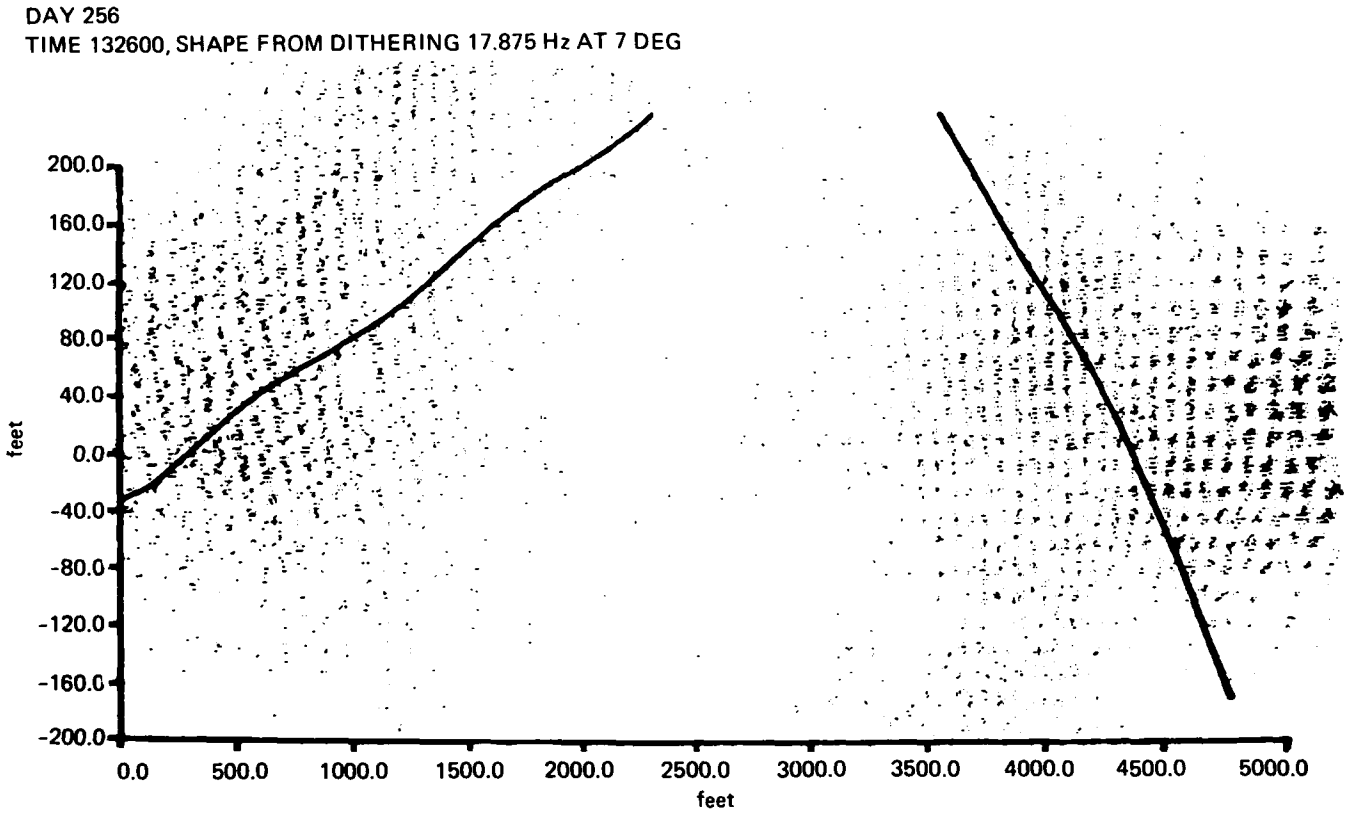

Figure 11ℓ. Array shape, self-cohering 17.875 Hz.

Most of the above frequencies were from target angles more or less broadside to the array (from 70° to 120°), but one frequency is from a target closer to endfire (142°). It is evident that the array shape self-cohered from one frequency can be used to improve beam patterns not only at other frequencies, but at other target angles as well.

Still at time 1326, the residual-phase self-cohering method with narrowed spatial filter was applied to some of the other frequencies. The resulting array shapes are shown in Figs. 11i through 11k. All these shapes show the same basic curvature as Fig. 11c. The shape from 21.75 Hz (Fig. 11i) is virtually identical to the shape from 19.625 Hz (Fig. 11c) except for the little upswing at the tail end; the residual-phase plot for 21.75 Hz shows an anomaly at that point, perhaps due to hydrophone failure or noise saturation. The shape from 29.375 Hz (Fig. 11j) is virtually identical to the shape from 19.625 Hz except for the first 900 ft of the array; cause unknown. The shape from 46.0 Hz (Fig. 11k) is virtually identical to the shape from 19.625 Hz for the first 3000 ft of the array; the deviation toward the tail end is possibly due to poor signal amplitude there, as shown in Fig. 2f. Shapes from 21.75 Hz and 29.375 Hz, when used to beamform at other frequencies, caused significant beam pattern improvement, though not as great as shown in the above table. The shape from 46.0 Hz did not improve beam patterns at any other frequencies.

In all cases, the self-cohering algorithm was applied using a straight array shape as an initial guess. Further work in this area should include using the self-cohered shape from one frequency as the initial guess for self-cohering a second frequency.

Frequency 17.875 Hz also shows a strong spectral level at time 1326 (Fig. 1h). When beamformed assuming a straight array, coherence was 0.613 with a target angle of 7° (very nearly endfire). Self-cohering successfully raised coherence to 0.858. The resulting array shape (Fig. 11ℓ) looks similar to the shape for 19.625 Hz, but neither beam pattern (17.875 Hz and 19.625 Hz) is improved when the other's array shape is used. The possible explanation is that the target arrival angles are too different: self-cohering at one angle causes correction of the y-component of array curvature and self-cohering at the other angle causes correction of the x-component of the array curvature, and small errors cause the two to be independent.

Figures 8a, 9a, 10, and 11c indicate a gradual progression over a period of 11 min of the array shape from nearly straight to well curved, as would be expected of an array being towed through a turn.

SIGNAL-TO-NOISE CONSIDERATIONS

Figures 11c through 11f have indicated that with a "strong" signal source, it is possible to recover a reasonable array shape from an intial guess which is in error by considerably more than a wavelength. This section is a simplistic analysis to establish an estimate of the signal-to-noise ratio required at the cohering frequency to effect beam pattern improvement at some other frequency.

Let there be N elements in the array. Signal amplitude S from a localized source and noise amplitude M from an isotropic source impinge on the array. The compensate-residual-phase method is used to self-cohere the array, with a spatial filter width of 2b + 1 elements (ie, b elements on either side of center). Steer the array toward the signal source; let ϕ_m be the residual phase at the m^{th} element due to imperfect knowledge of the element locations. Noise is independent from element to element, so the noise phase θ_m is a random variable, uniformly distributed from 0 to 2π, uncorrelated between elements. The total voltage received at the m^{th} element is

$$S\, e^{j\phi_m} + M\, e^{j\phi_m}$$

The spatial filtering operation (part of the residual-phase method of self-cohering) involves averaging over adjacent elements, so that the result at the n^{th} element is

$$Z_n = \frac{1}{2b+1} \sum_{m=n-b}^{n+b} \left(S\, e^{j\phi_m} + M\, e^{j\theta_m} \right) .$$

Now Z_n is a random variable. Its expected value is

$$E(Z_n) = \frac{1}{2b+1} \sum_{m=n-b}^{n+b} \left[S\, E(e^{j\phi_m}) + M\, E(e^{j\theta_m}) \right] .$$

The variable θ_m is completely random, so $E(e^{j\theta_m}) = 0$. The variable ϕ_m is deterministic, being due to the unknown (but presumably fixed) array shape. The usefulness of the spatial filtering is predicated upon a much slower element-to-element variation in ϕ_m than in θ_m, so that for m within b of n, $\phi_m \approx \phi_n$:

$$E(e^{j\phi_m}) \approx e^{j\phi_n} \text{ for } n - b \leq m \leq n + b$$

$$E(Z_n) = \frac{1}{2b+1} \sum_{m=n-b}^{n+b} (S\, e^{j\phi_n} + 0) = S\, e^{j\phi_n} . \qquad (2)$$

This means that, on the average, the spatial filtering procedure is able to extract the true residual phase (due to array shape) from the midst of random phase (due to noise).

Now find the variance contributed by the noise.

$$Z_n^2 = \frac{1}{(2b+1)^2} \sum_m \sum_p \left(S\, e^{j\phi_m} + M\, e^{j\theta_m}\right)\left(S\, e^{-j\phi_p} + M\, e^{-j\theta_p}\right)$$

$$= \frac{1}{(2b+1)^2} \sum_m \sum_p \left[S^2\, e^{j(\phi_m - \phi_p)} + SM\, e^{j(\phi_m - \theta_p)} + SM\, e^{j(\theta_m - \phi_p)} + M^2\, e^{j(\theta_m - \theta_p)}\right] .$$

To compute $E(Z^2)$, note that:

ϕ and θ are uncorrelated, so $E\left[e^{j(\phi-\theta)}\right] = 0$.

θ_m and θ_p are uncorrelated if $m \neq p$, so $E\left[e^{j(\theta_m - \theta_p)}\right] = 0$ for $m \neq p$.

ϕ_m and ϕ_p are approximately equal for all m and p.

Therefore,

$$E(Z^2) = \frac{1}{(2b+1)^2}\left[(2b+1)^2 S^2 + (2b+1) M^2\right] = S^2 + \frac{M^2}{2b+1} .$$

The variance is

$$\sigma^2 = E(Z_n^2) - E^2(Z_n) = \frac{M^2}{2b+1} ,$$

$$\sigma = \frac{M}{\sqrt{2b+1}} . \qquad (3)$$

Equations (2) and (3) may be interpreted as saying that the output of the spatial-filtering process of the residual-phase self-cohering method is the sum of two vectors (in complex space). One of those vectors has amplitude S and phase ϕ_n [Eq. (2)]. The second vector has amplitude $M/\sqrt{2b+1}$ and completely random phase [Eq. (3)]. (See diagram a.)

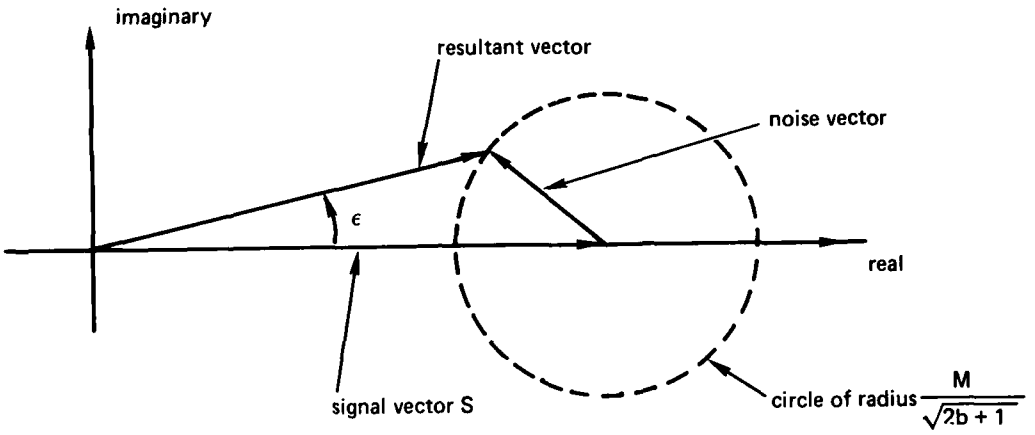

Diagram a.

The output of the spatial filter is the self-cohering algorithm's best estimate of the residual phase ϕ_n due to array non-straightness. Suppose that the signal arrival angle is more or less broadside to the array; then the algorithm compensates for residual phase by translating it directly into element y-coordinate displacement:

$$Y_n = \lambda \frac{\phi_n}{2\pi} \quad .$$

However, as indicated in Diagram a, the algorithm's best estimate of residual phase will be in error by an angle ϵ, and therefore the calculated y-coordinate displacement will be in error by

$$\Delta Y_n = \lambda \frac{\epsilon_n}{2\pi} \quad ,$$

where λ is the wavelength of the self-cohering frequency.

Worst-case ϵ occurs when the noise vector is more or less perpendicular to the signal vector, at which point:

$$\epsilon = \arctan\left(\frac{\text{noise}}{\text{signal}}\right) = \arctan\left(\frac{M}{S\sqrt{2b+1}}\right) \quad .$$

Up until the point where the argument of the arctan is about 2, the arctan may be approximated by its argument:

$$\epsilon \approx \frac{M}{S\sqrt{2b+1}} \quad .$$

So

$$\Delta Y_n \approx \frac{\lambda M}{2\pi S\sqrt{2b+1}} \quad .$$

The self-cohered array shape is built up element by element by adding to the $(n-1)^{th}$ y-coordinate an amount sufficient to compensate for the estimated phase difference between the n^{th} and $(n-1)^{th}$ elements. Thus, there is a tendency for errors to accumulate. When random errors are added, the rms error increases as the square root of the number of independent terms in the sum. There are N elements in the array, but because of the spatial filtering, only N/2b+1 of the Δy terms are independent. The total error in the self-cohering method's estimate of how much the array shape is likely to differ from straight is:

$$\delta = \Delta Y \sqrt{\frac{N}{2b+1}} = \frac{\lambda M}{2\pi S\sqrt{2b+1}} \sqrt{\frac{N}{2b+1}} = \frac{\lambda M\sqrt{N}}{2\pi S(2b+1)} \quad . \tag{4}$$

Suppose that the true array shape differs from the initial-guess shape by an amount ξ. The self-cohered shape will effect some improvement of beam patterns of other targets only if the self-cohered shape error is less than the initial-guess error:

$$\delta < \xi \quad .$$

From Eq. (4), this means that

$$\frac{S}{M} > \frac{\lambda\sqrt{N}}{2\pi\xi(2b+1)} \quad . \tag{5}$$

Equation (5) gives a lower bound on the signal-to-noise ratio at a single array element in order that the array shape may be calculated (via a self-cohering algorithm) with sufficient accuracy to effect improvement in the beam patterns of targets at other frequencies. This bound does not guarantee that the beam patterns of other frequencies will be improved up to the limits established by their own signal-to-noise ratios (ie, a beam pattern cannot be made perfect if noise is present, even if the array shape is known exactly); it only guarantees that the beam patterns won't get any worse by using the self-cohered array shape than they already were with the use of the initial-guess array shape.

Obviously, the derivation of Eq. (5) is not rigorous. The most glaring deficiencies are the "small-noise" approximation, the elimination of steering angle from consideration, and the sort of haphazard use of the concept of array shape "deviations from the initial guess." Probably the equation is adequate for a ballpark estimate of required signal-to-noise ratios. For example, for the array considered in this report:

N = 40 elements,

2b+1 = 7-element-wide spatial filter,

ξ = 1 wavelength deviation of true array shape from initial guess $\left(\frac{\lambda}{\xi} \approx 1\right)$

$$\frac{S}{M} > \frac{\lambda\sqrt{40}}{2\pi\lambda(7)} \approx \frac{1}{7} = -16.8 \text{ dB} \quad .$$

This is an overly optimistic prediction, since a noise voltage 7 times larger than the signal voltage (at one element) obviously exceeds the "small noise" approximation used in deriving Eq. (5).

A computer simulation has been performed that verifies that self-cohering can indeed be successful with a signal-to-noise ratio (at one array element, at the cohering frequency) as poor as 1/2. An arbitrary array shape was chosen (Fig. 12a). Signals at two frequencies (19 Hz and 25 Hz) and two arrival angles (100° and 70° from endfire) were simulated (the noise-free 19-Hz beam pattern is shown in Fig. 12b) and then corrupted with various amounts of noise. In the noise-free case, the 19-Hz beam pattern is severely degraded if the array is assumed to be straight (Fig. 12c); but the compensate-residual-phase self-cohering method can recover a reasonable estimate of the array shape (Fig. 12d) (using a straight line as an initial guess) and restore the beam pattern to near perfection (Fig. 12e). Figures 12f through 12h show a similar sequence for the case of noise equal in amplitude to the signal; the self-cohered array shape (Fig. 12g) is still recognizable, and the self-cohered beam pattern (Fig. 12h) is nearly as good as the beam pattern which uses perfect knowledge of the array shape (Fig. 12f). Figures 12i through 12ℓ show a similar sequence for the case of noise amplitude twice as large as signal amplitude. The beam pattern is not very good, even using the true array shape (Fig. 12i). When the array is assumed to be straight, the beam pattern is so poor that the target is lost (Fig. 12j). (The apparent peak at about 80° is a false sidelobe, not the target). The self-cohered array shape (Fig. 12k) has only slight resemblance to the true array shape, but is nevertheless close enough to the true shape to recover the target in the beam pattern (Fig. 12ℓ). With noise twice as large as signal, the 25-Hz target (Fig. 12m) also disappears when the beam pattern is drawn using a straight array shape (Fig. 12n); but the 25-Hz target reappears (Fig. 12o) when the array shape (Fig. 12k) resulting from self-cohering 19 Hz is used.

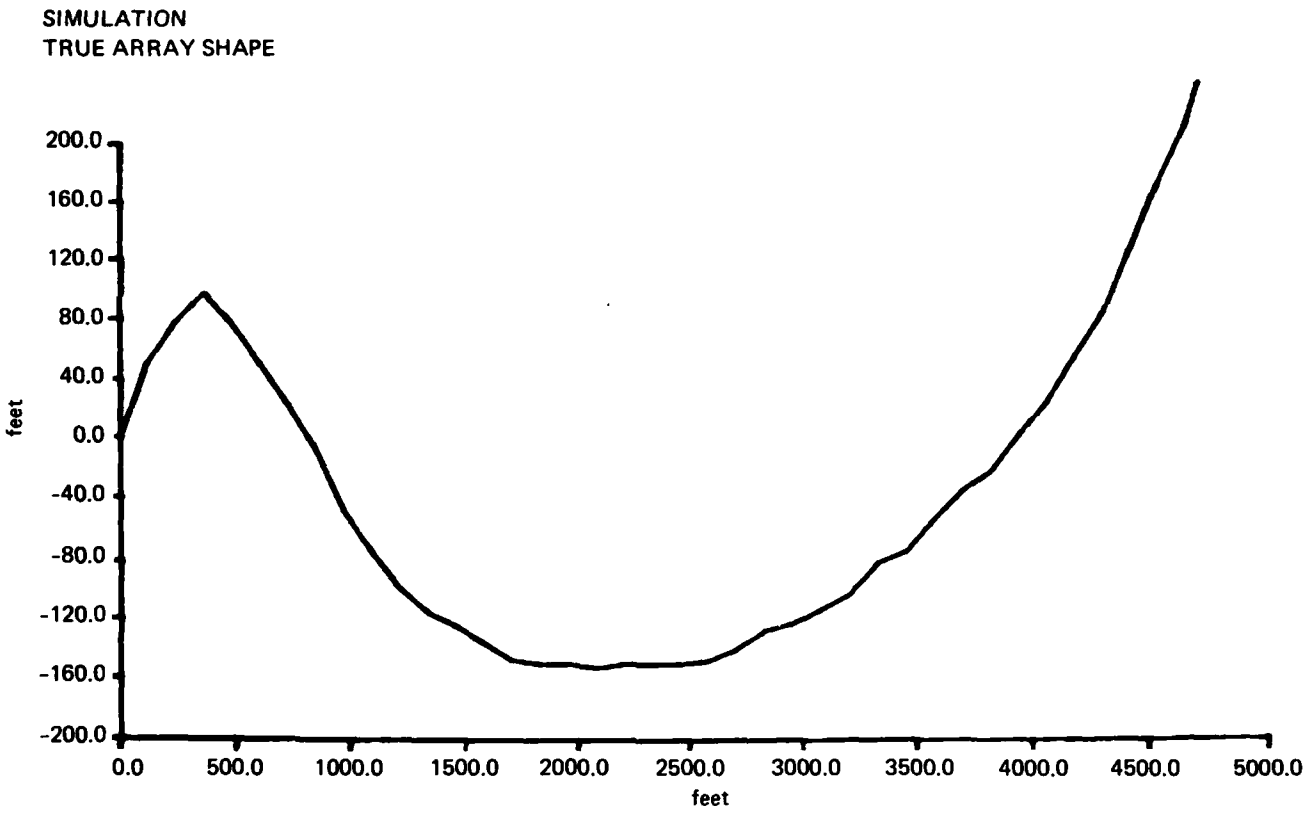

Figure 12a. Simulated true array shape.

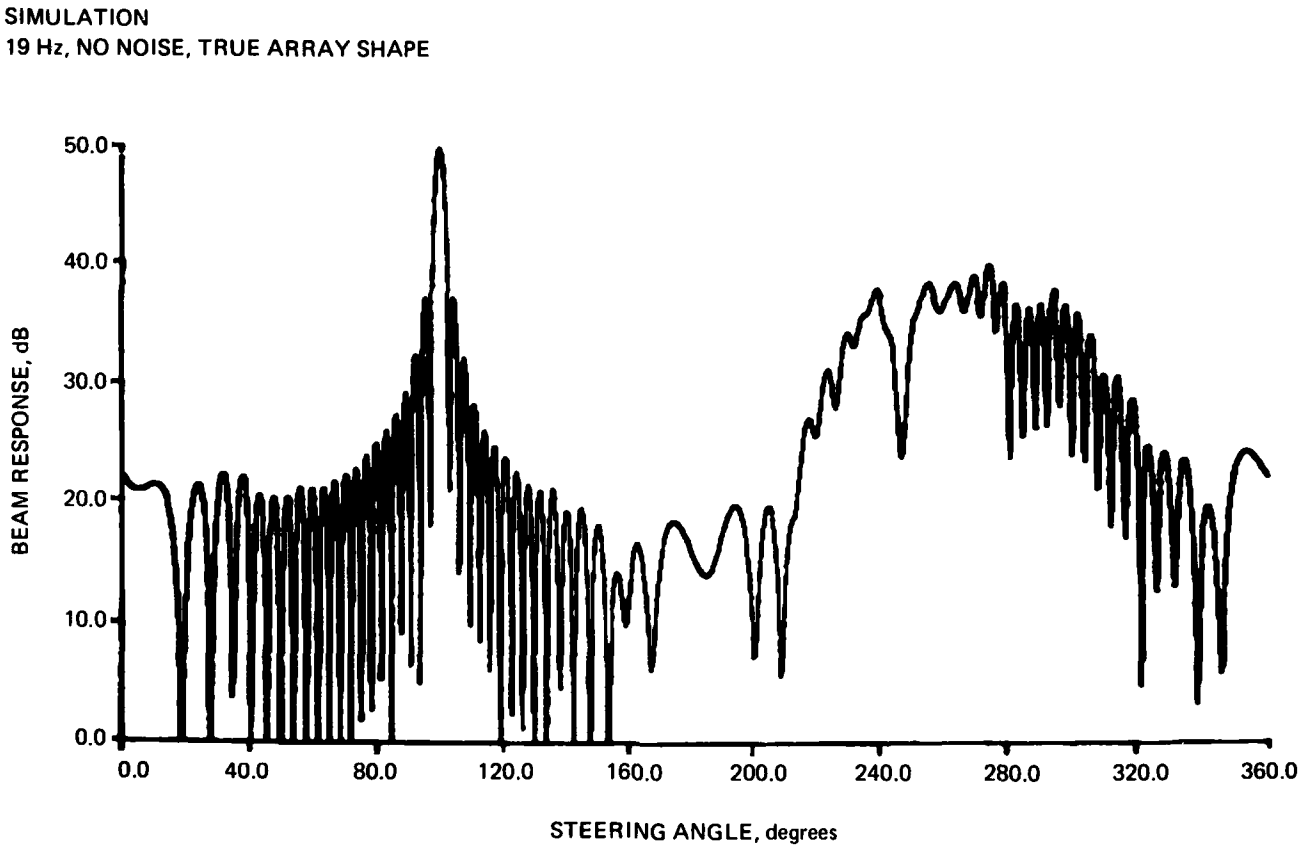

Figure 12b. Ideal beam pattern at 19 Hz.

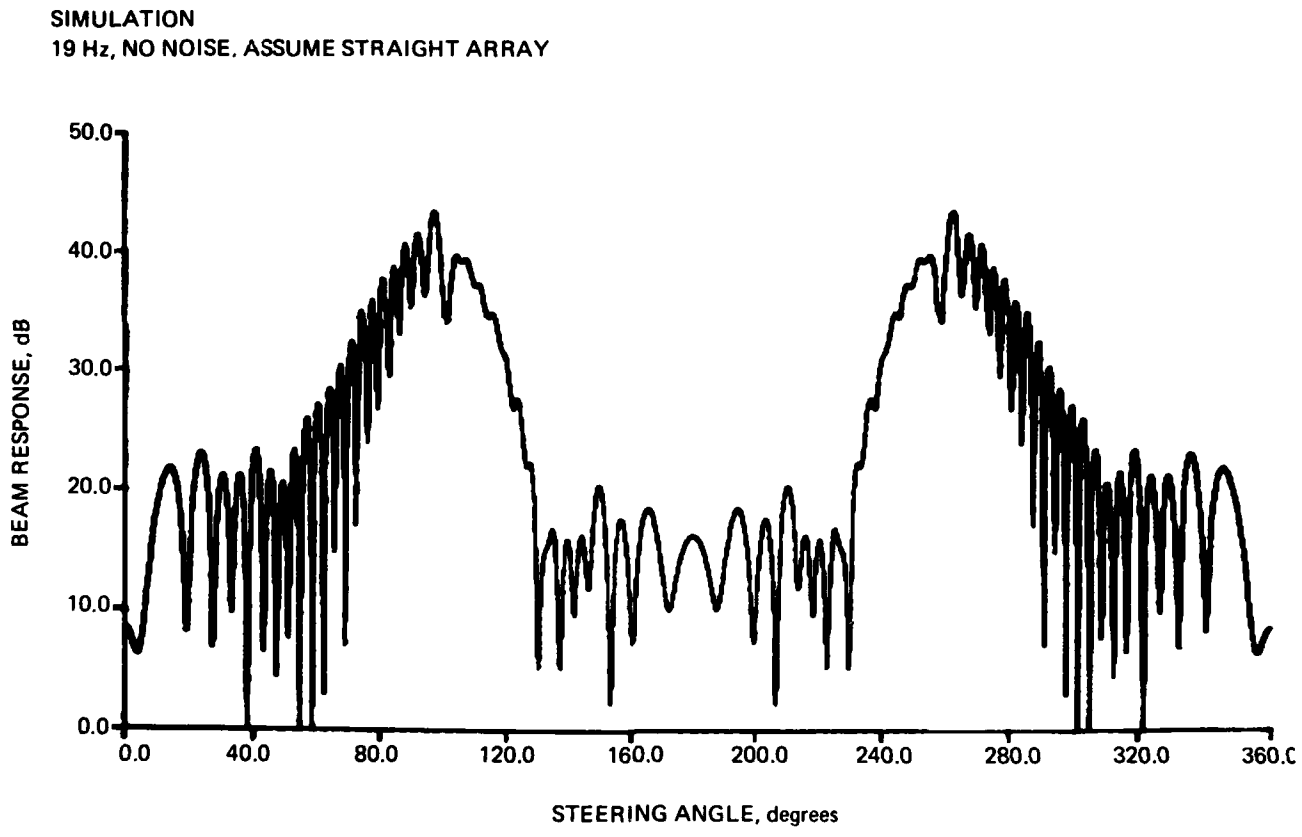

Figure 12c. 19-Hz beam pattern corrupted by incorrect array shape.

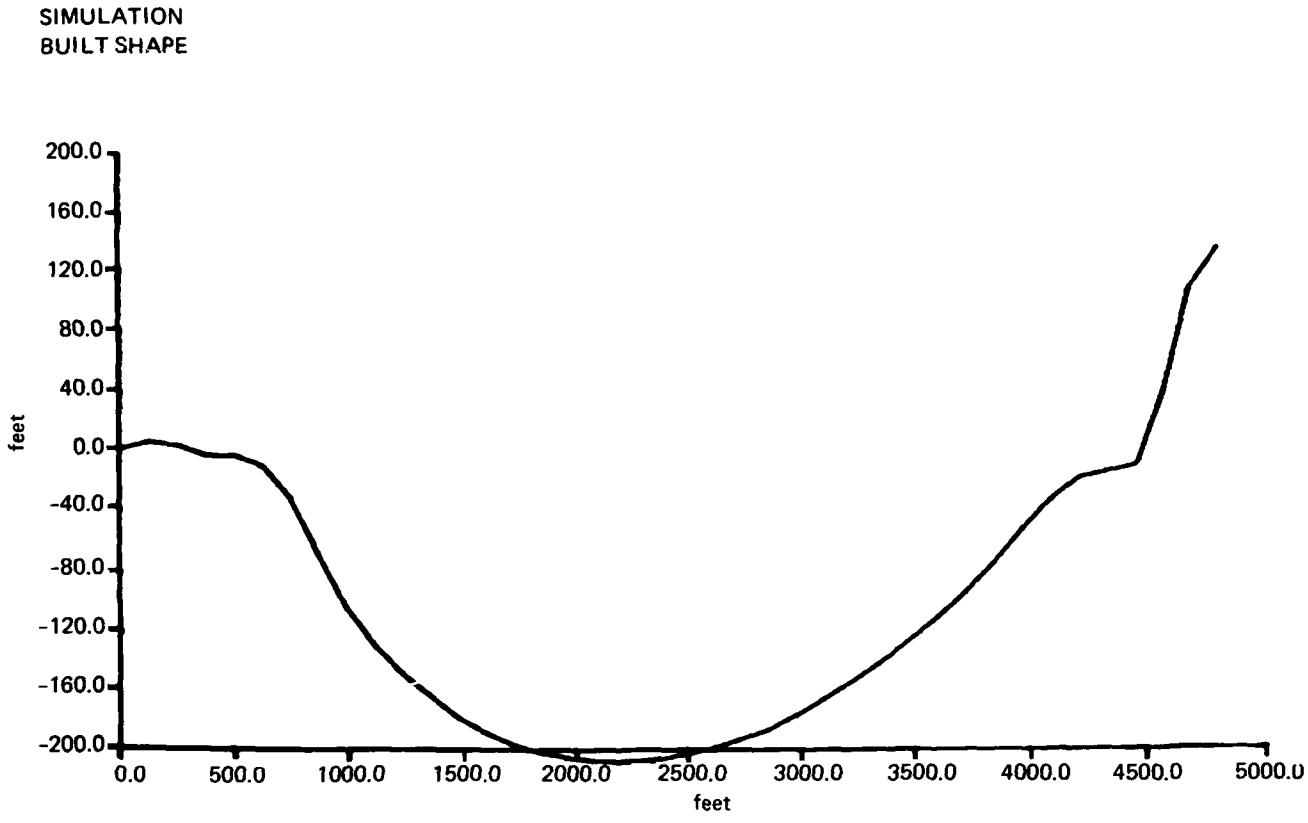

Figure 12d. Self-cohered array shape.

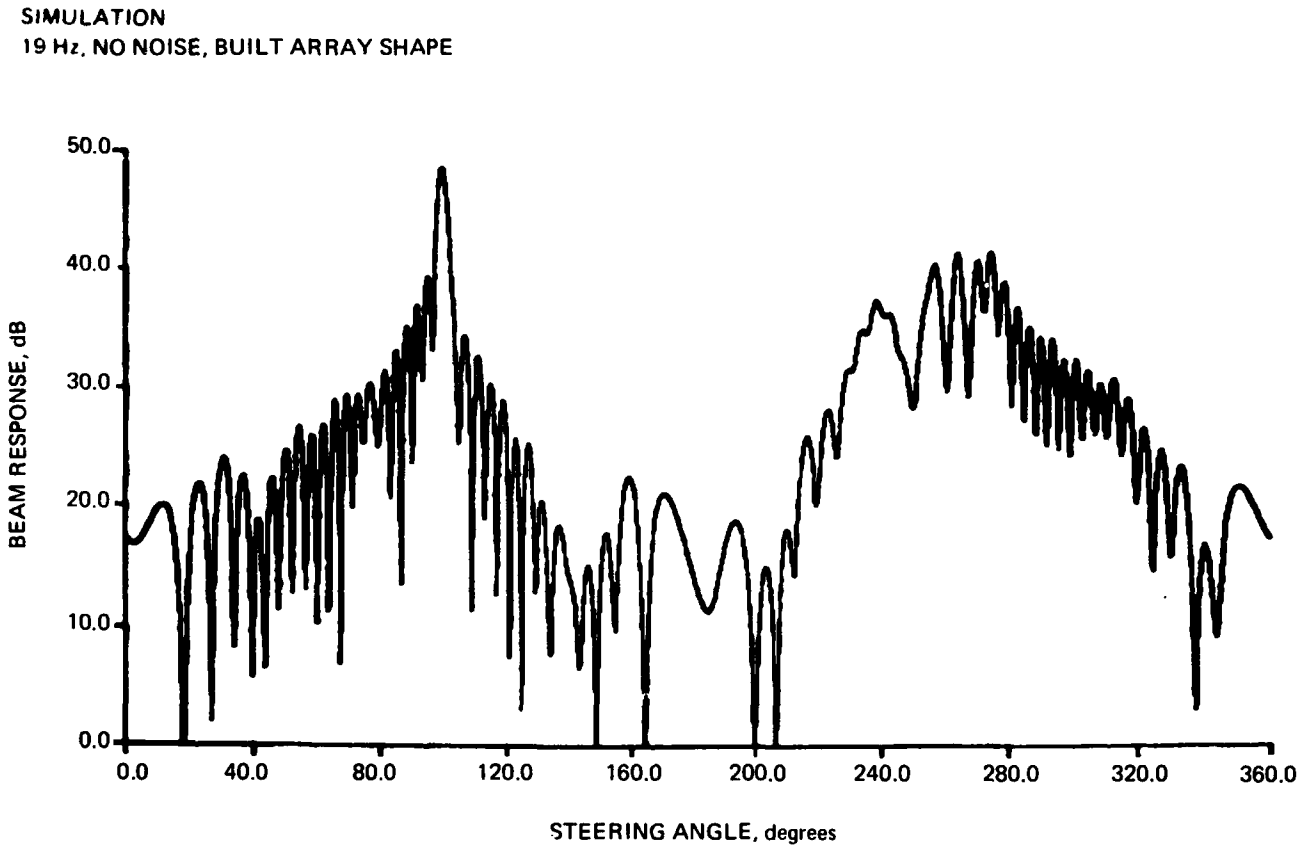

Figure 12e. 19-Hz beam pattern after self-cohering.

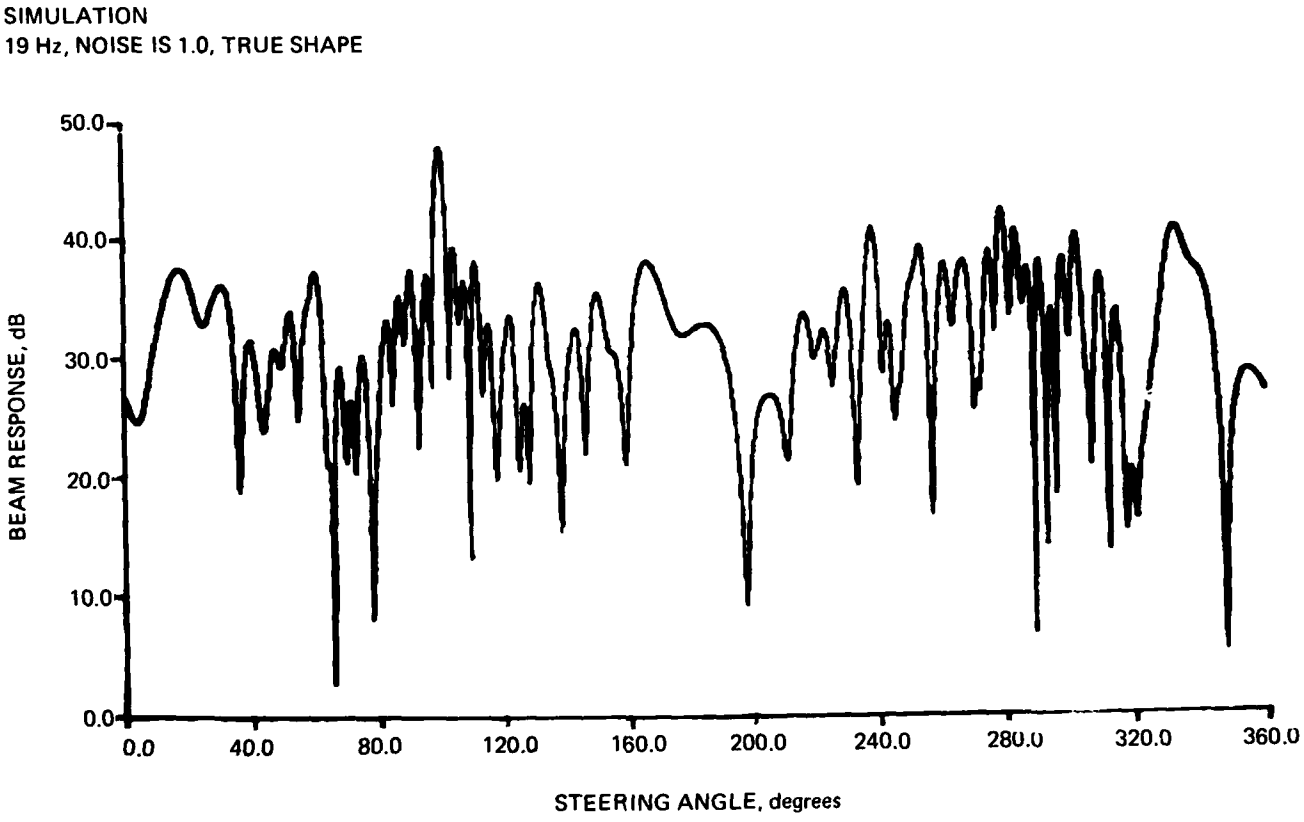

Figure 12f. 19-Hz beam pattern corrupted by noise.

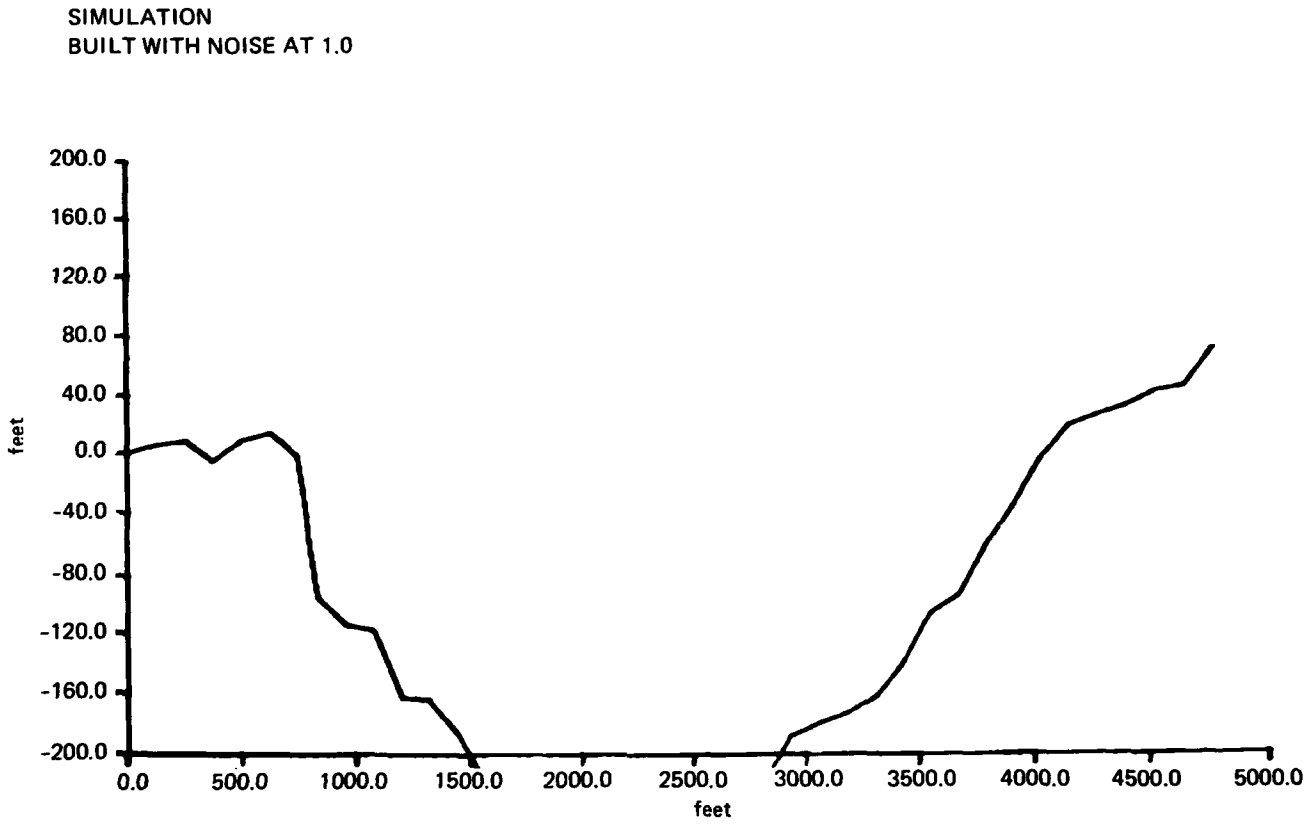

Figure 12g. Array shape self-cohered from noisy signal.

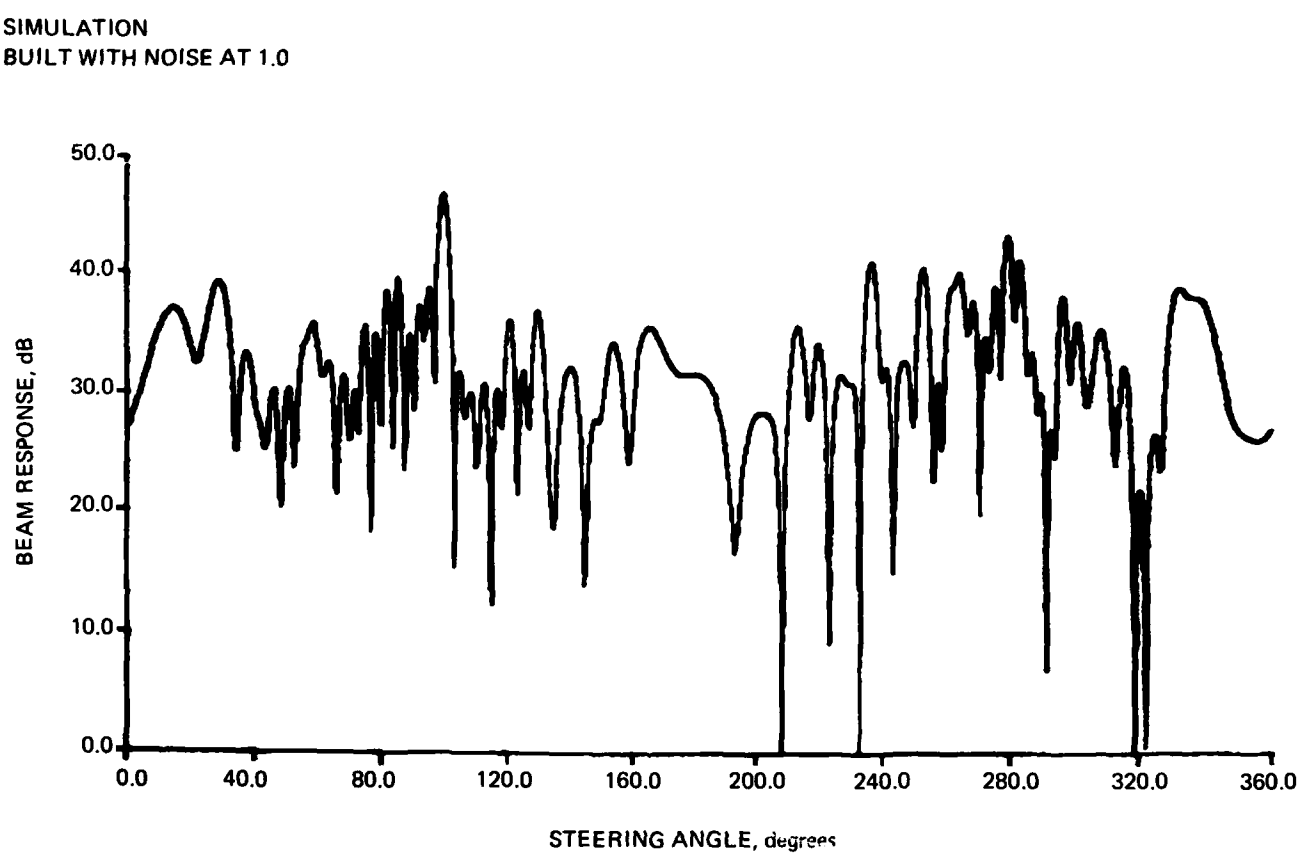

Figure 12h. 19-Hz beam pattern after self-cohering on noisy signal.

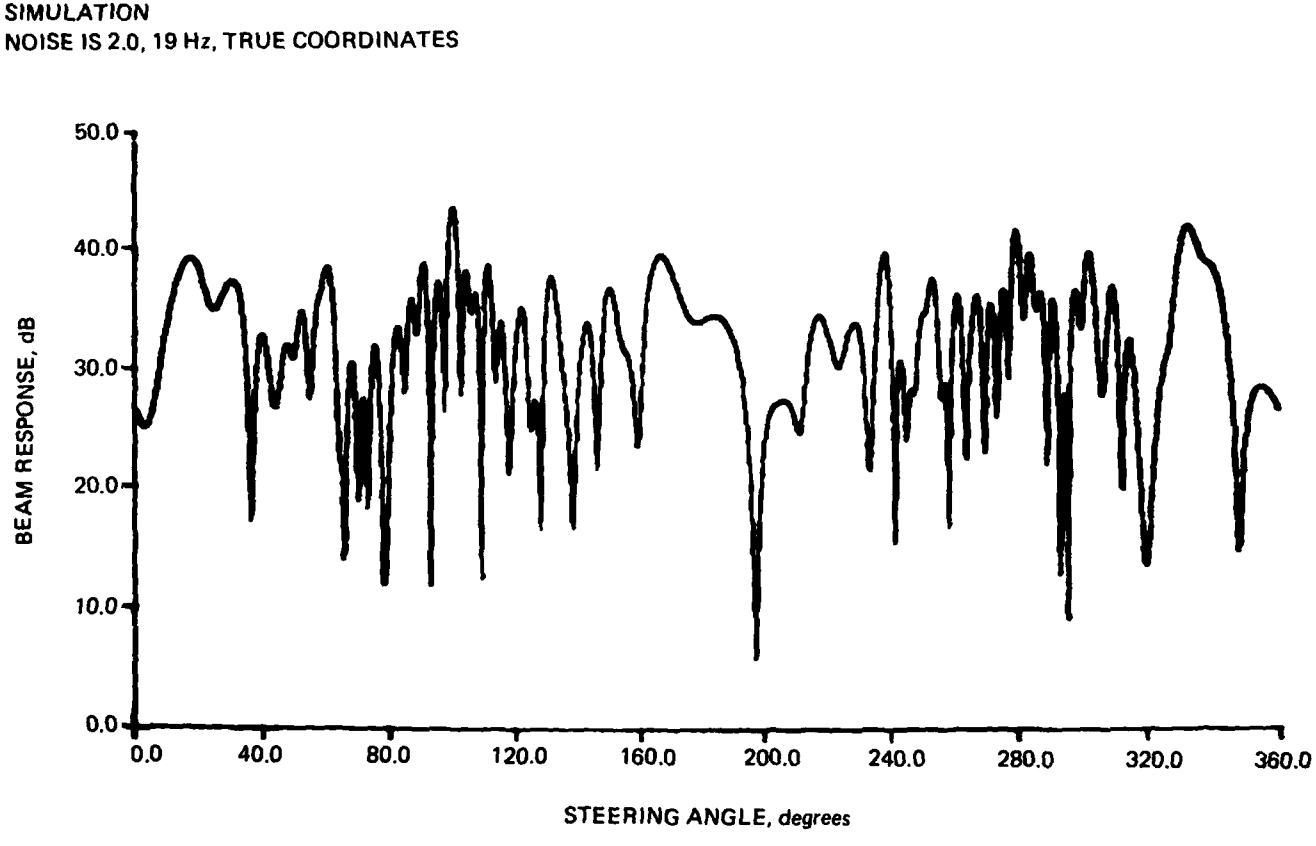

Figure 12i. 19-Hz beam pattern corrupted by even more noise.

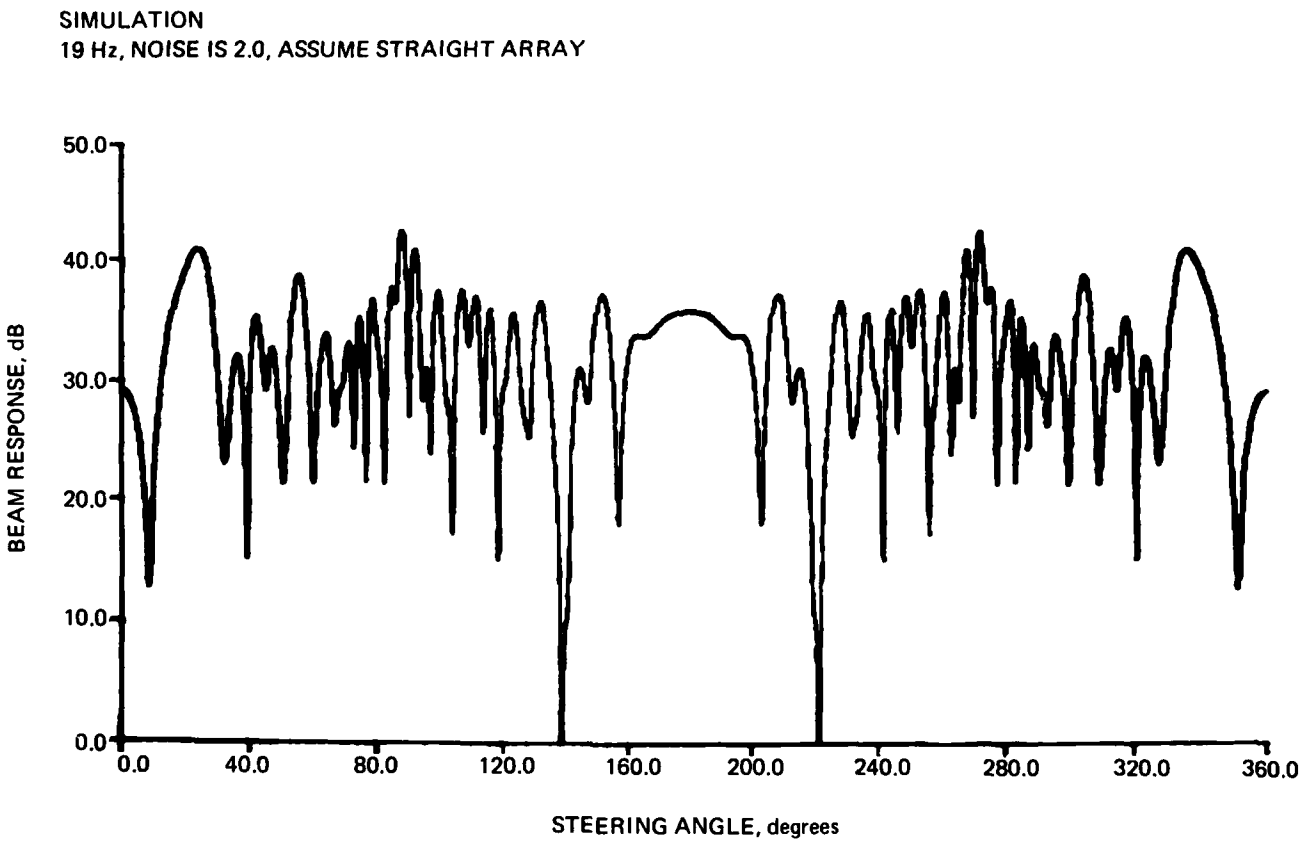

Figure 12j. 19-Hz beam pattern corrupted by noise and incorrect array shape.

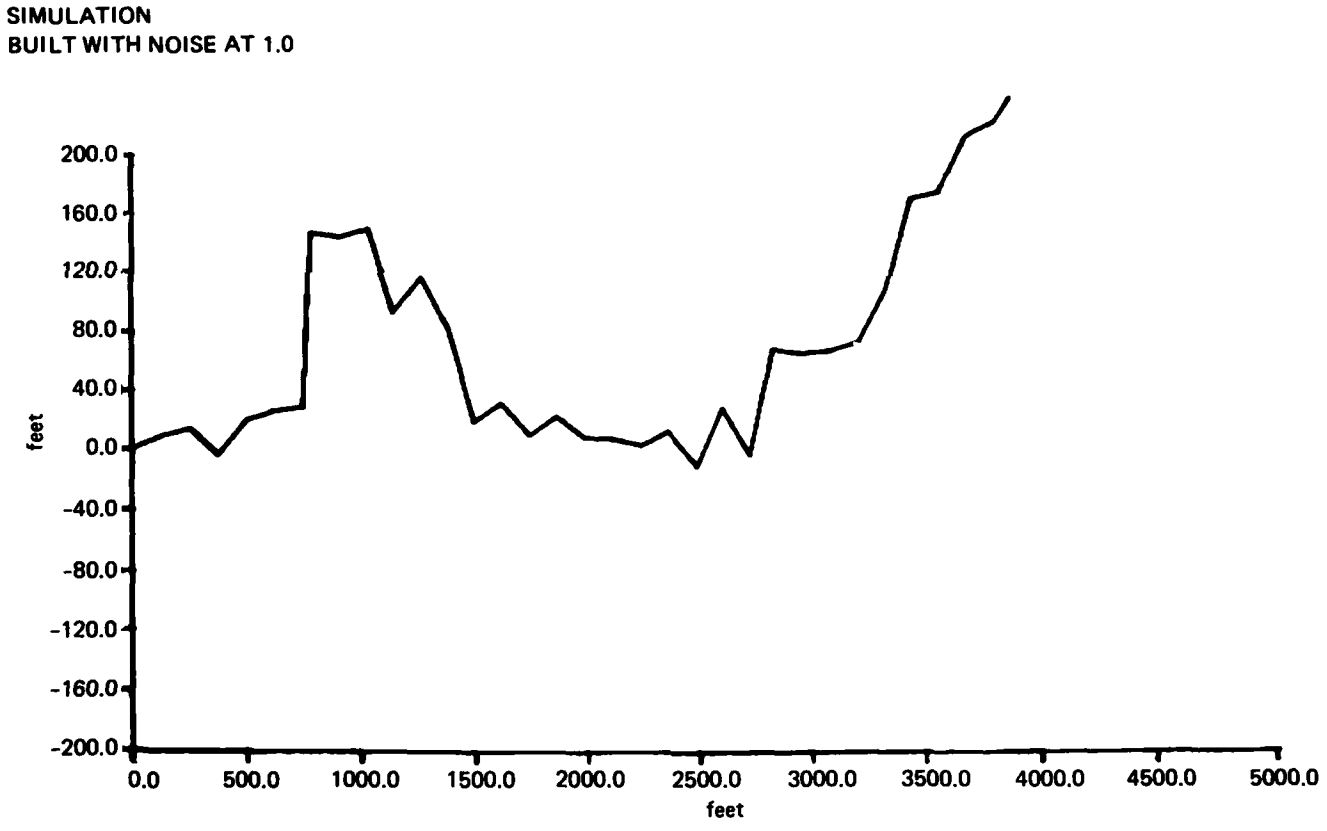

Figure 12k. Array shape self-cohered from noisy signal.

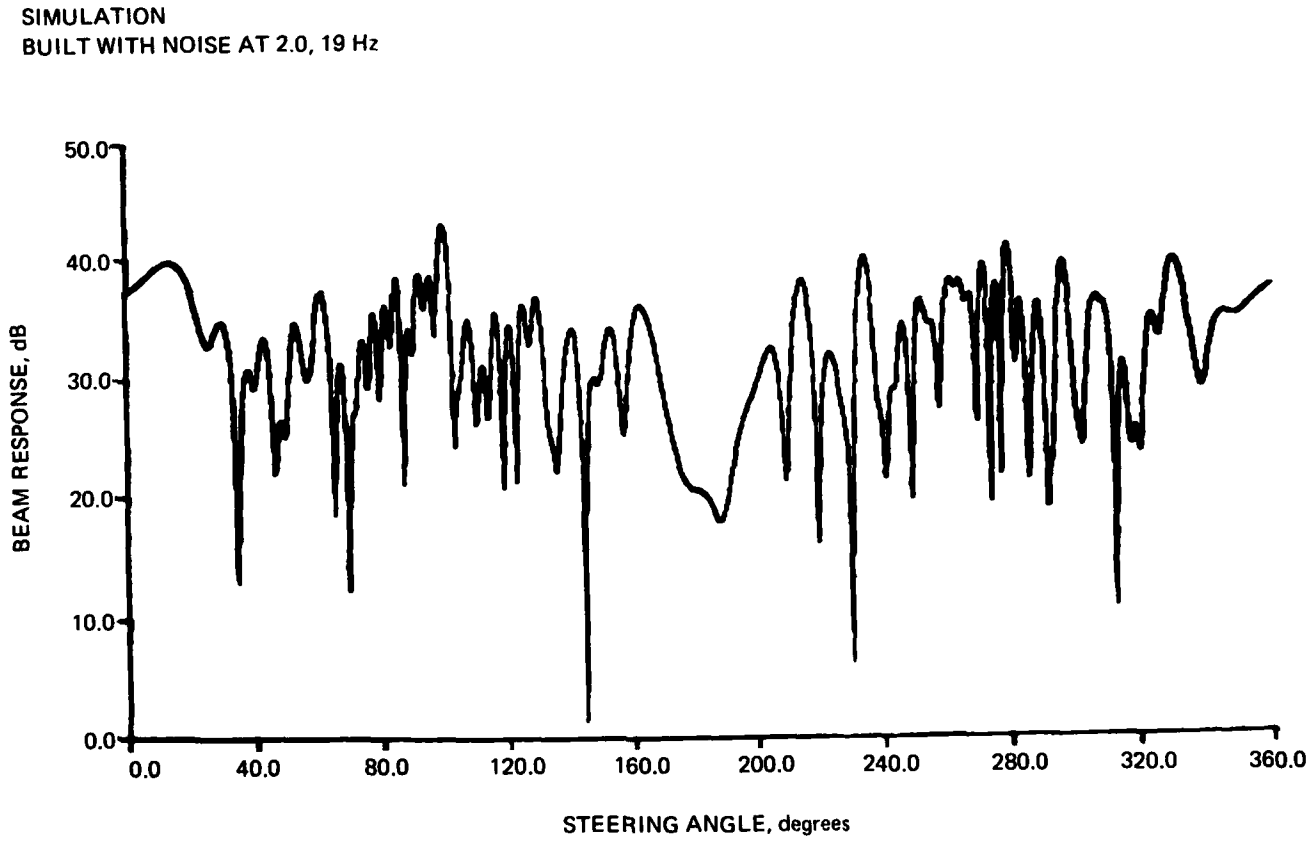

Figure 12ℓ. 19-Hz beam pattern after self-cohering on noisy signal.

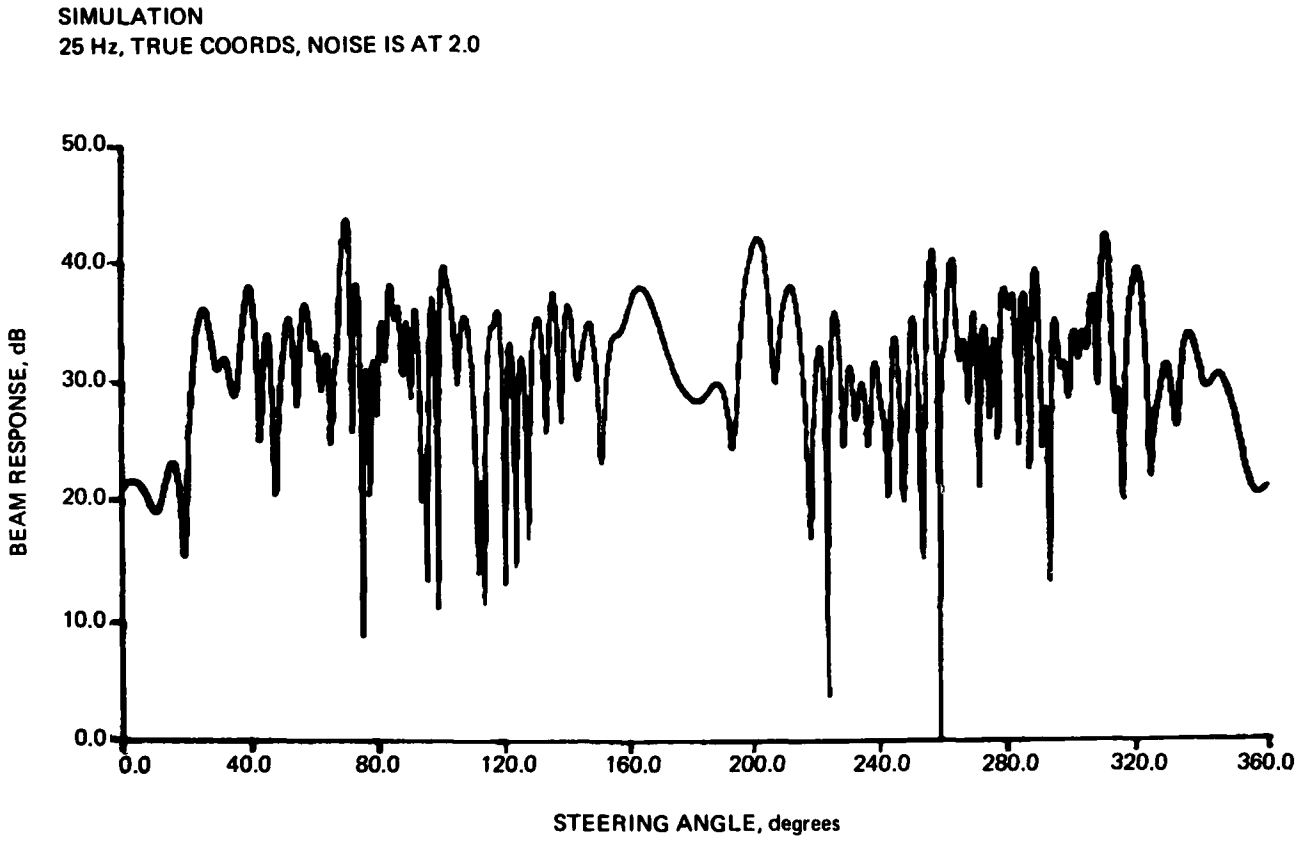

Figure 12m. 25-Hz beam pattern corrupted by noise.

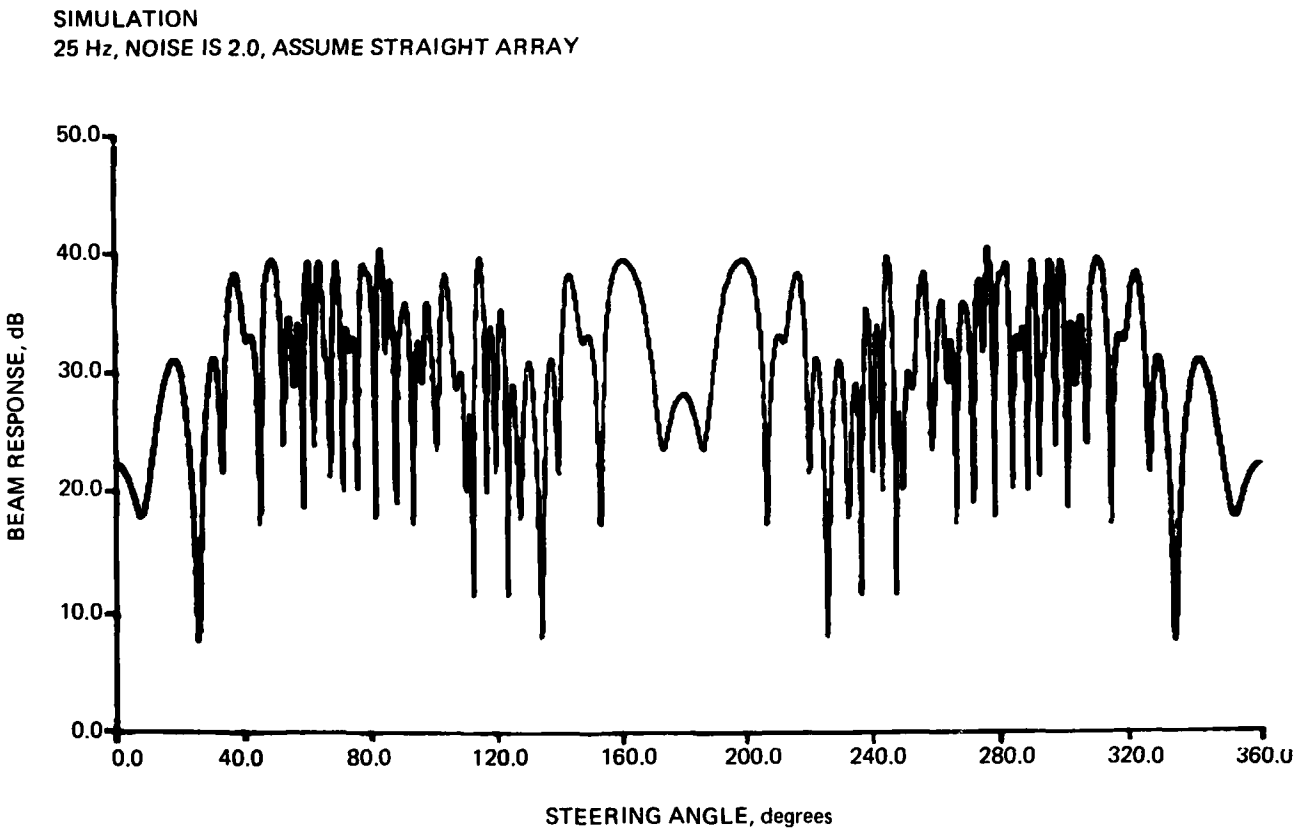

Figure 12n. 25-Hz beam pattern corrupted by noise and incorrect array shape.

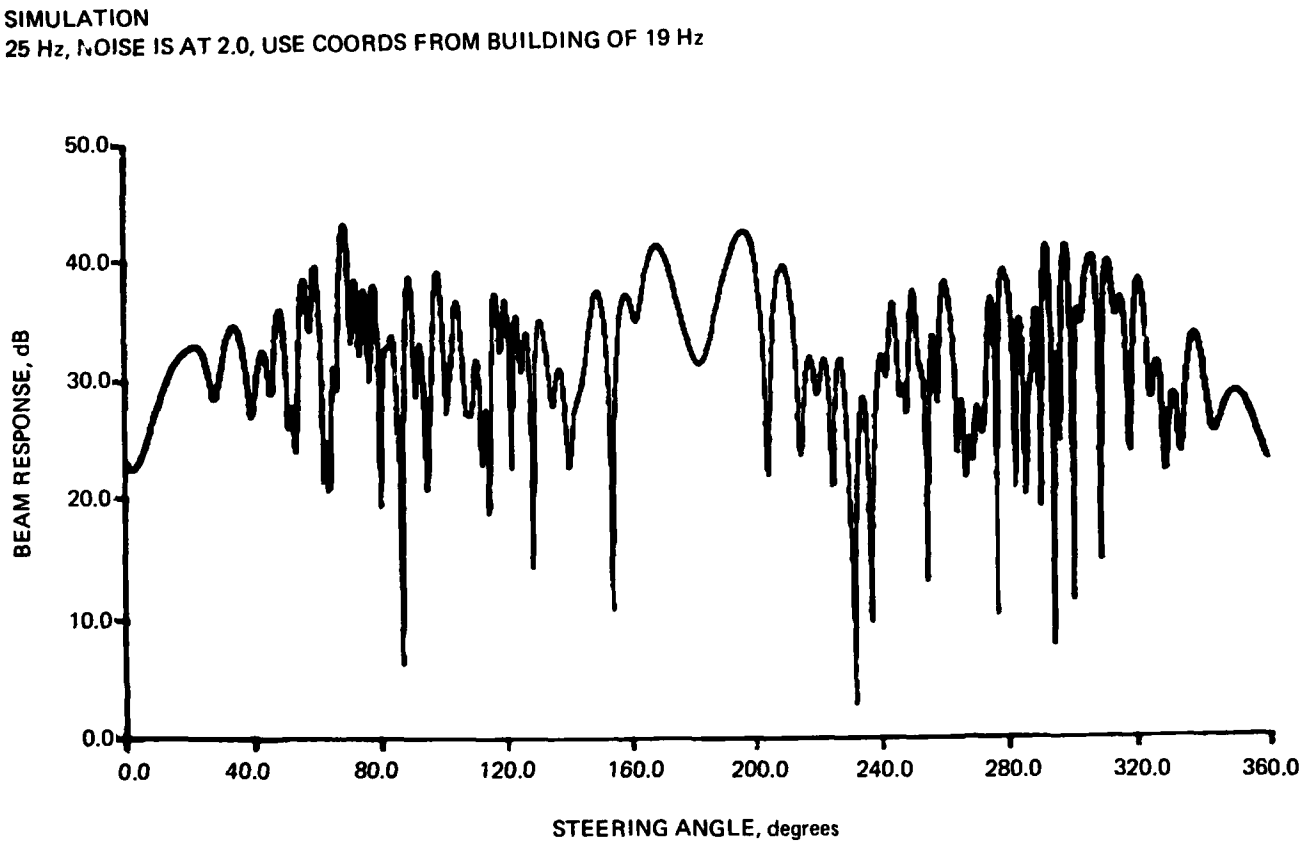

Figure 12o. 25-Hz beam pattern recomputed using array shape from Fig. 12k.

SUMMARY

Self-cohering has been tested with apparent success on recorded data from a 5000-ft towed line array. While the towing ship was on a "straight" course, the array apparently deviated from a straight line by less than 10 ft over its entire length. While the towing ship was turning, signals from a target at 20 Hz with an arrival angle near broadside were used to calculate a two-dimensional array shape differing by nearly three wavelengths (600 ft) from a straight-line initial guess. The calculated array shape was used to beamform at other frequencies, uncovering a 46-Hz target which was completely obscured prior to self-cohering. These results are summarized as follows.

Summary of Self-Cohering Improvements

frequency, Hz	coherence assuming straight array	coherence using array shape from 19.625 Hz	steering angle, deg
19.625	0.440	0.882	77
21.75	0.460	0.771	142
29.375	0.515	0.738	78
46.000	0.374 (Fig. 11e)	0.617 (Fig. 11f)	70
56.500	0.487 (Fig. 11g)	0.571 (Fig. 11h)	120

Especially note: the target at 46.000 Hz is undetectable if the array is assumed straight (Fig. 11e), but is easily detectable after self-cohering (Fig. 11f).

Several different algorithms for self-cohering have been developed and tested. The simplest has been the most successful. No single set of algorithm parameters has yet been found which works well for all conditions.

Right-for-left ambiguity and beam aliasing, plus lack of control over the experimental conditions, cause uncertainty about true target locations and characteristics. Possibly the apparent array shapes found by self-cohering are due to near-field wavefront curvature rather than to turns by the towing ship.

Theoretical calculations indicate that self-cohering can be accomplished with a signal-to-noise amplitude ratio at the cohering frequency as poor as 1/2 (which is -6 dB). Computer simulations confirm weak-signal recovery under those conditions.

INITIAL DISTRIBUTION

NAVAL ELECTRONIC SYSTEMS COMMAND
ELEX-320 (5)

NAVAL RESEARCH LABORATORY
CODE 5000 (LIBRARY)

NAVAL RESEARCH AND DEVELOPMENT
ACTIVITY

NAVAL UNDERWATER SYSTEMS CENTER

OFFICE OF NAVAL RESEARCH
ONR-200 (CAPT W. T. BOYER, JR.)

UNIT X
LIBRARY OF CONGRESS

DEFENSE TECHNICAL INFORMATION CENTER (12)